Supplementary Material

Synthesis of 1,4- and 1,4,4-substituted piperidines for the inhibition of neuronal T-type Ca^{2+} channels and mitigation of neuropathic pain in mice

Medha J. Gunaratna,[a] Duy H. Hua,[*a] Bende Zou,[b] Conrado Pascual,[b] William Cao,[b] Man Zhang,[a] Sahani Weerasekara,[a] Thi D. T. Nguyen,[a] Kui Xiao,[b] and Xinmin Simon Xie[*b]

[a]Department of Chemistry, Kansas State University, Manhattan, KS 66506, U.S.A.
[b]AfaSci Research Laboratories, Redwood City, CA, U.S.A.
Email: duy@ksu.edu; simonxie@afasci.com

Table of Contents

Biological evaluation of T-type channel inhibitors

For the primary screen of our synthesized molecules for T-type channel activities, we used patch clamp recordings of either dissociated mouse dorsal root ganglion (DRG) neurons or $Ca_{v3.2}$ channel expressed in human embryonic kidney (HEK)-293 cells from a tetracycline inducible expression system (Invitrogen; see Experimental Section shown below). The active compounds were then evaluated *in vivo* for resistance of neuropathic pain by either one of the following two methods. Firstly, because knockout or antisense knockdown of the $Ca_{v3.2}$ isoform produces analgesic effects in neuropathic and inflammatory pain in mice,[1] a reported Complete Freund adjuvant (CFA)-inflammatory pain mouse model[1] was used to examine the drug effects. Secondly, because an over activation of T-channel results in the generation of seizure activity,[2] prolonged latencies to seizures and decreasing the fatality rate in pentylenetetrazole (PTZ)-induced seizure mouse model was also used to determine the inhibition of T-channel activity. Two previously reported T-type calcium channel inhibitors ML218 and Z944 were compared, and gabapentin was used as a standard in the analgesic study. Results of the *in vitro* and *in vivo* studies are summarized in Table S1. From the *in vitro* inhibition of T-type and $Ca_{v3.2}$ channel data (second and third columns of Table S1), the synthesized molecules are not as strong inhibitors as ML218 or Z944 with the exception of molecule **6**, which possessed similar activity in DRG neurons. However, because molecule **6** showed a weak inhibitory activity in PTZ-induced fatality model, it was not investigated further. Compounds **2**, **5**, and **6** possessed low inhibitions of seizure; therefore, they were also not investigated further. Notably, the two reported calcium channel inhibitors ML218 and Z944 showed only weak protective effect in PTZ-induced fatality model (17 and 33%, respectively). Compounds **3**, **7**, **9**, and **10** did not show promising inhibition of either T-channels or $Ca_{v3.2}$ channel; hence, they were not studied further. Molecules **4** and **8** displayed acceptable analgesic activity (strong and medium, respectively) and inhibition of seizure (86 and 89%, respectively). Therefore, these two compounds were investigated further for their analgesic effects using a spared nerve injury (SNI) model, which is an acute pain and neurogenic inflammatory pain rat model.

Table S1. Bioactivities *in vitro* and *in vivo* of molecules **1** – **10** and ML218 and Z944. (NT = not tested)

Compound	Inhibition (%) of T-channel in DRG neurons at 1 μM (unless specified)	Inhibition (%) of $Ca_{v3.2}$-channel in HEK 293 cells at 1 μM (unless specified)	Analgesic Max: ++++ at 30 mg/Kg, (unless specified) (n = 6 - 8)	Inhibition (%) of seizure in PTZ-induced fatality, at 30 mg/Kg, via i.p. (n = 6)
1	43.6±13.2 (n=3)	NT	+	80
2	47	NT	NT	0
3	NT	40 (at 10 ?M)	NT	NT
4	NT	62.6 (n=2)	+++	86
5	83±6.4 (n=3)	NT	+	0
6	100 (n = 2)	NT	NT	14
7	43.6 (n=2)	NT	NT	63
8	40.1±6.9 (n=7)	47 (n=2)	++	89
9	0	NT	NT	NT
10	0	NT	NT	NT
ML218	99	91.8±1.8 (n=3)	+++	17
Z944	93.7 (n=2)	82.8±3,3 (n=19)	+++	33
Gabapentin	NT	NT	+++ (100 mg/kg)	0

The tested compounds **4** and **8** showed increases of thermal and mechanical thresholds compared to vehicle. The drug actions started around one hour post-injection and peaked between 3 and 4 hours. The drug effects gradually declined to pre-treatment levels over 7-8 hours (Figures S1 and S2). These tested compounds produced analgesic effects on both thermal and mechanical pain thresholds, while the Spared Nerve Injury (SNI)-vehicle group remained thermal hyperalgesia and mechanical allodynia conditions. Therefore, compounds **4** and **8** have the ability to mitigate neuropathic pain induced in rats and **4** appears to have a greater effect than **8** at a 3-hour time point (an 80% increase in mechanical threshold for **4** and ~60% for **8**)

In the SNI studies, baseline thermal and mechanical thresholds of male rats (Sprague-Dawley rats) were taken prior to surgery, and baseline thresholds were measured on the rats' left hind paws. A group of rats underwent surgery without injury of the nerves, i.e., a sham surgery group (n = 6 – 8/group). Two weeks post-surgery, the thermal and mechanical pain thresholds of each rat were assessed at pre-dosing, and 1, 2, 3, 4, 5, 6, 7, and 8 hours post-treatment (of drug) using Hargreaves test and von Frey monofilament test, respectively. Results are depicted in Figures S1 and S2.

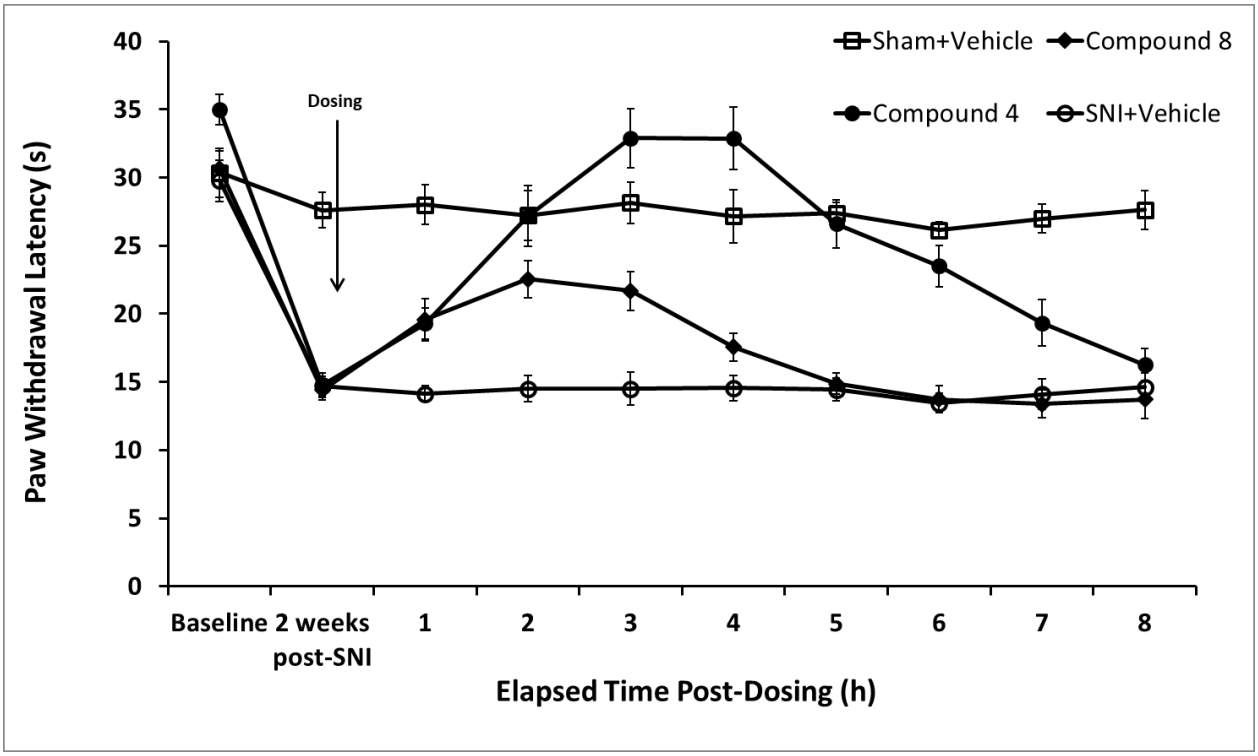

Figure S1. Spared Nerve Injury (SNI) rats' left hind paw withdrawal latencies in response to thermal stimulation (Hargreaves test; number of rats: n = 6 - 8).

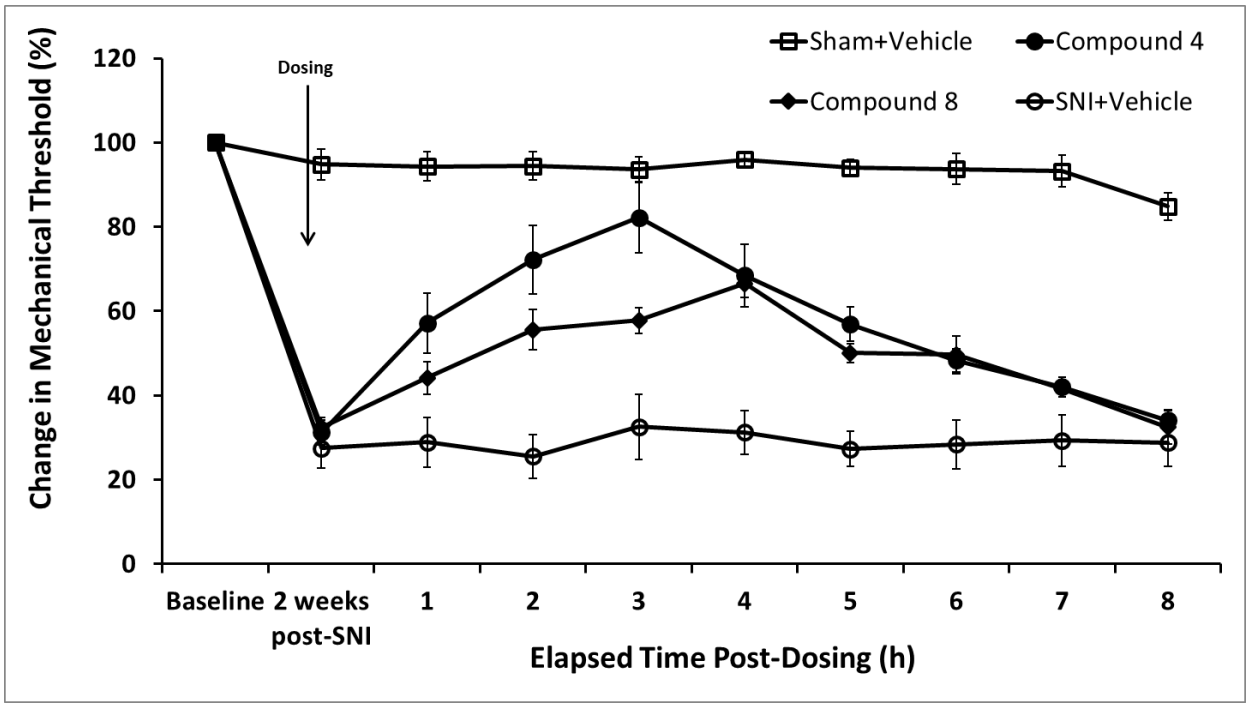

Figure S2. Mechanical pain threshold assessment (von Frey monofilament test) of SNI rats' left hind paws (number of rats: n = 6 - 8).

Biological Experimental Section.

Bio-evaluation methods

Inhibition of T-channel in DRG neurons. Mouse dorsal root ganglion (DRG) neurons were prepared from 1 – 2 months old C57/BC6 mice. All the procedures related to animal handling were conducted at AfaSci Research Laboratory and were in strict accordance with NIH guidelines and IACUC approved protocols. The spine was removed and split into two halves from the middle line after sacrificing the mice by decapitation. Lumbar DRG neurons were collected into a modified Krebs solution (130 mM NaCl, 10 mM HEPES-Na, 5 mM KCl, 1 mM $CaCl_2$, 10 mM glucose, 2 mM $MgCl_2$, pH adjusted to 7.35 with 1 N HCl) in a 1.5 mL-tube. The DRG neurons were removed for digestion into 0.5 mL of Hank's balanced salt solution (HBSS) with 1 mg/mL Collagenase and 0.5 mg/mL Trypsin added. The DRG neurons were minced with fine scissors and incubated at 35°C for 50 min. After removing the HBSS solution, the DRG neurons were dispersed into modified Krebs solution and triturated with fire polished glass pipettes until no clumps were visible. The cells were then dispersed onto poly-L-ornithine-coated cover slips and maintained in a modified Krebs solution and streptomycin sulfate (0.2 mM), Penicillin G Sodium (0.3 mM), and Gentamycin (0.1 mM) at 21°C.

Preparation of HEK293 cells expressing $Ca_{v3.2}$ channels. $Ca_{v3.2}$ channels were expressed in human embryonic kidney (HEK)-293 cells using a tetracycline inducible expression system (Invitrogen). Cells were placed in 25-cm^2 tissue culture flasks at 37°C, 5% CO_2, and 100% relative humidity in D-MEM/F12 (Dulbecco's Modified Eagle Medium/Nutrient Mixture F-12; Gibco) supplemented with fetal bovine serum (FBS, 10% v/v/), sodium pyruvate (0.5 mM, Gibco), penicillin-streptomycin (100 U/mL, 100 μg/mL) and Geneticin^R Selective antibiotic (G418; 0.5 mg/mL). Cells were detached from the flask base using a non-enzymatic cell dissociation solution (Cellstripper, Corning), removed, and reseeded onto poly-D-lysine coated glass coverslips in 35-mm dishes. Cells in dishes were further supplemented with G418 at a final concentration of 1 mg/mL and after 24 hours, expression of $Ca_{v3.2}$ was induced with 1 □g/mL tetracycline. The medium for the HEK-293 was composed of D-MEM/F-12 and 15 mM HEPES buffer, with L-glutamine and pyridoxine hydrochloride. It was supplemented with FBS, P/S (penicillin/streptomycin) (Gibco, #15140-122), and sodium pyruvate 100 mM.

Patch clamp recordings. Whole-cell voltage clamp recordings were performed on mouse DRG neurons within 2 days after acutely dissociation or cultured HEK293 cells expressing T-type channels (encoded by $Ca_{v3.2}$ channels). All experiments were performed at ~21°C and whole-cell currents were recorded using a MultiClamp 700B amplifier and analyzed off-line with Pclamp10.4 software (Molecular Devices, LLC, Sunnyvale, CA, USA). To record calcium currents in DRG and HEK293 cells, the external solution was composed (in mM) of 115 choline-Cl, 30 TEA-Cl, 2 $CaCl_2$, 10 glucose and 10 HEPES (pH 7.3 – 7.4 adjusted with TEA-OH; osmolality verified as 295 mOsm/kg). The internal solution was composed (in mM) of 125 CsCl, 10 HEPES (acid), 10 EGTA (ethylene glycol tetraacetic acid), 1 $CaCl_2$, 1 $MgCl_2$, 4 MgATP, and 0.3 MgGTP (pH 7.3 – 7.4 adjusted with CsOH; osmolality verified as 295 mOsm/kg). Since sodium ions were absent in the external solution, tetrodotoxin was not needed. Calcium currents were recorded at a holding potential of -100 mV and then depolarized to -30 mV for 100 ms to activate $Ca_{v3.2}$ expressed in HEK cells. An interpulse interval of 10 seconds allowed the channel recovery from inactivation and achieved stable current recordings. All reagents were purchased from Sigma unless specified otherwise. Test compounds were usually applied via a rapid-solution-exchange system with 8 fine polyplastic tubings (100 mm OD) glued in a holder in parallel and located closely to the recorded cells. The current responses were normalized to the control, percent inhibition was

calculated, and sigmoidal dose-response curves were generated using XLFit (IDBS, Surrey, UK) or Prism (GraphPad Software, La Jolla, CA, US) for calculation.

Analgesic effect using Complete Freund adjuvant (CFA)-inflammatory pain mouse model. The reported protocol[4] of Complete Freund adjuvant (CFA)-inflammatory pain in mice was followed for the study of inhibition of pains. Tested molecules and a reference, gabapentin (100 mg/kg, I.P.), was individually administered to mice (n = 6 - 8) that had CFA-induced inflammatory on their left hind paws. The maximum inhibition was rated at ++++, strong inhibition at +++, medium at ++, and weak at +, comparing with gabapentin.

Inhibition of seizure in pentylenetetrazol (PTZ)-induced fatality in mice. It has been reported that antiepileptics, such as carbamazepine, lamotrigine and gabapentin, are used for the treatment of neuropathic pain.[1] Overactivation of T-channel involves the generation of seizure activity.[1] Following the reported protocol[2] in the pentylenetetrazol (PTZ)-induced seizure model in mice (n = 6 per drug) was used to evaluate the inhibition of pains. Prolonged latencies to seizure and decrease of fatality rate were studied comparing to vehicle (2% DMSO in 0.5% HPC). Fatality latency and rate – the percentage (%) of mice in each treatment group that died within a 20-minutes cutoff of the observational period, were recorded and calculated. Average fatality latency and rate of each treatment group were used to evaluate the molecule's ability to either prevent or delay the onset of PTZ-induced seizures and death.

***In vivo* analgesic effects in spared nerve injury (SNI) pain models**. To evaluate the therapeutic effects and safety of highly active compounds, the spared nerve injury (SNI) model, one of the reliable neuropathic pain models in mice or rats,[3] was used to assess the effects of compounds **4** and **8**. Baseline thermal and mechanical thresholds of male rats (Sprague-Dawley rats, 275 – 325 g, Harlan) were taken prior to surgery. Baseline thresholds were measured on the rats' left hind paws. Drug-tested rats (n = 6 - 8 per drug) and without-drug-treated rats underwent the SNI surgery on their left hind leg. A group of rats (n = 6 – 8/group) underwent surgery without injury of the nerves as a sham group. Two weeks post-surgery, the thermal thresholds of each rat were reassessed. The SNI rats displayed approximate 55% reduction in thermal pain thresholds and 75 – 80% reduction in mechanical pain thresholds, confirming the presence of hyperalgesia and mechanical allodynia in the SNI rats. Each rat received either compounds **4**, **8** (each 30 mg/kg, 1 mL I.P.) or vehicle (2% DMSO in 0.5% HPC). Thermal and mechanical thresholds were measured at 1, 2, 3, 4, 5, 6, 7, and 8 hours post-treatment/dosing. The tested compounds were shown to elevate both thermal and mechanical thresholds compared to vehicle.

References.

1. Perez-Reyes, E. *Mol. Pharm.* **2010**, *77*, 136. https://doi: 10.1124/mol.109.062133
2. Xie, X.; Lancaster, B.; Peakman, T.; Garthwaite, J. *Pflugers Archiv.: Eur. J. Phys*. **1995**, *430*, 437. https://doi:10.1007/BF00373920
3. Decosterd, I.; Woolf, C. J. *Pain* **2000**, *87*, 149. https://doi.org/10.1016/S0304-3959(00)00276-1

4. Choi, S.; Na, H.; Kim, J.; Lee, J.; Lee, S.; Kim, D.; Park, J.; Chen, C. C.; Campbell, K.; Shin, H. S. *Genes Brain Behav.* **2007**, *6*, 425. https://doi.org/10.1111/j.1601-183X.2006.00268.x

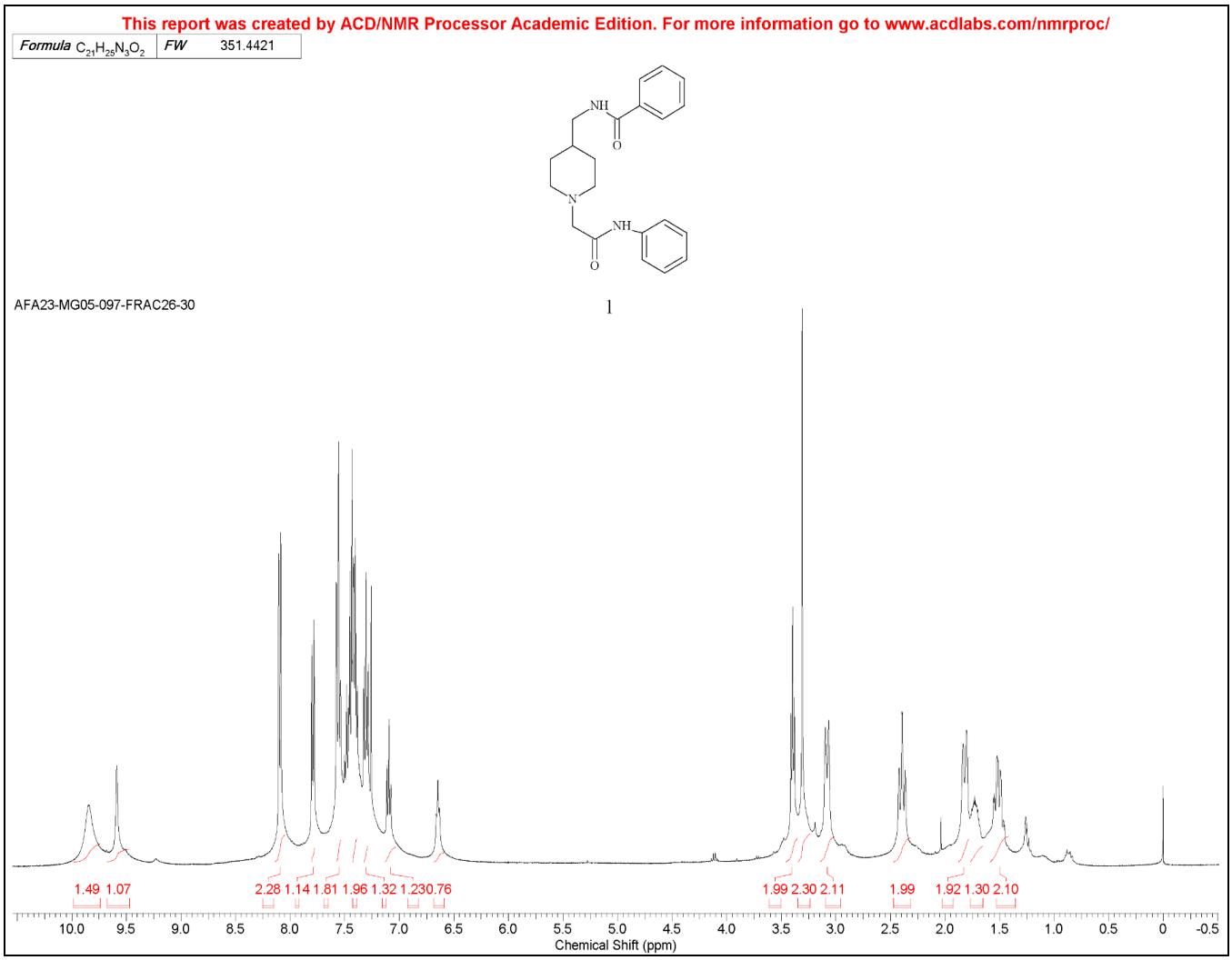

Figure S3. ^{1}H NMR spectrum of compound **1**.

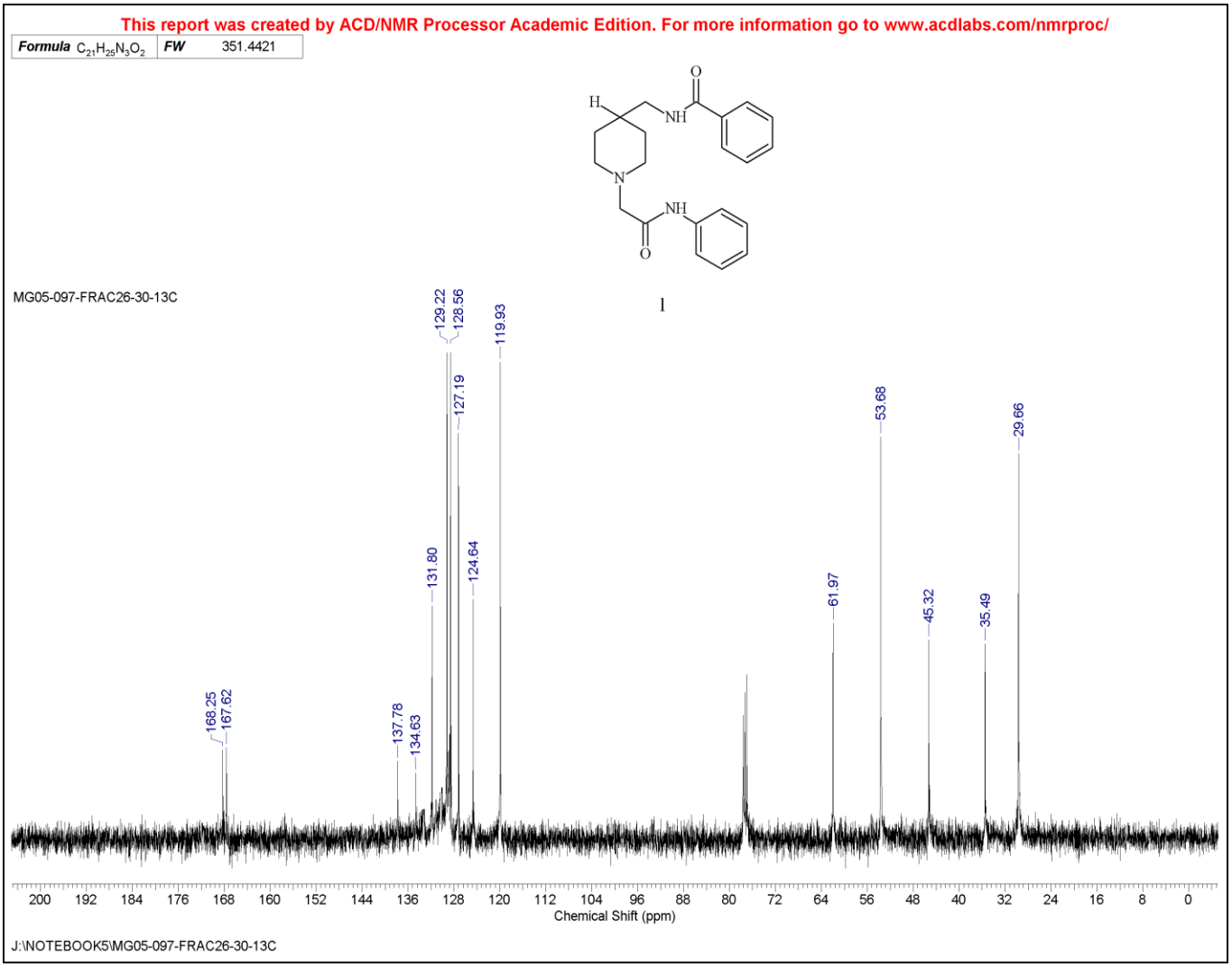

Figure S4. ^{13}C NMR spectrum of compound **1**.

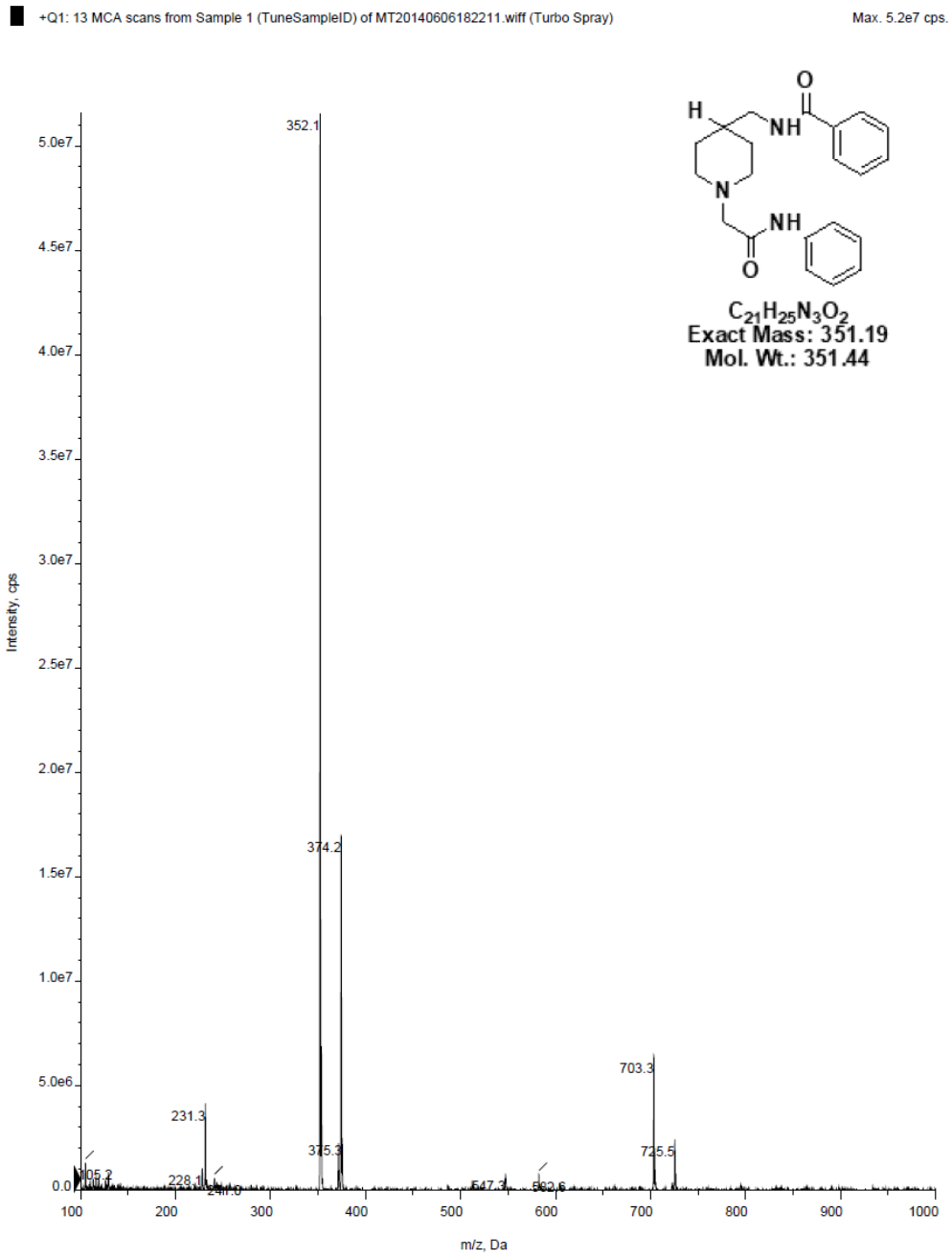

Figure S5. MS spectrum of compound **1**.

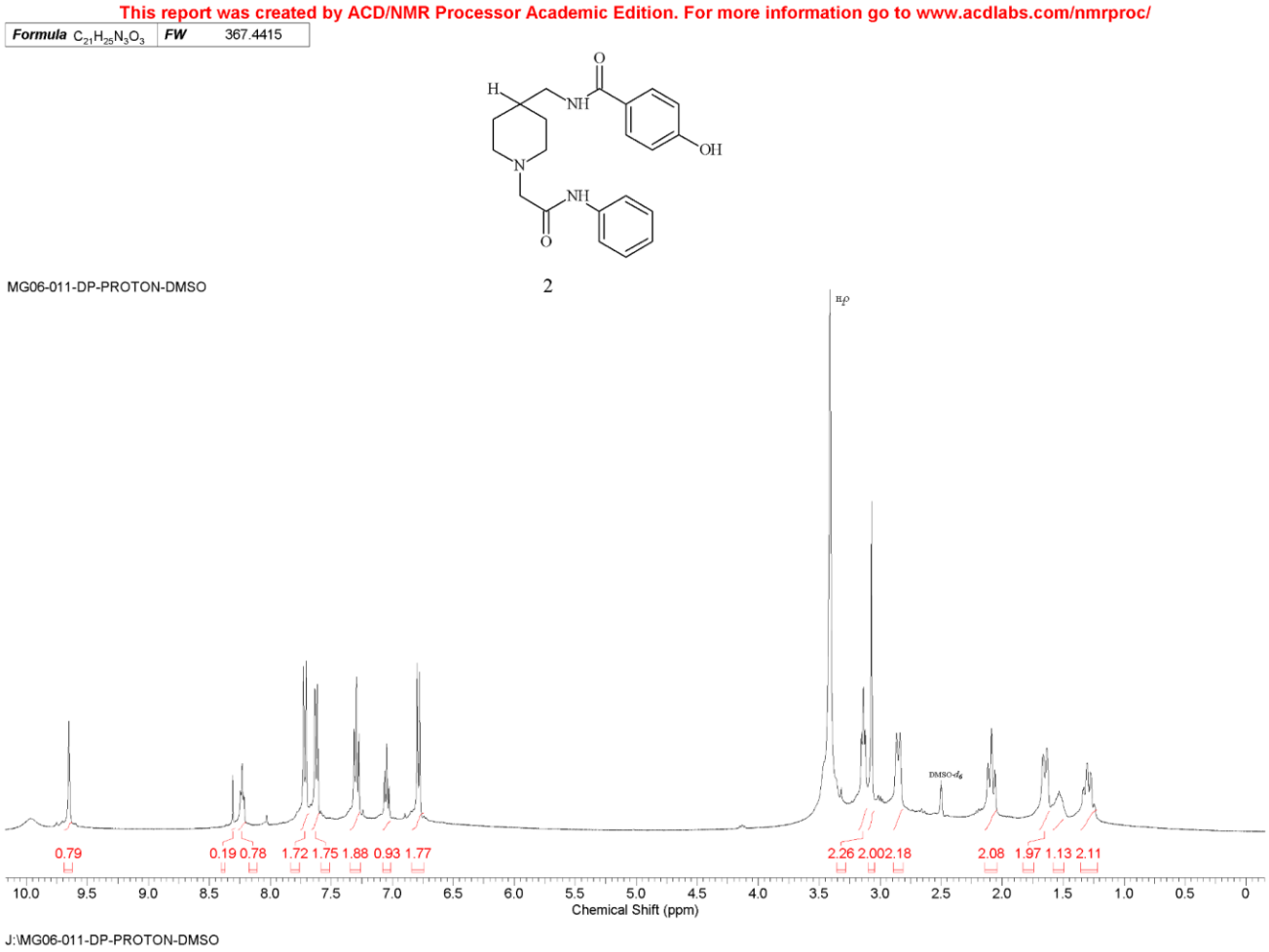

Figure S6. ^{1}H NMR spectrum of compound **2**.

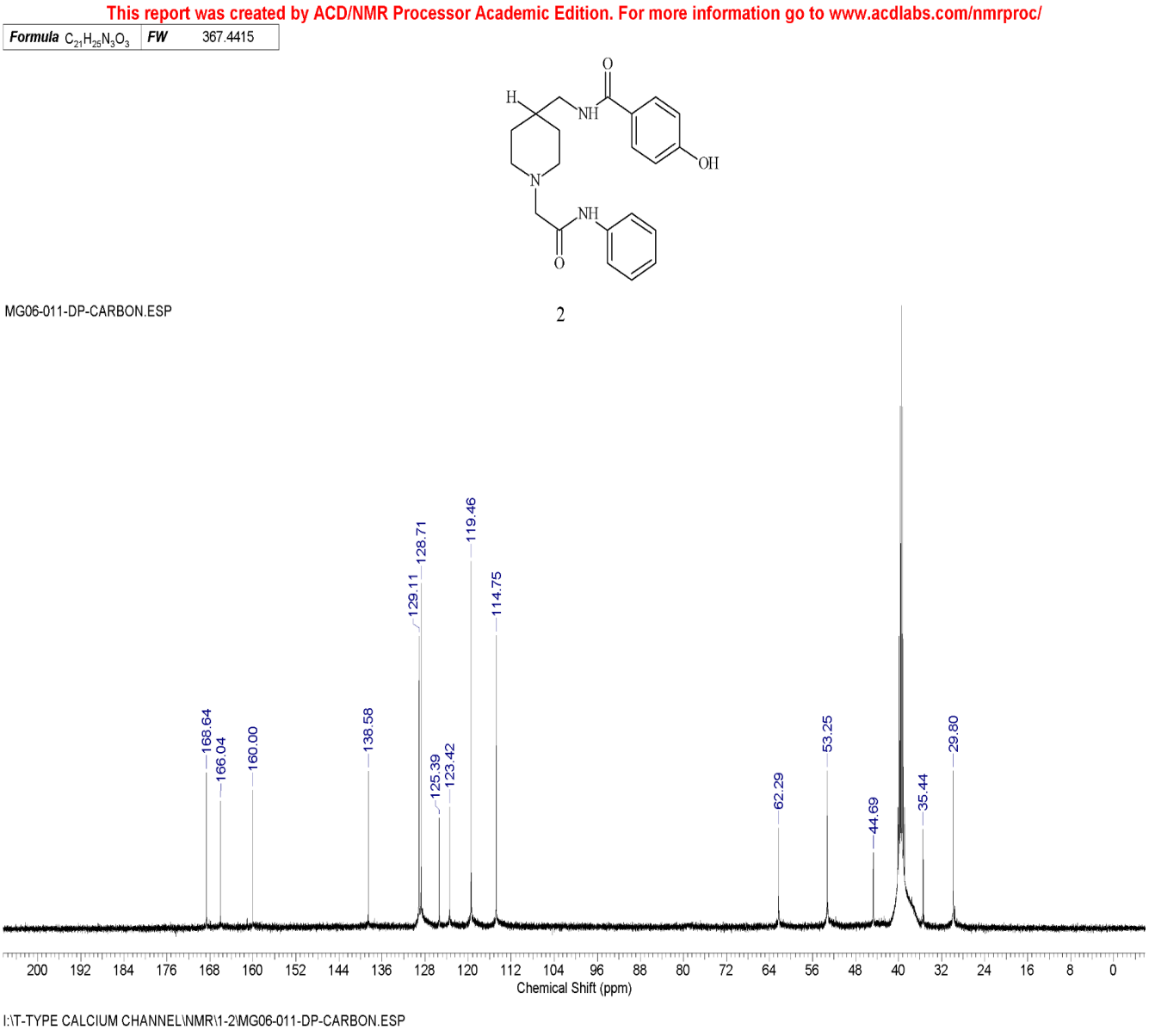

Figure S7. ^{13}C NMR spectrum of compound **2**.

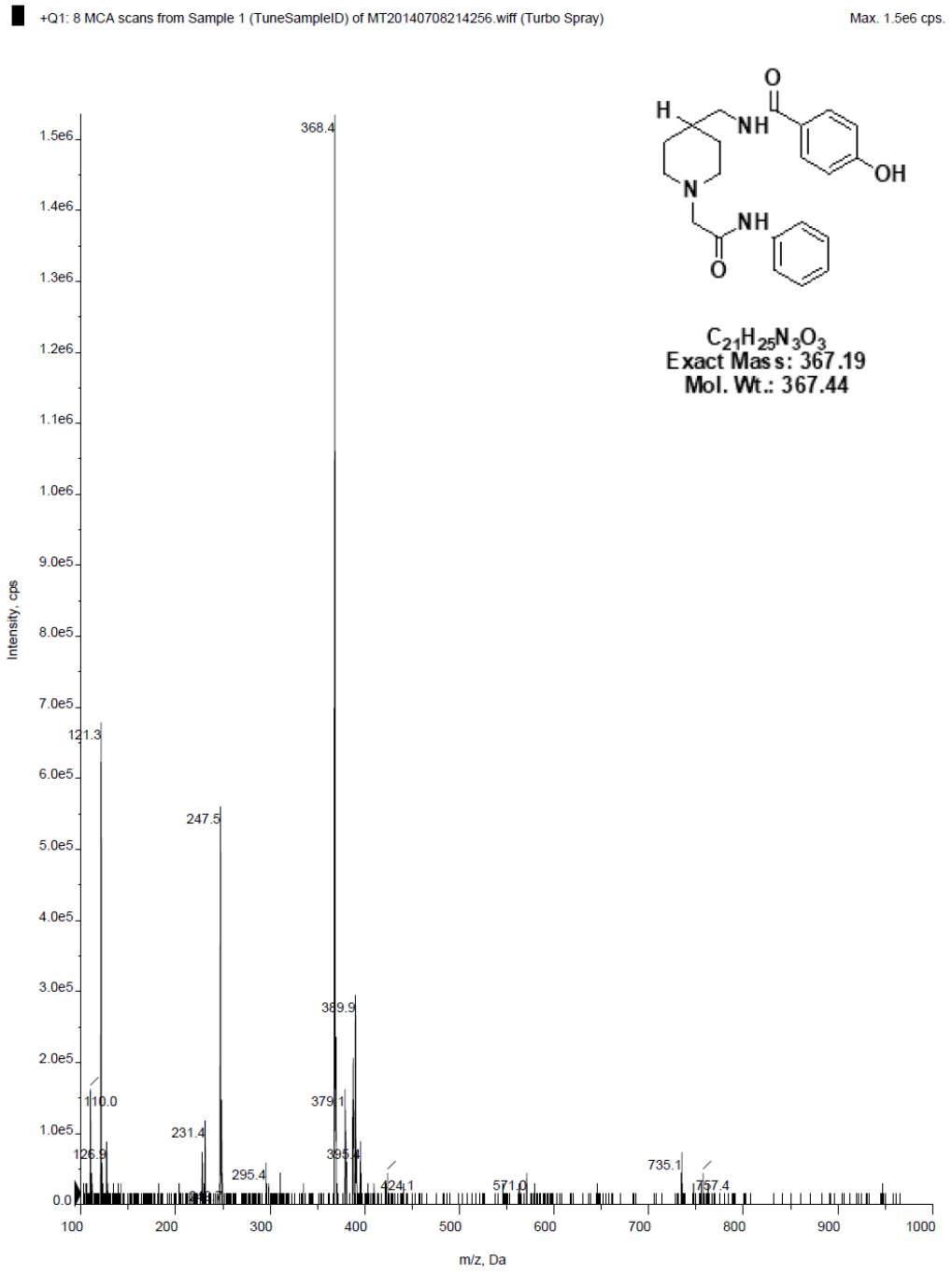

Figure S8. MS spectrum of compound **2**.

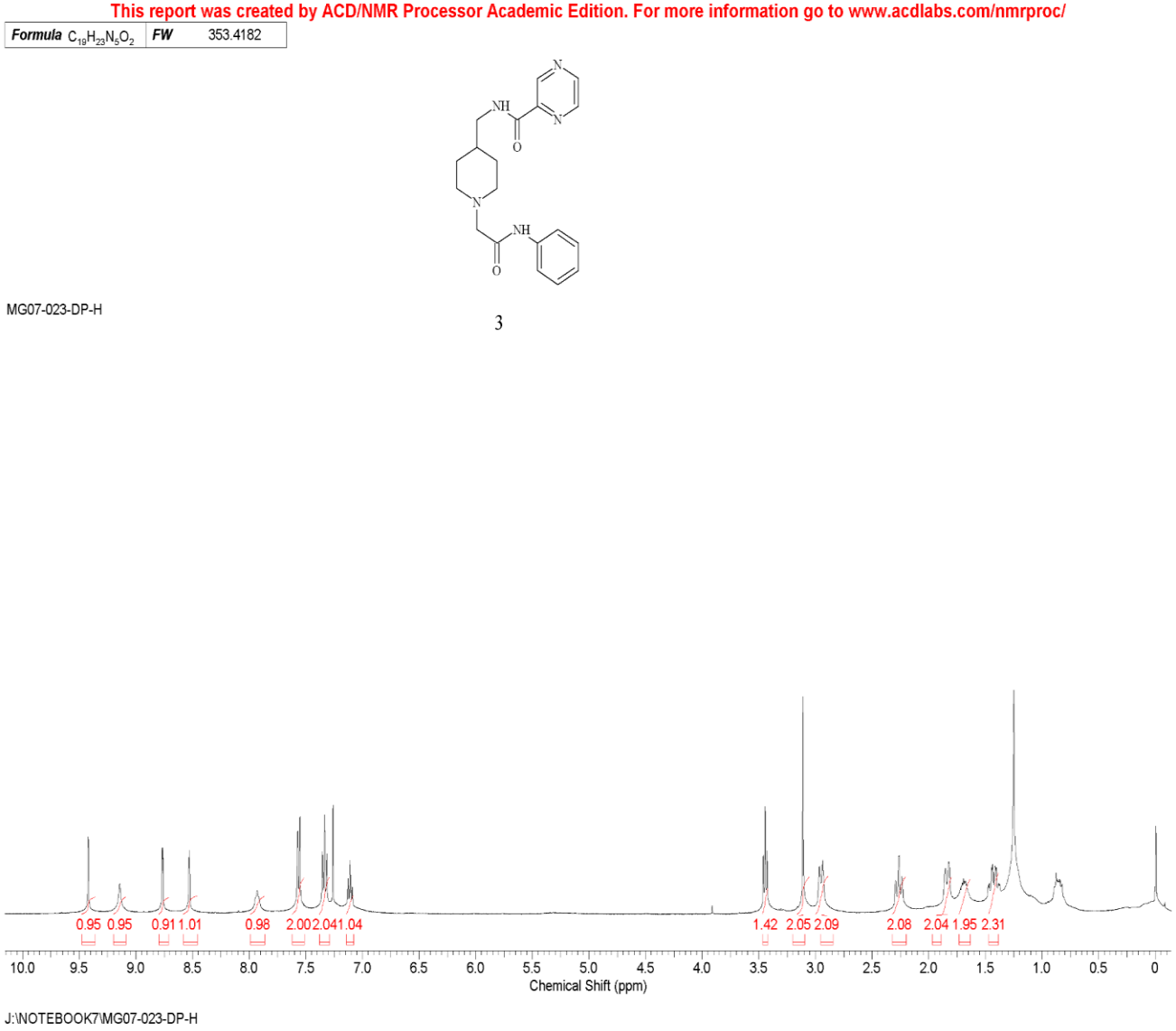

Figure S9. ^{1}H NMR spectrum of compound **3**.

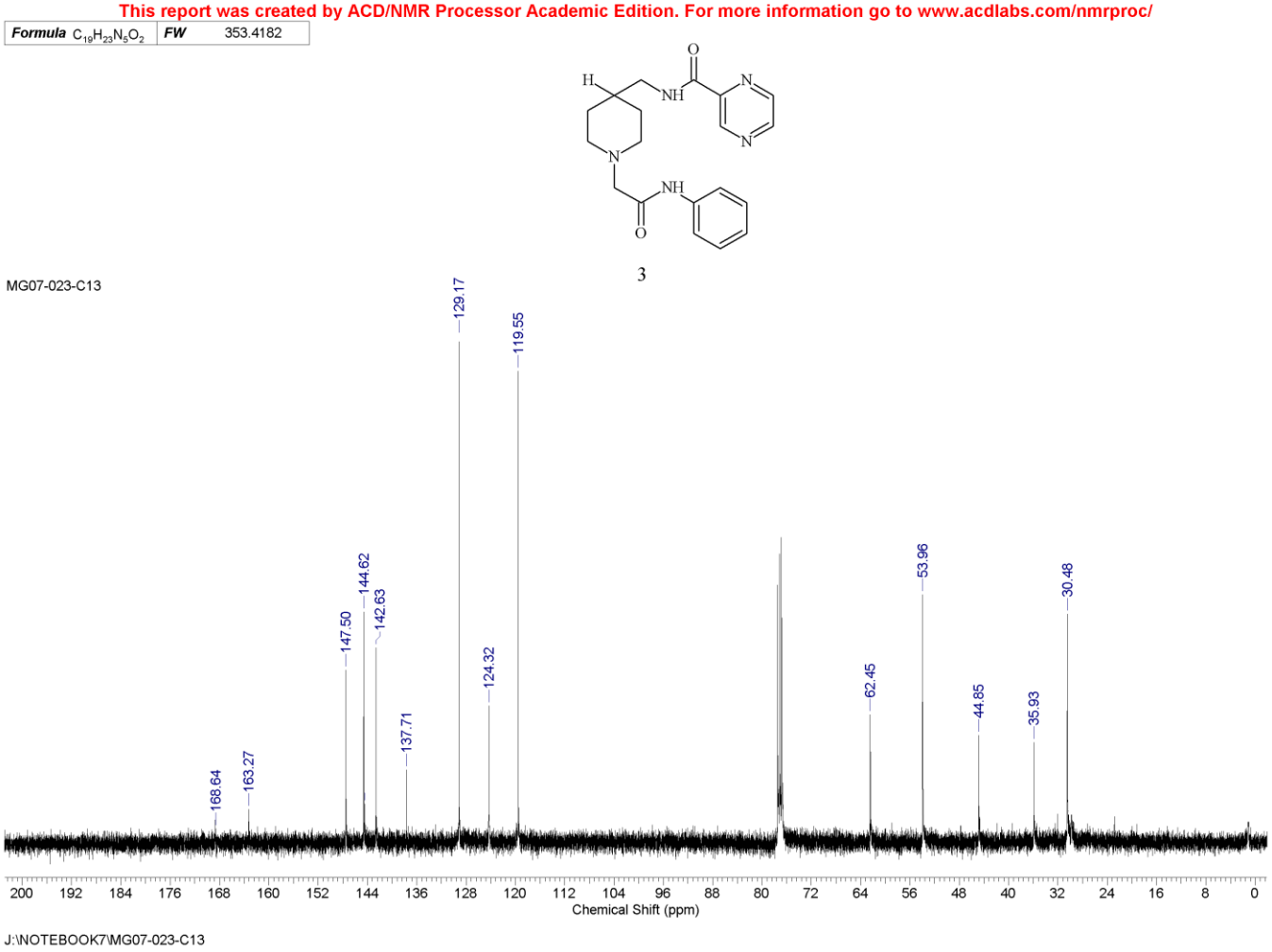

Figure S10. ^{13}C NMR spectrum of compound **3**.

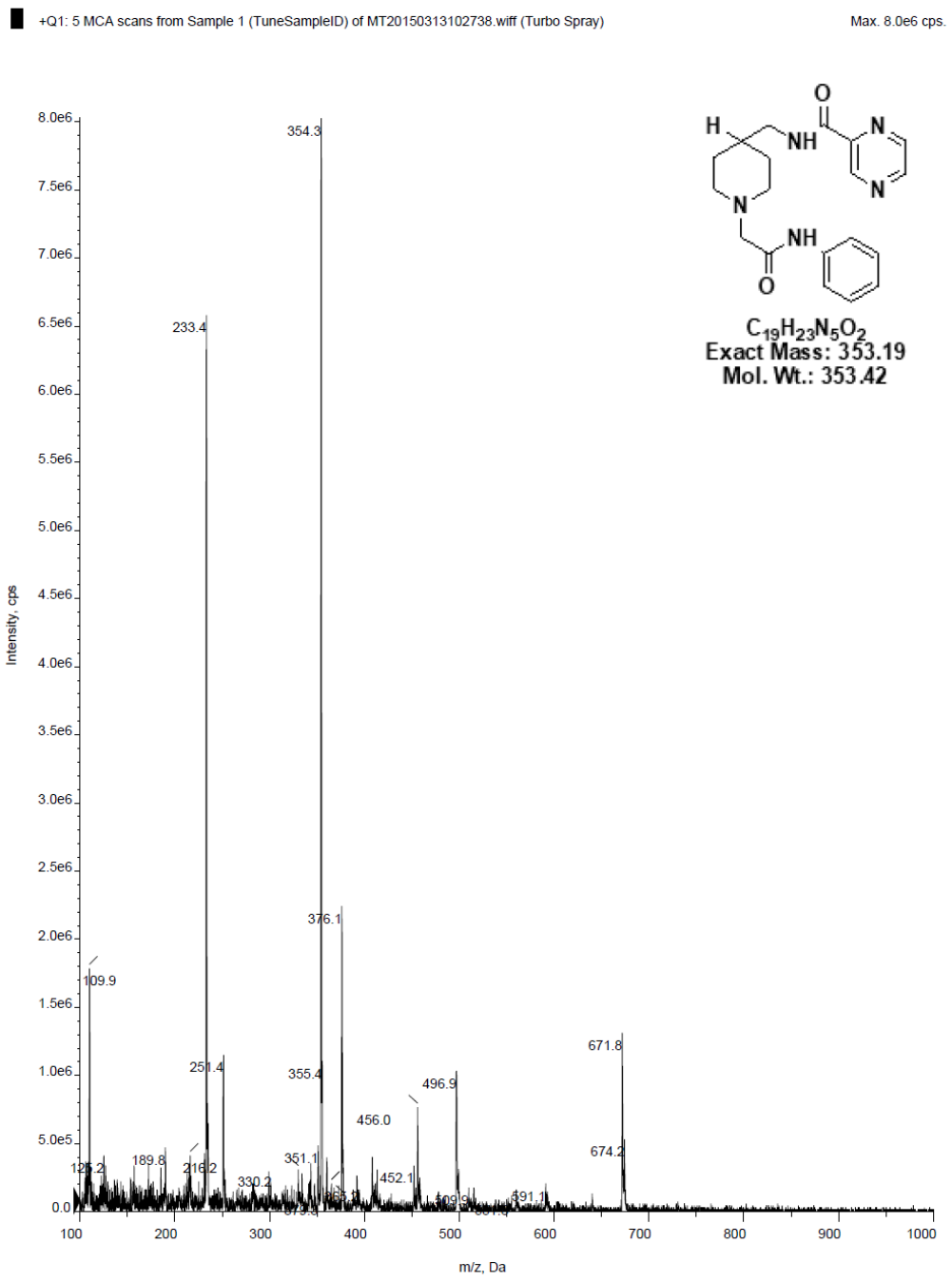

Figure S11. MS spectrum of compound **3**.

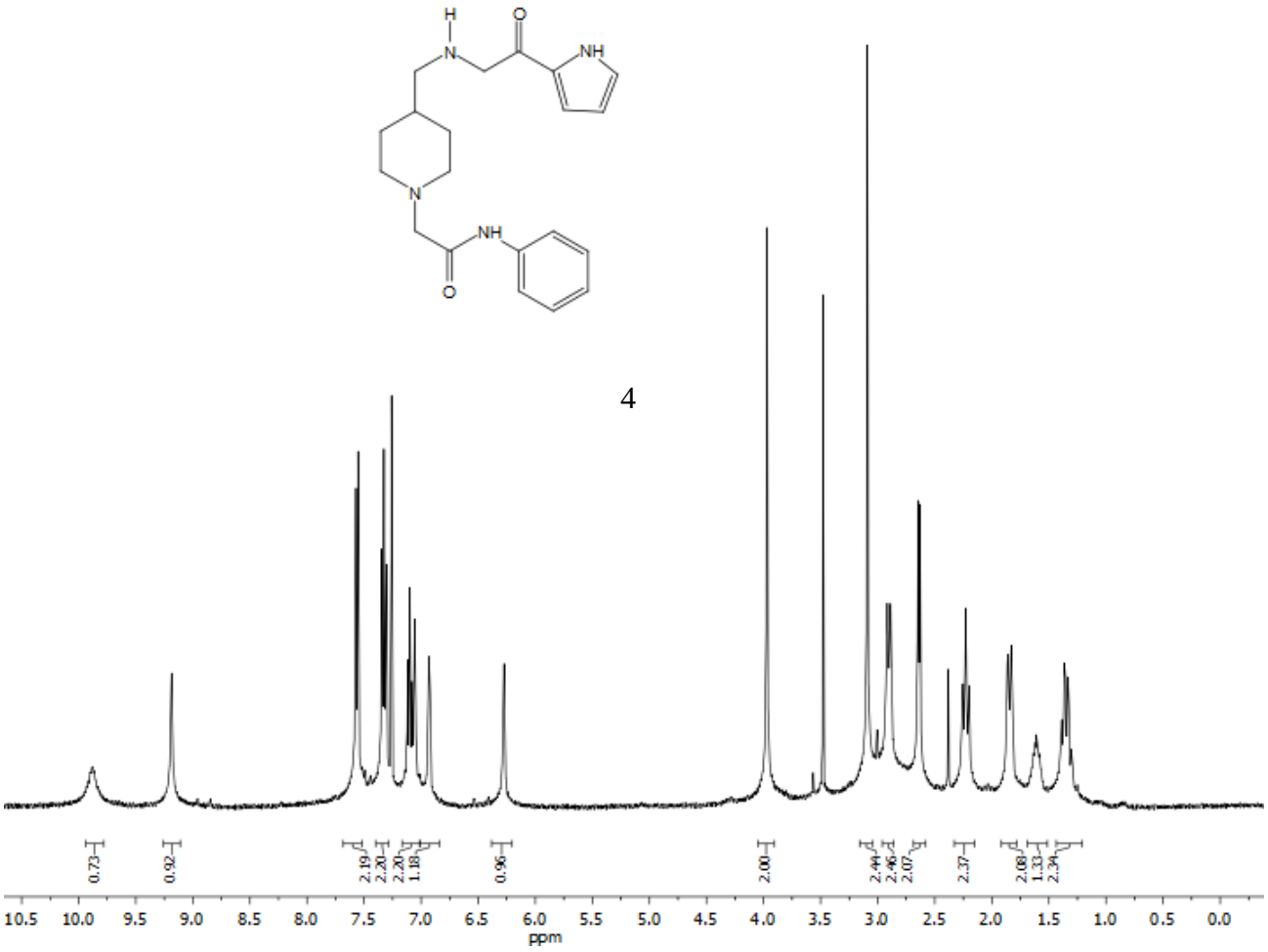

Figure S12. ^{1}H NMR spectrum of compound **4**.

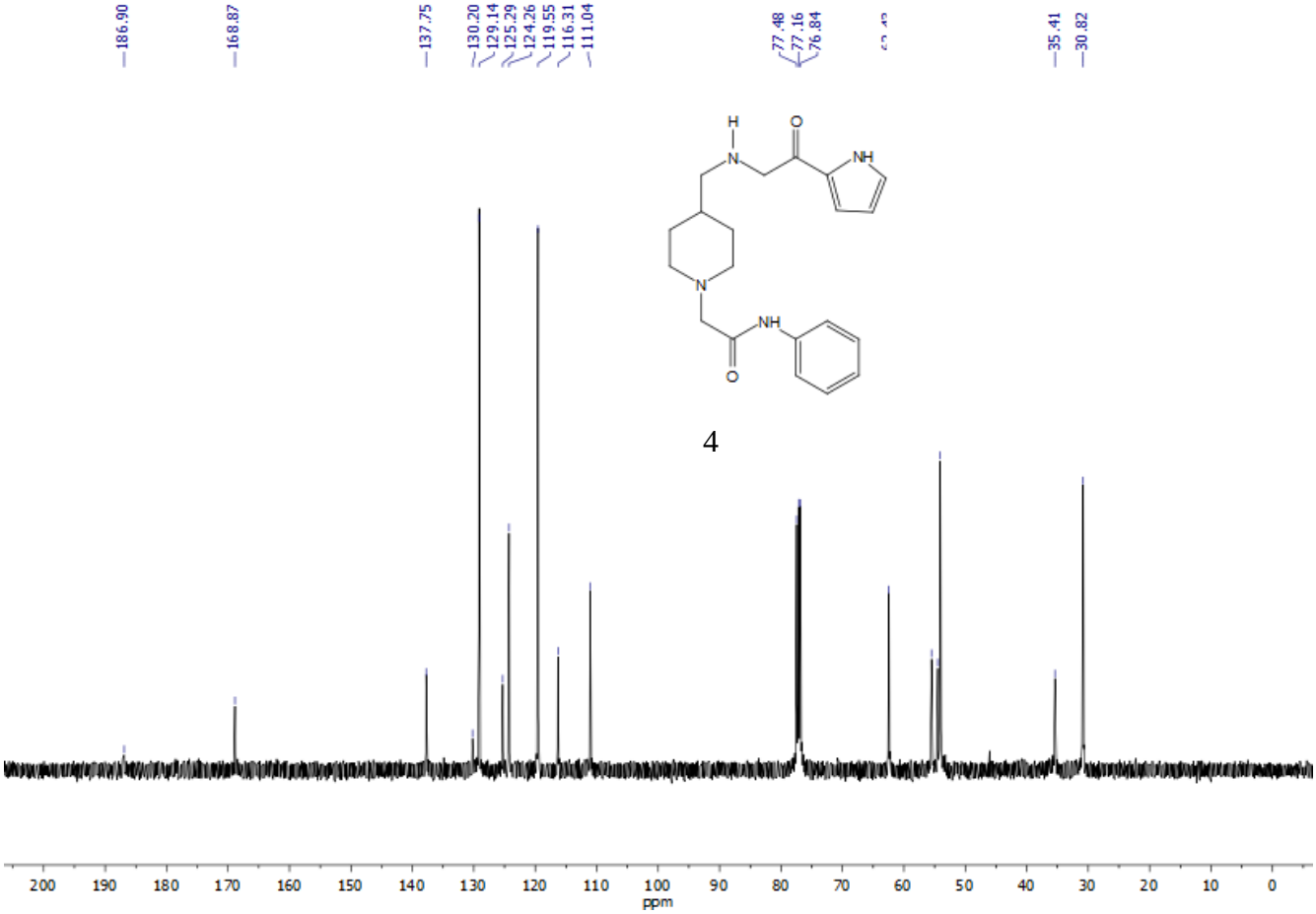

Figure S13. ^{13}C NMR spectrum of compound **4**.

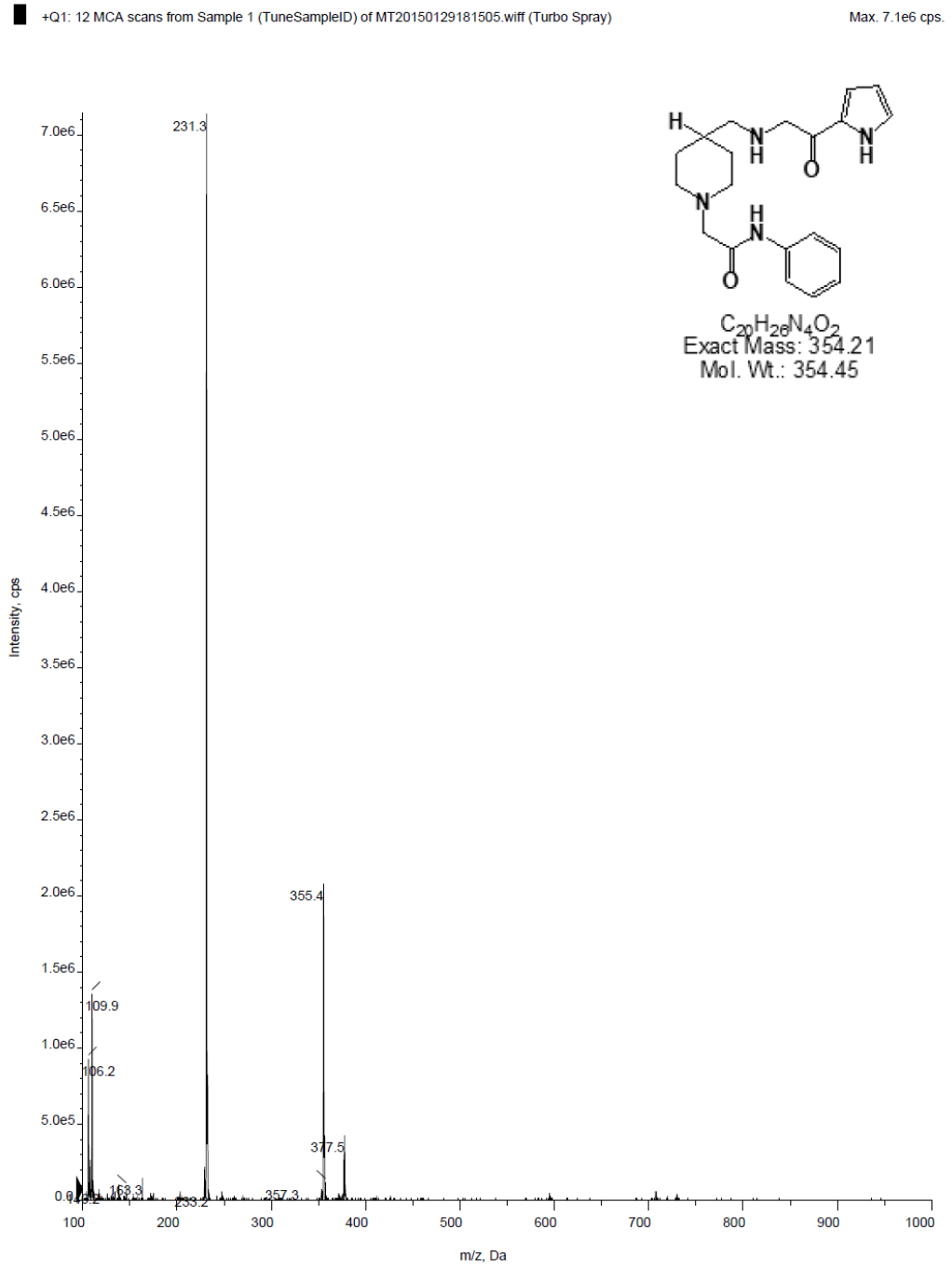

Figure S14. MS spectrum of compound **4**.

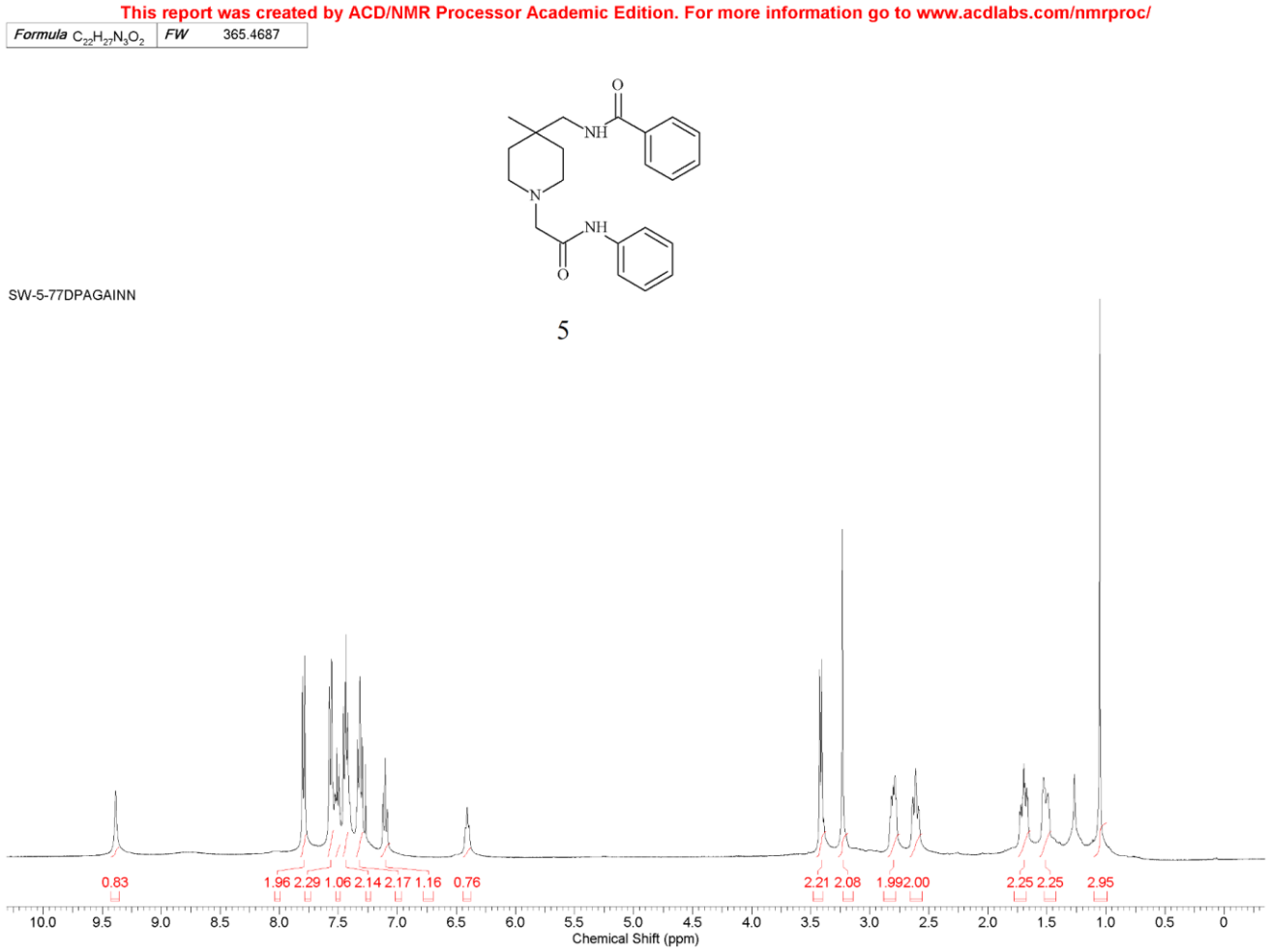

Figure S15. ^{1}H NMR spectrum of compound **5**.

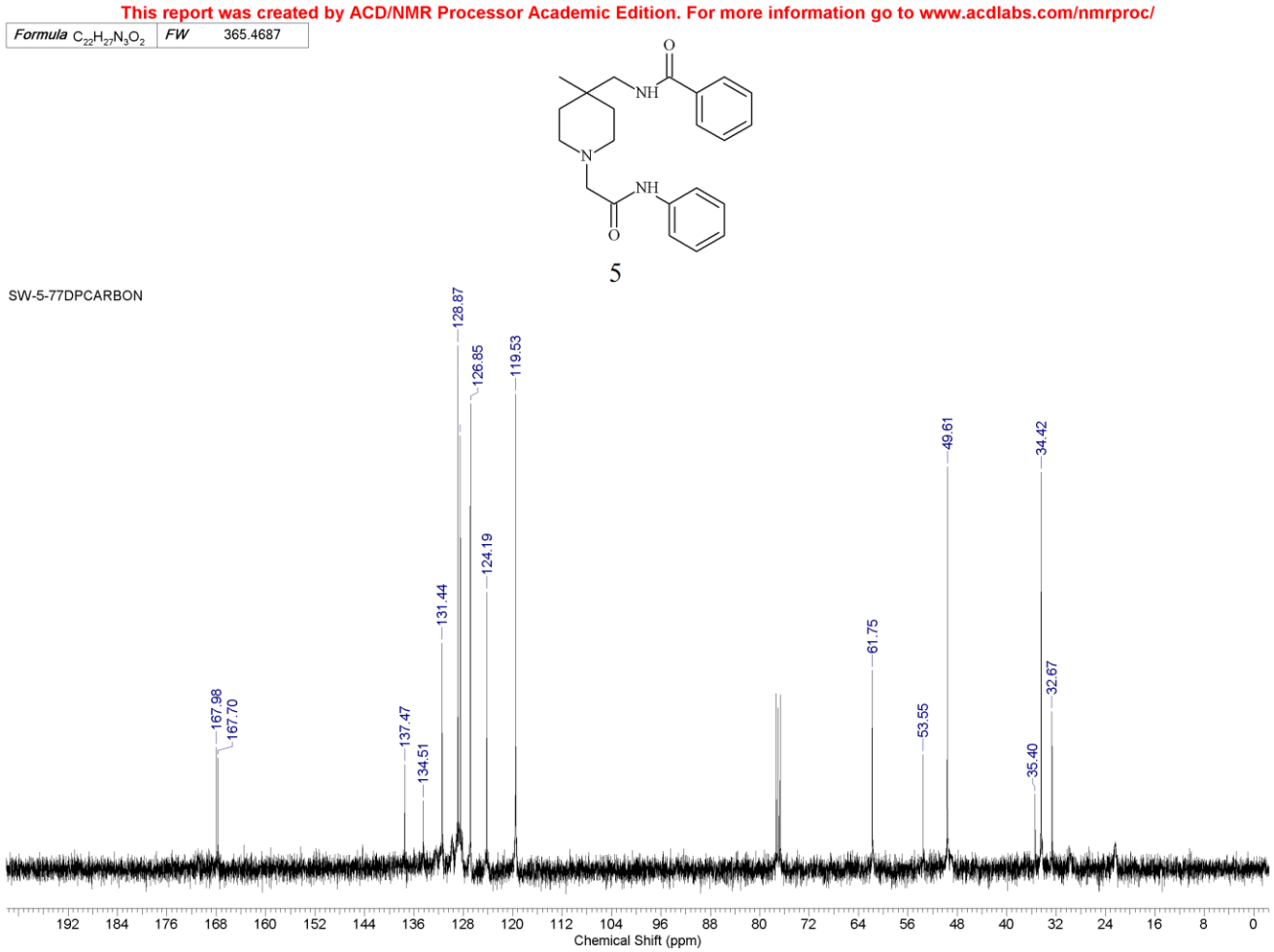

Figure S16. ^{13}C NMR spectrum of compound **5**.

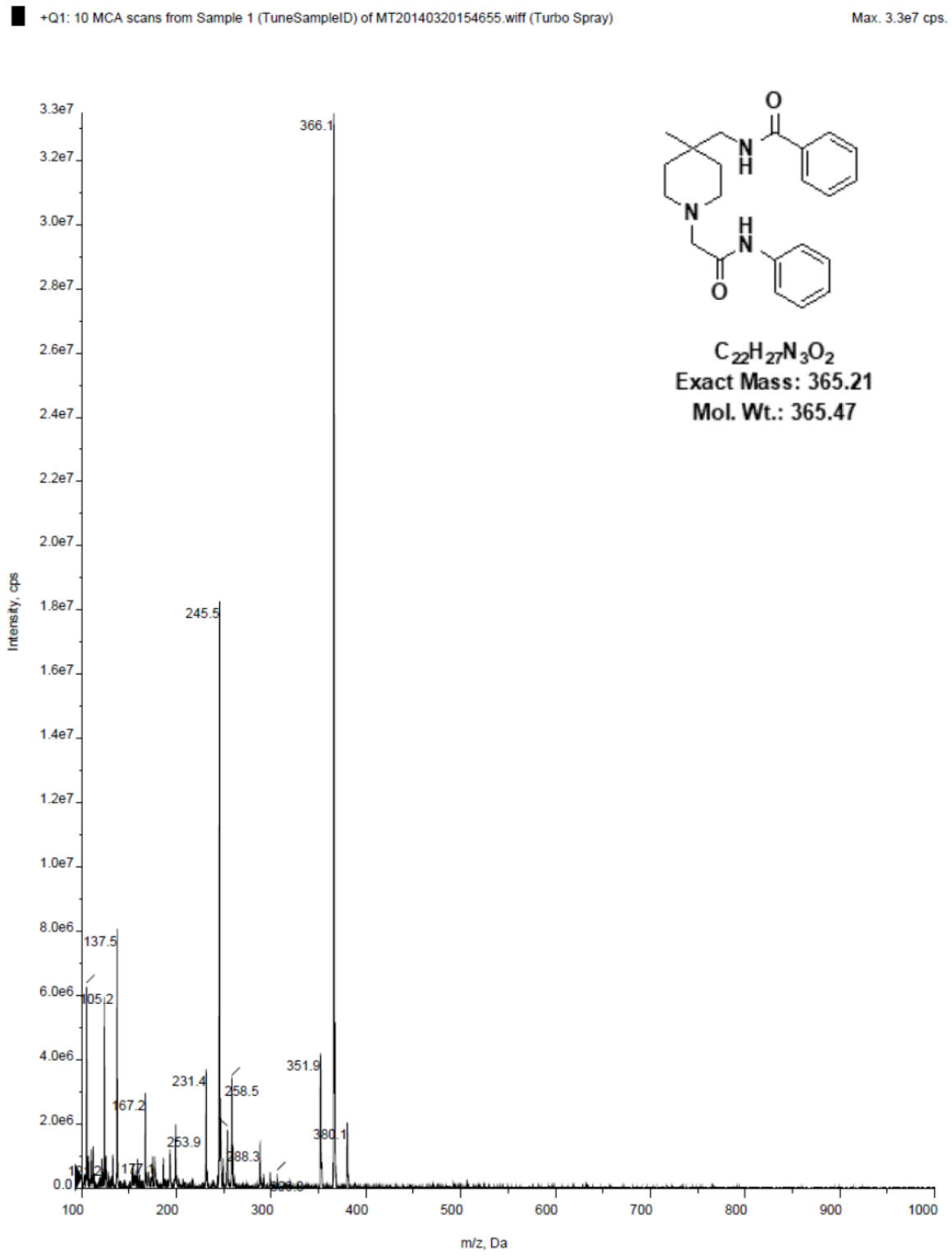

Figure S17. MS spectrum of compound **5**.

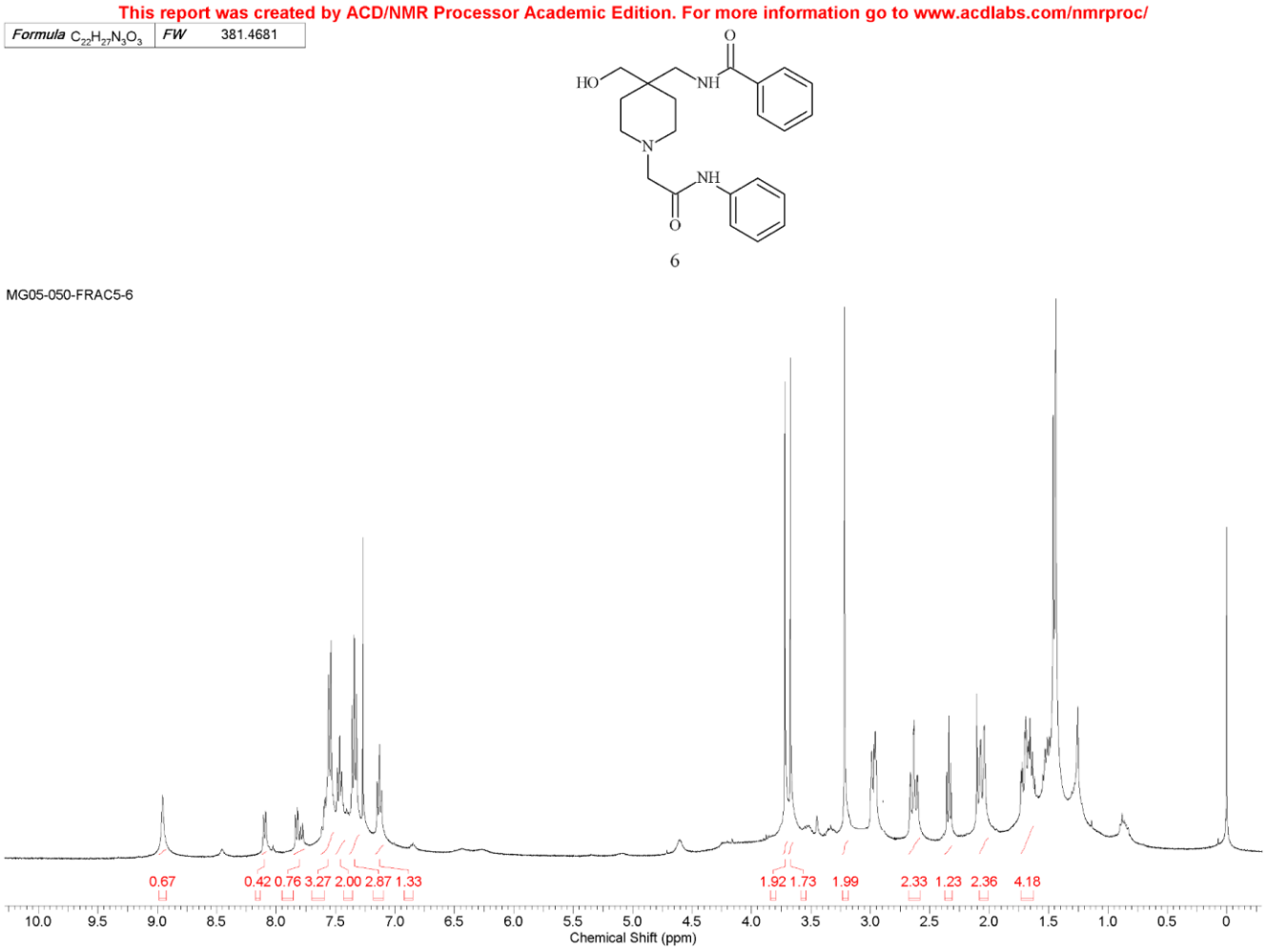

Figure S18. ^{1}H NMR spectrum of compound **6**.

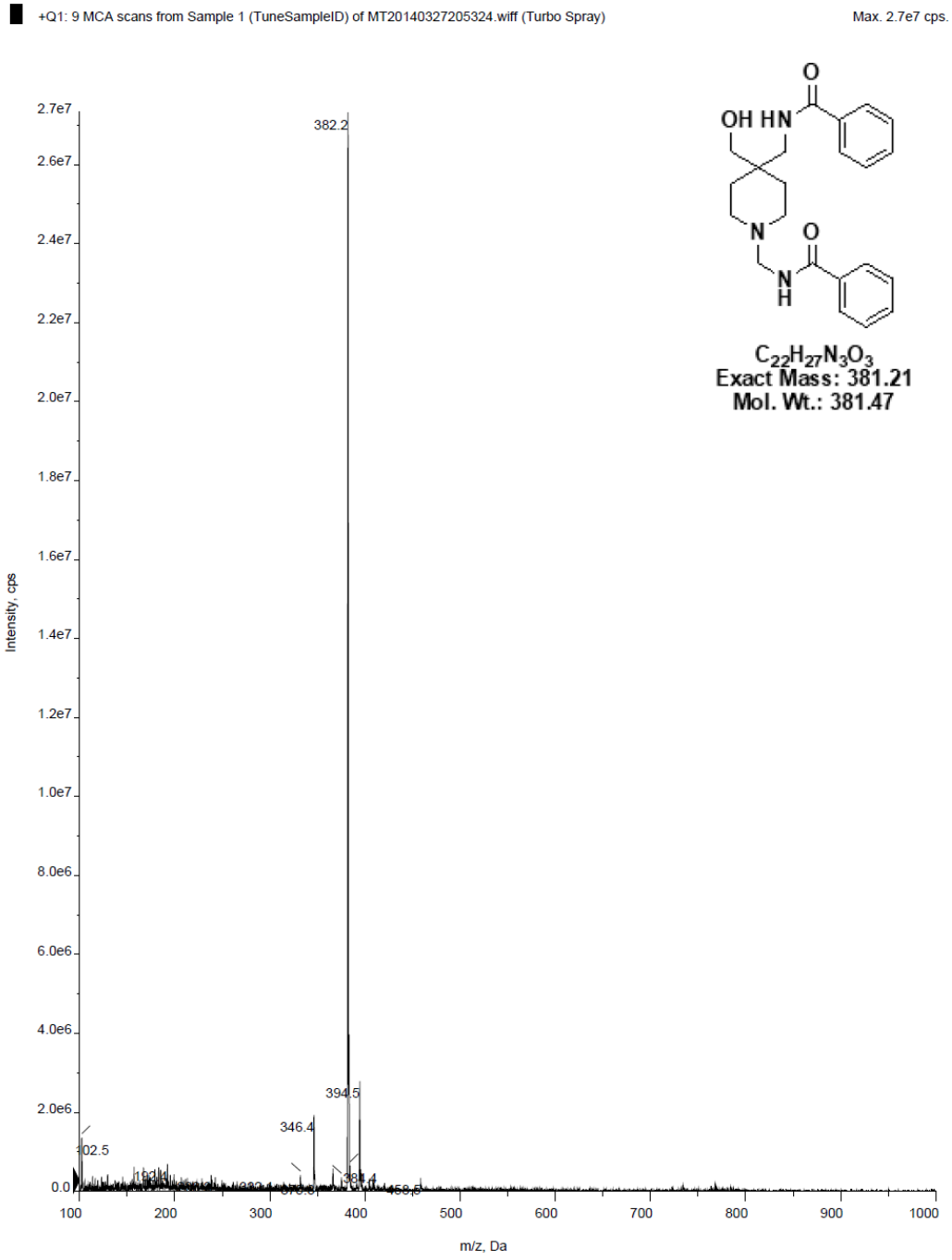

Figure S19. MS spectrum of compound **6**.

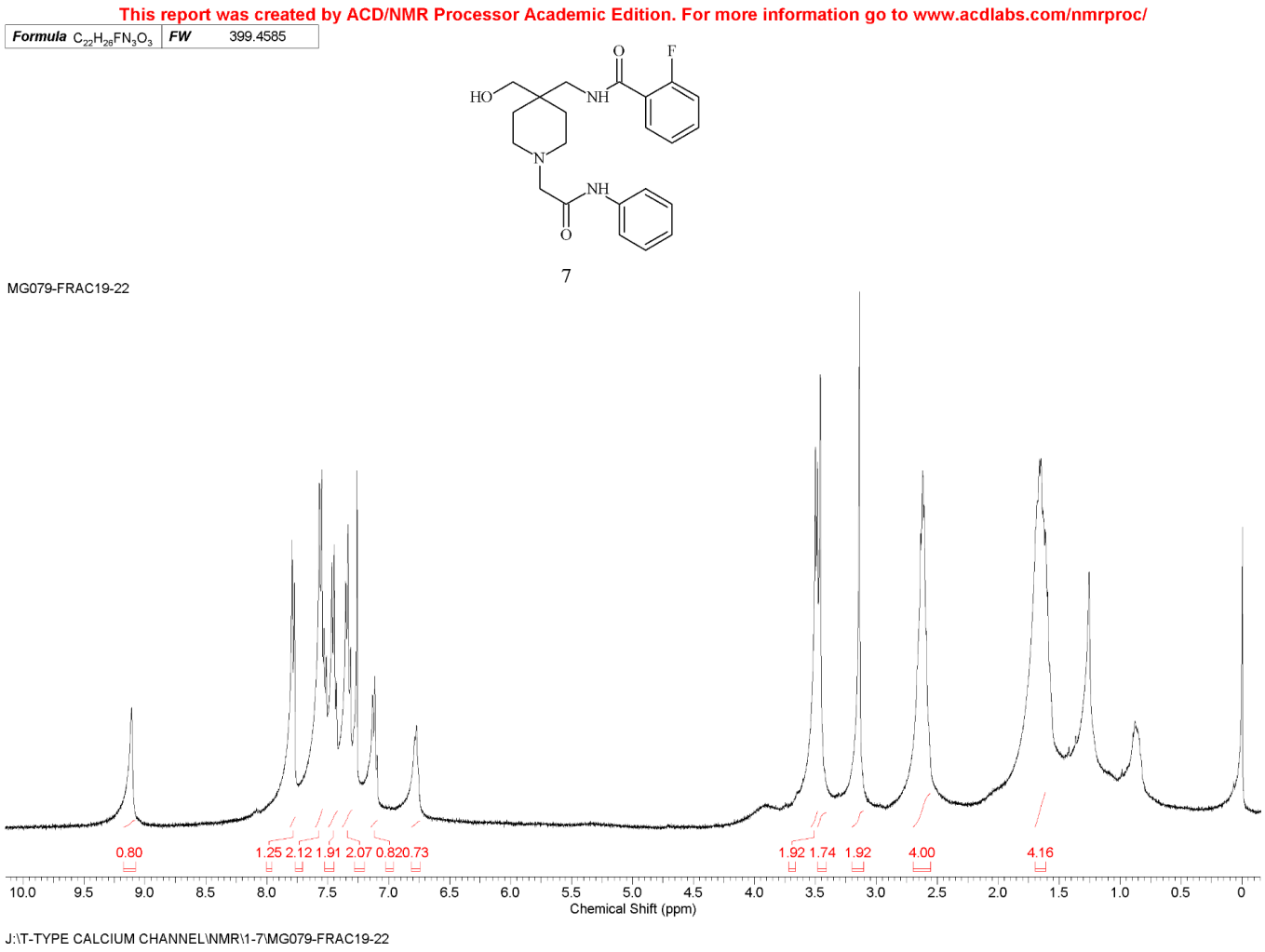

Figure S20. ^{1}H NMR spectrum of compound **7**.

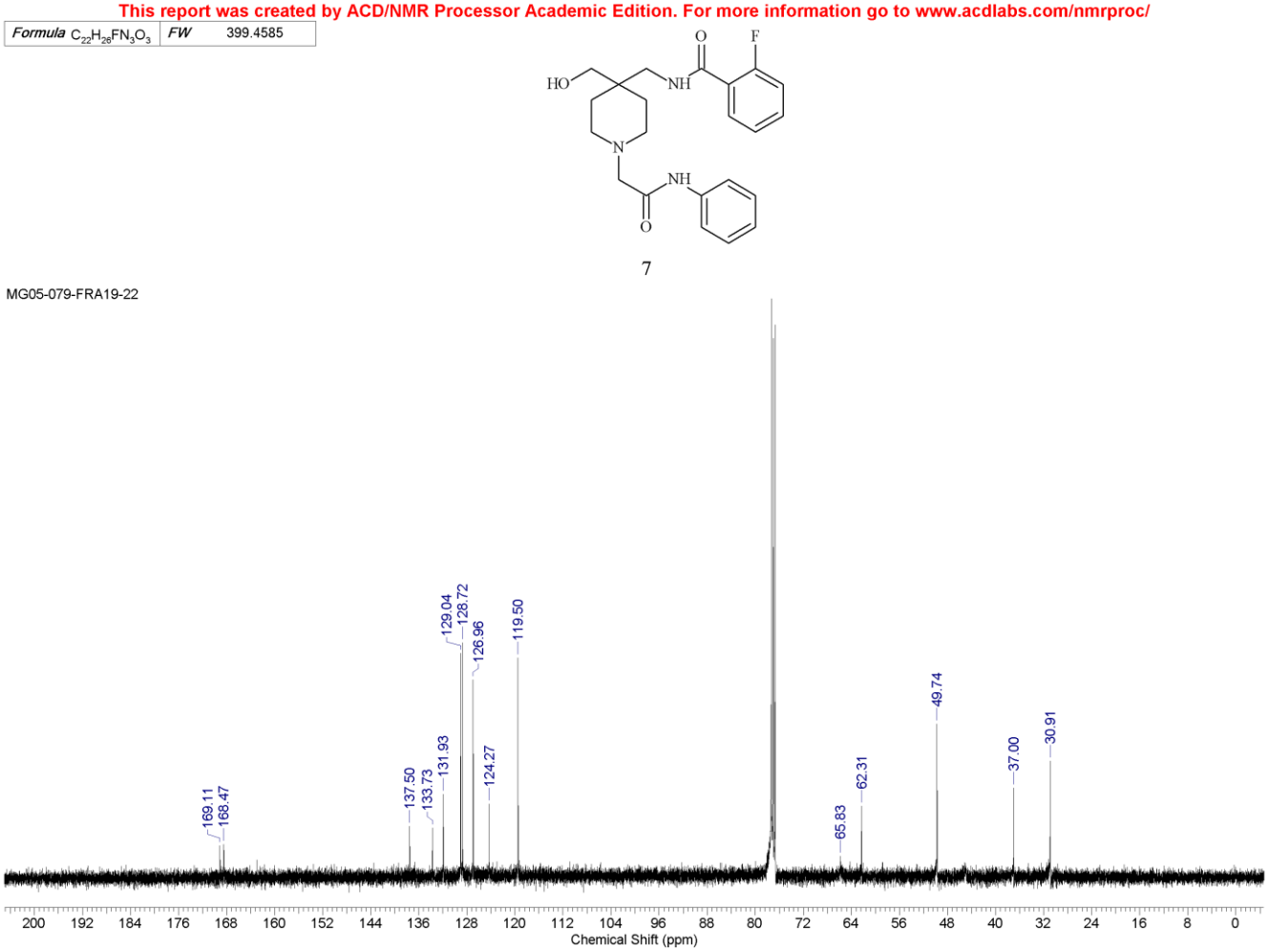

Figure S21. ^{13}C NMR spectrum of compound **7**.

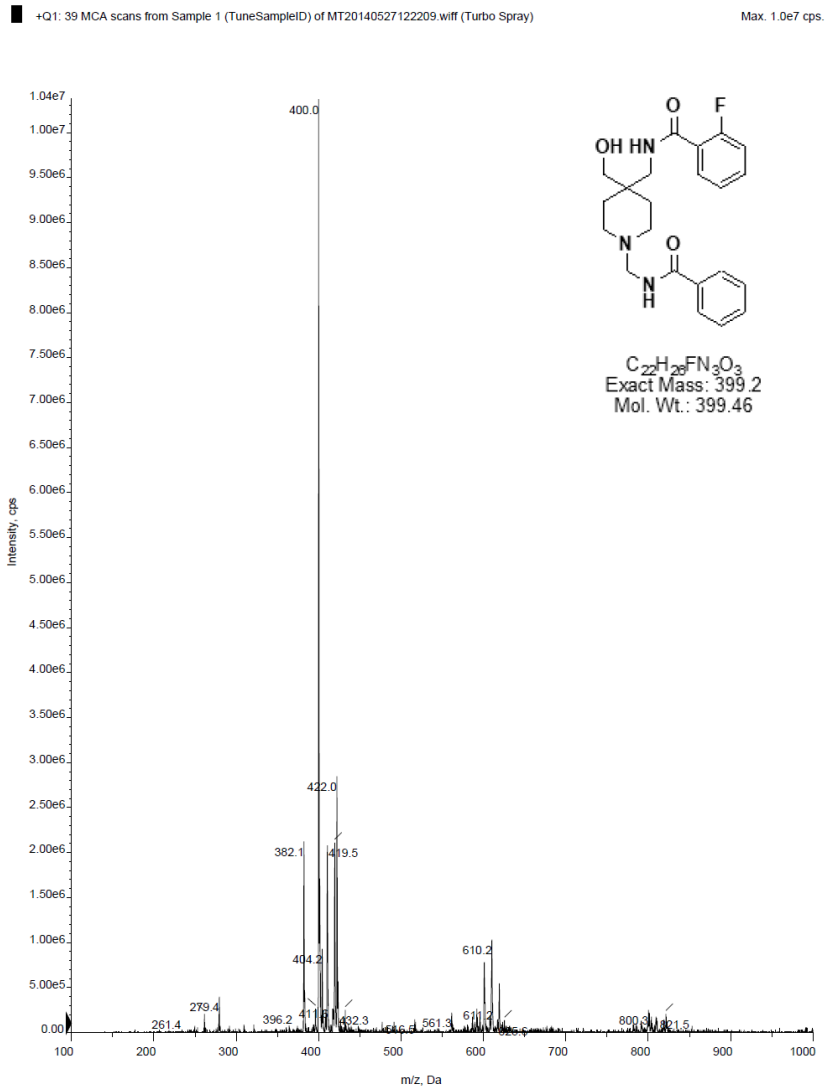

Figure S22. MS spectrum of compound **7**.

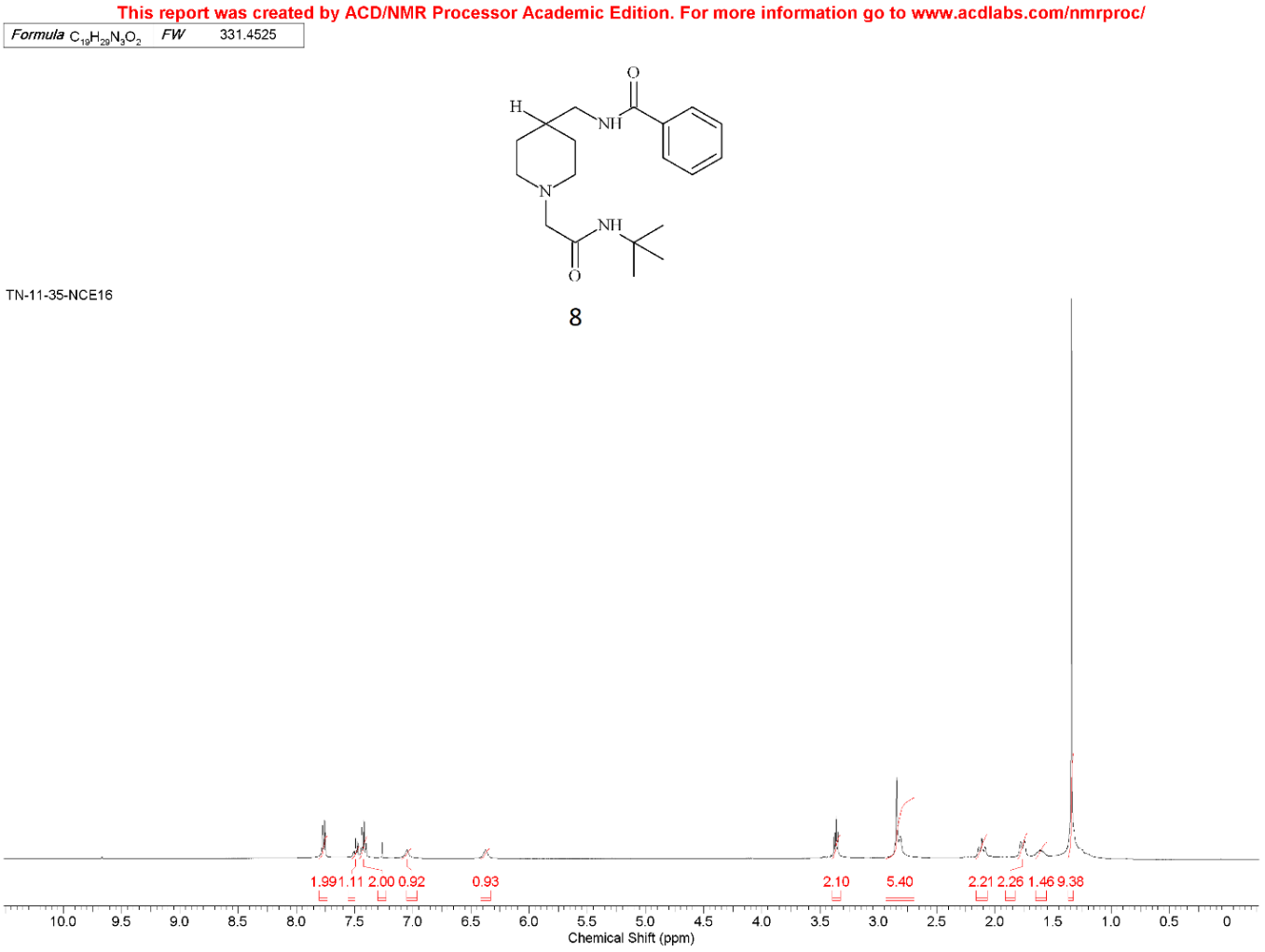

Figure S23. ^{1}H NMR spectrum of compound **8**.

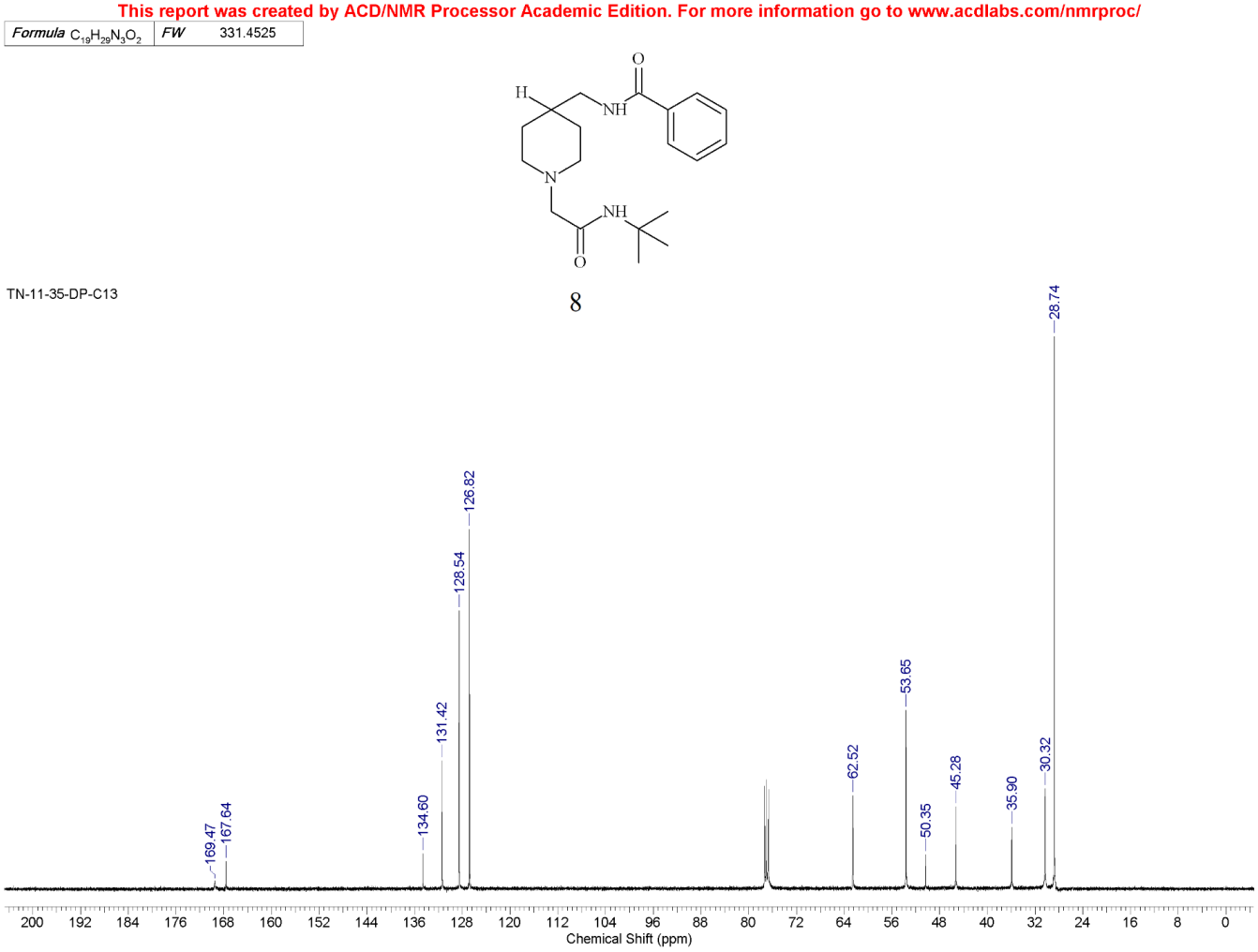

Figure S24. ^{13}C NMR spectrum of compound **8**.

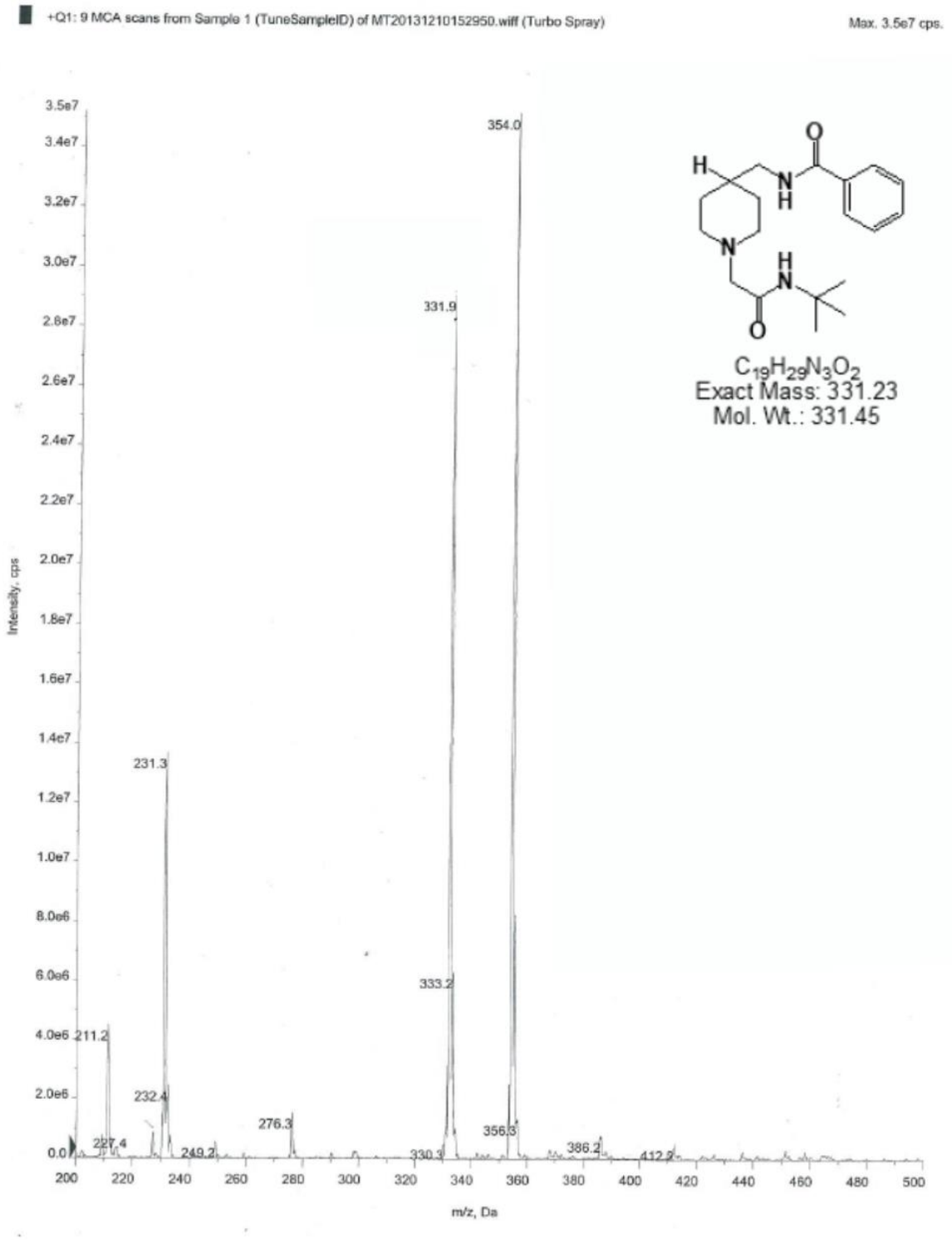

Figure S25. MS spectrum of compound **8**.

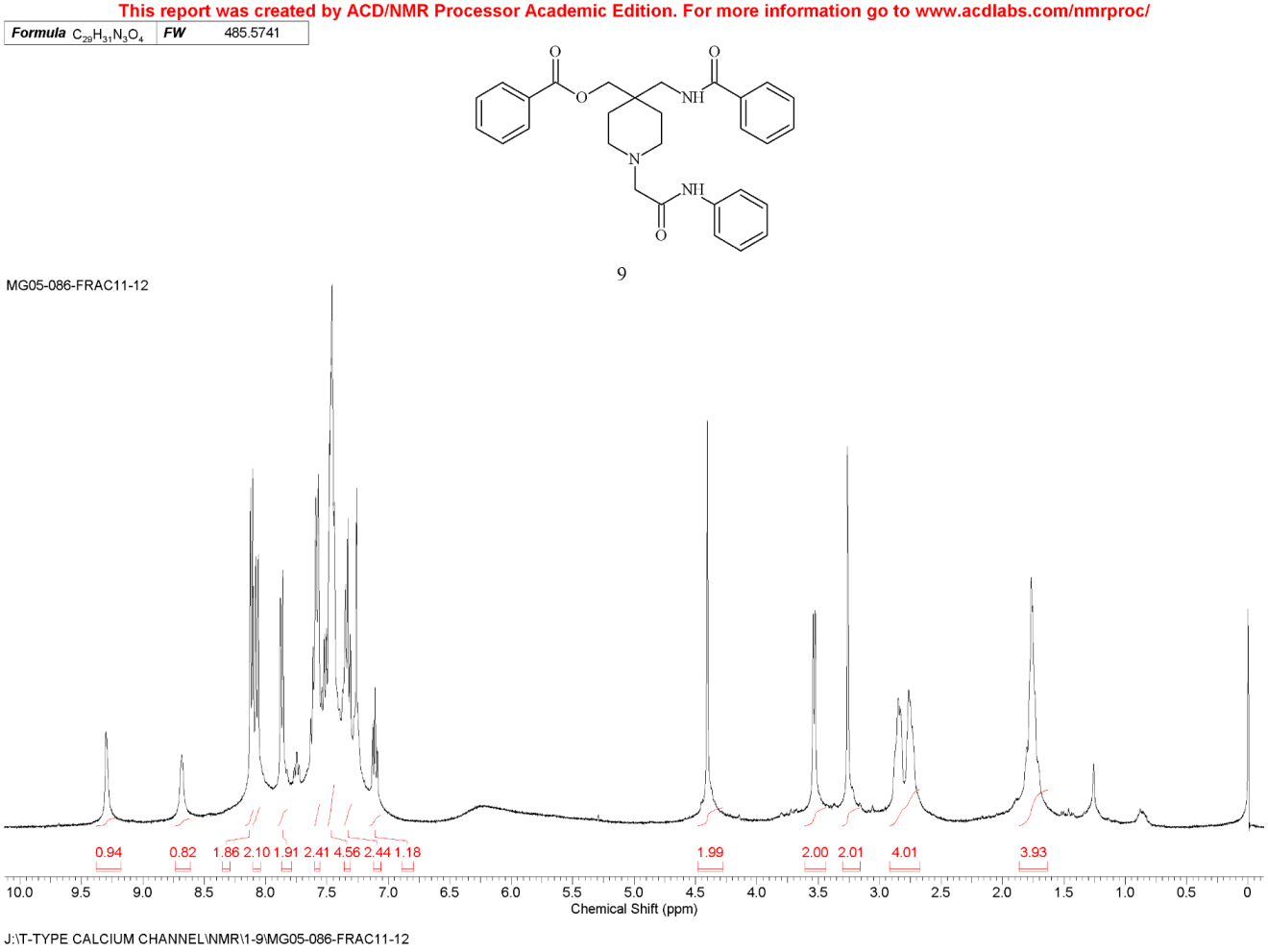

Figure S26. ^{1}H NMR spectrum of compound **9**.

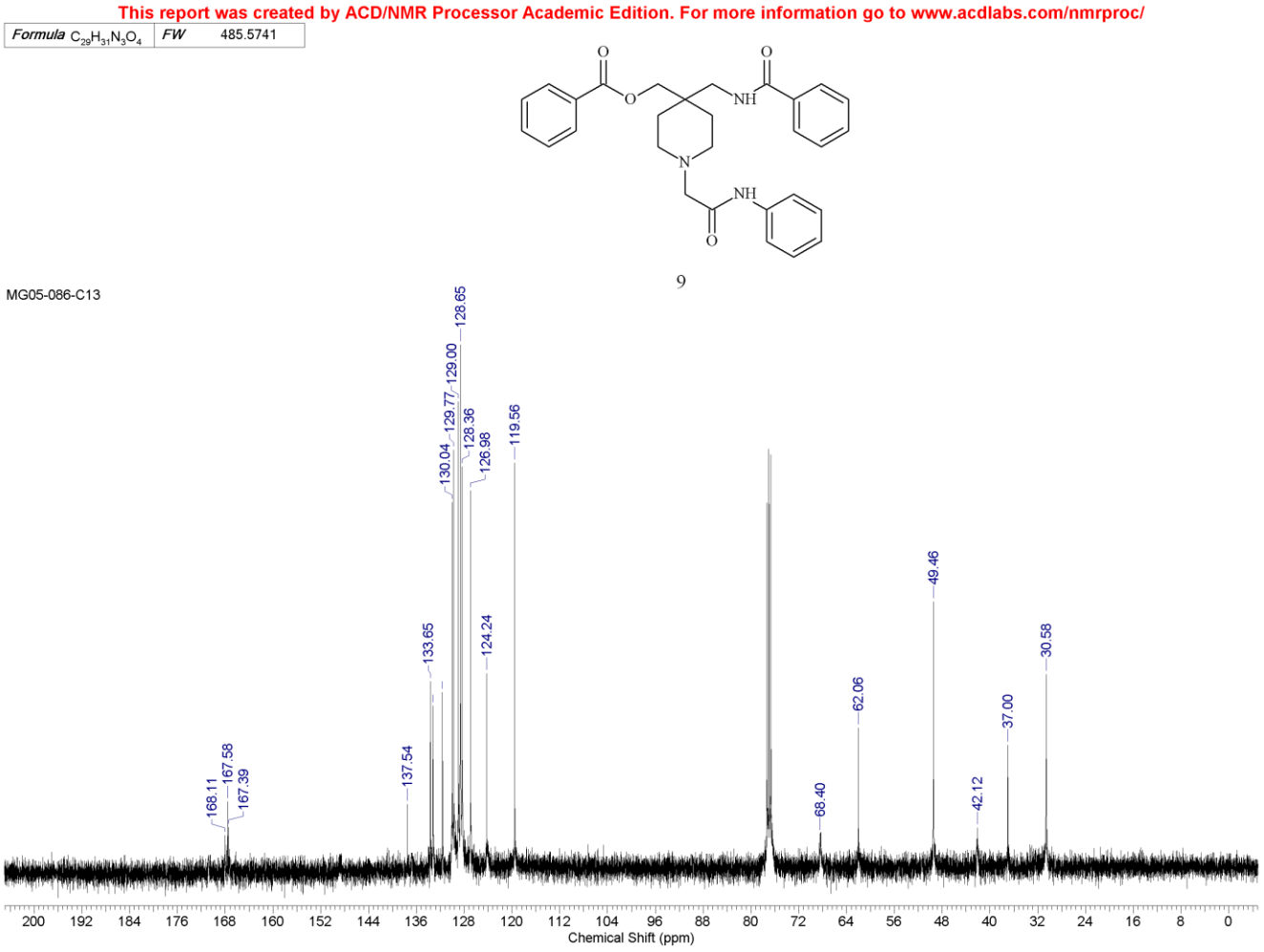

Figure S27. ^{13}C NMR spectrum of compound **9**.

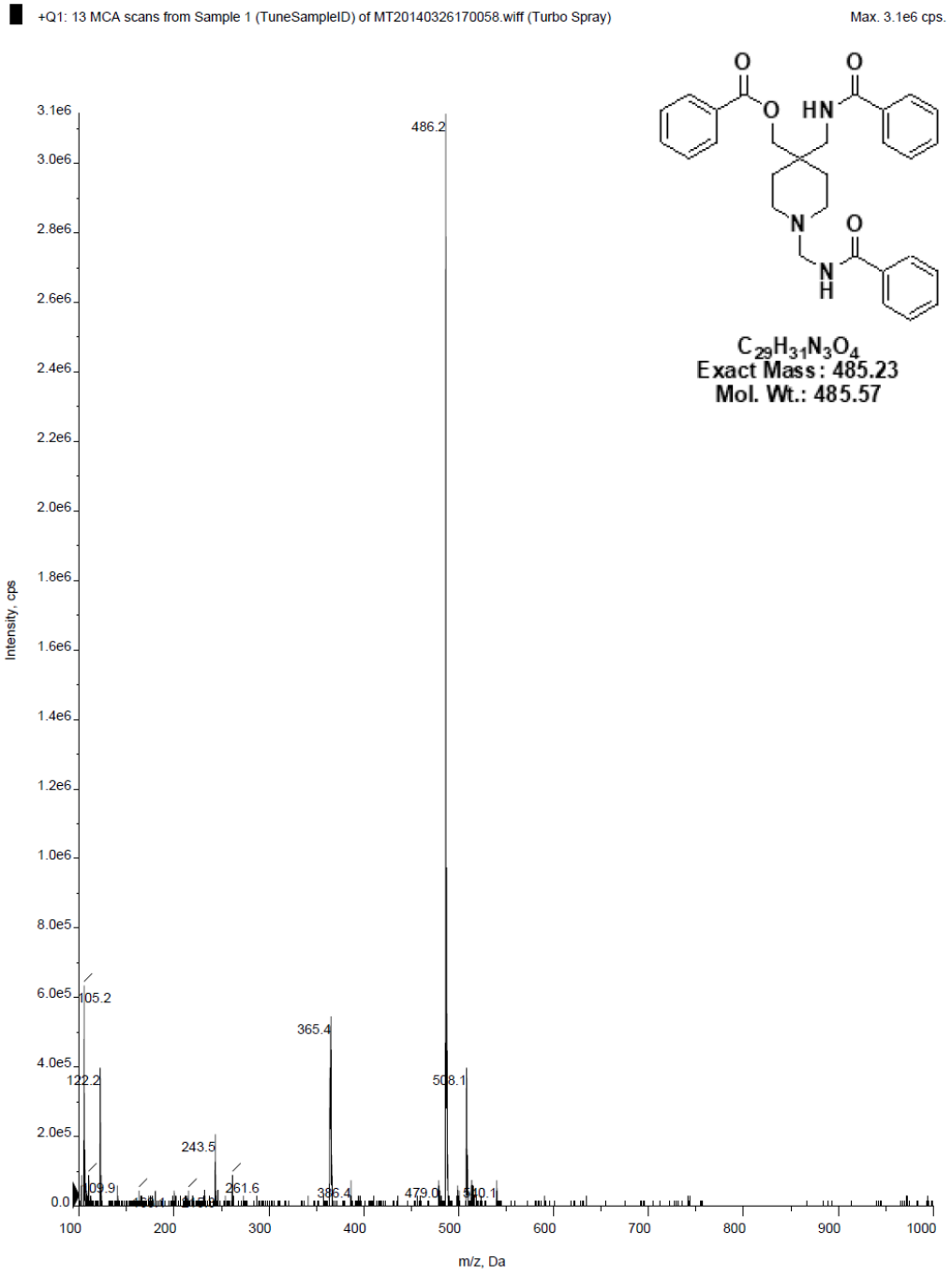

Figure S28. MS spectrum of compound **9**.

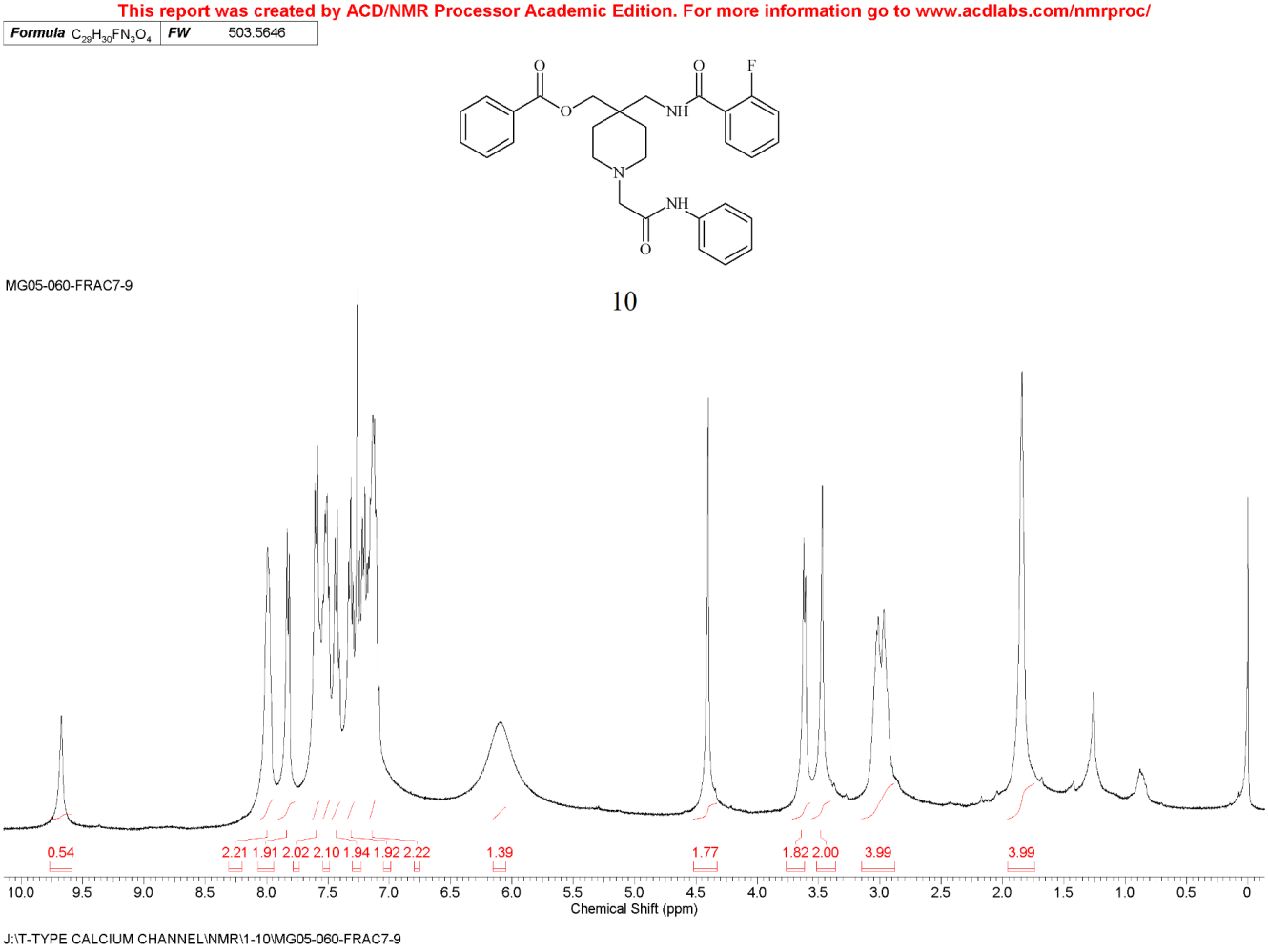

Figure S29. ^{1}H NMR spectrum of compound **10**.

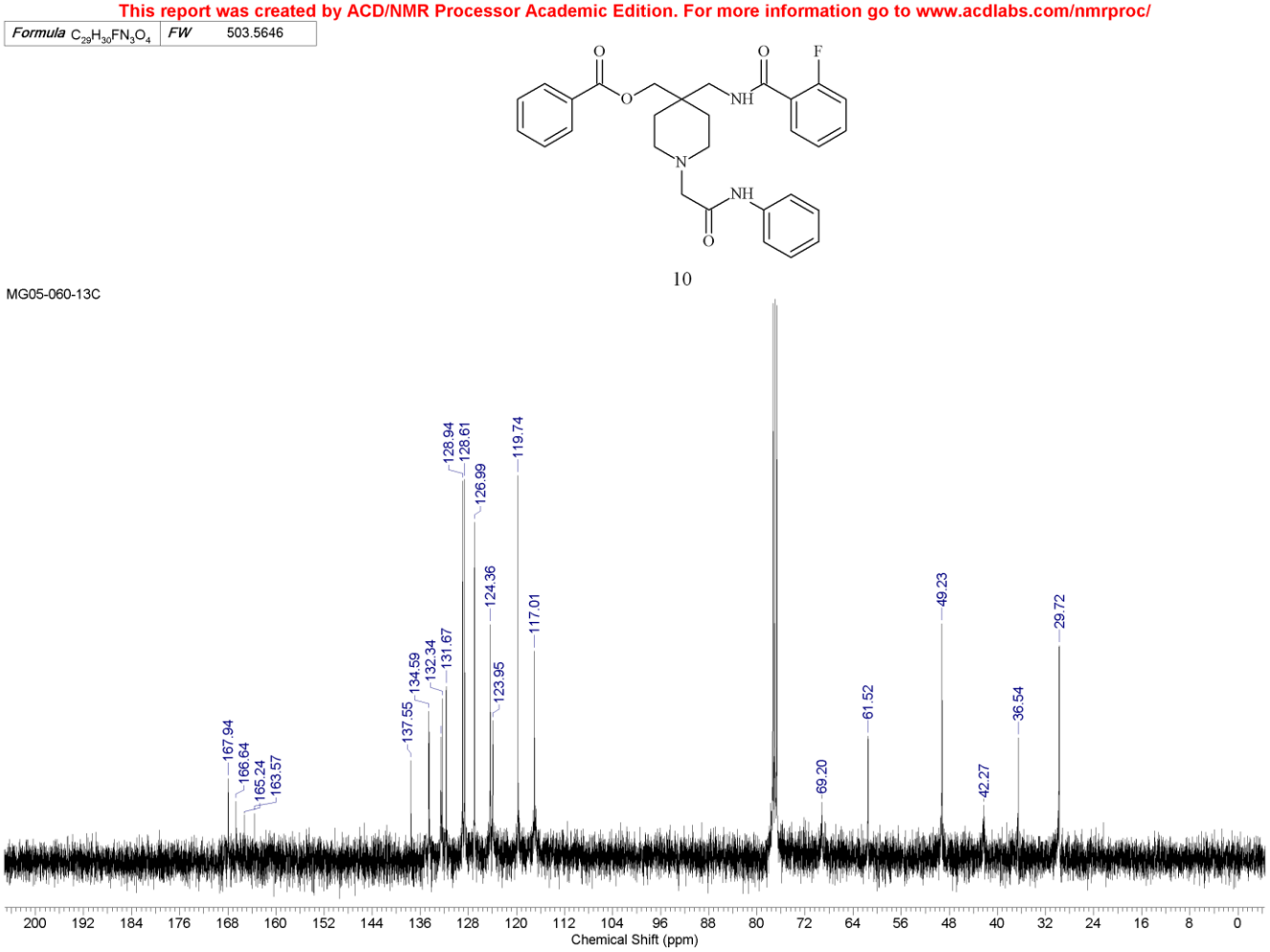

Figure S30. ^{13}C NMR spectrum of compound **10**.

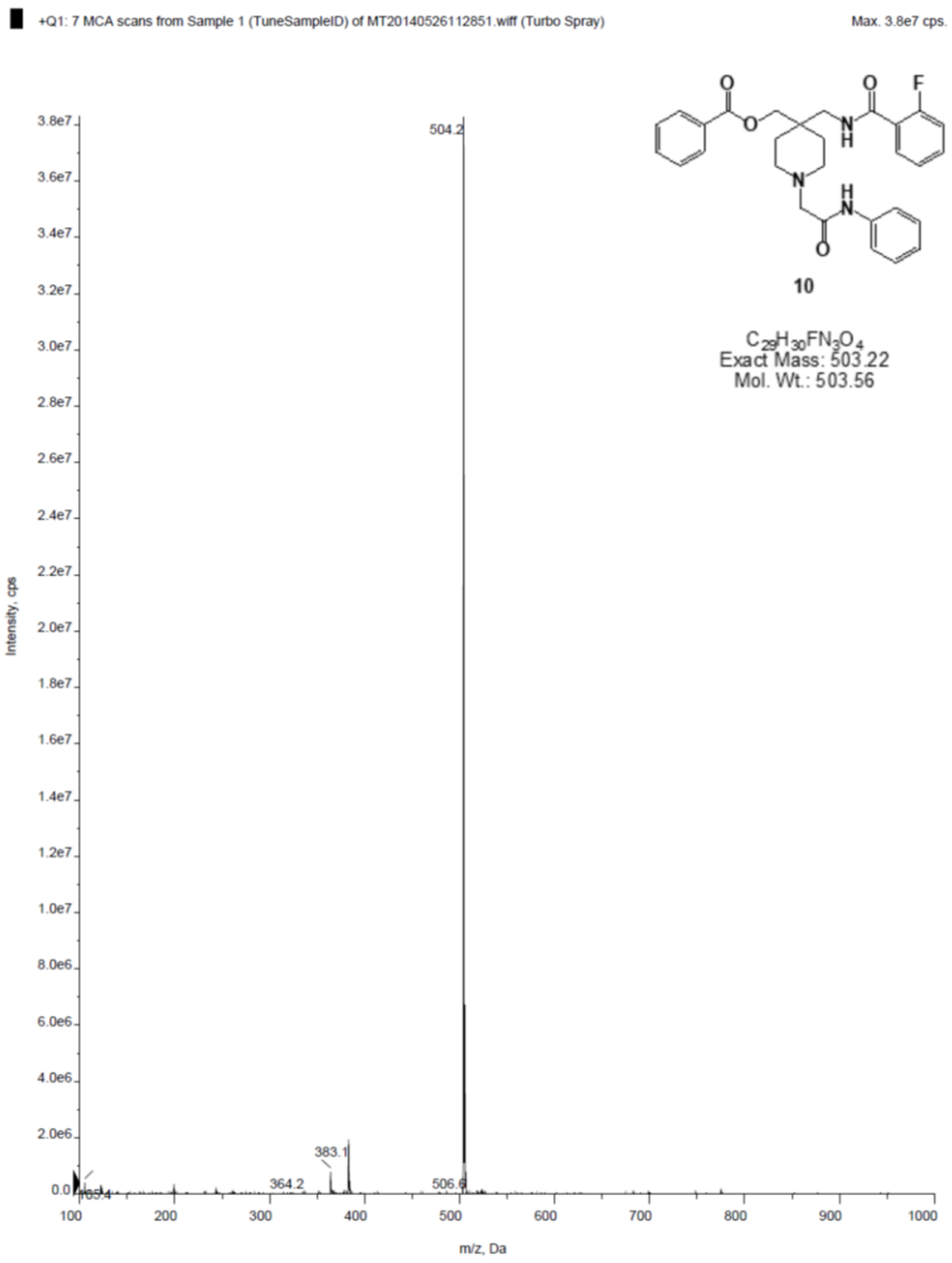

Figure S31. MS spectrum of compound **10**.

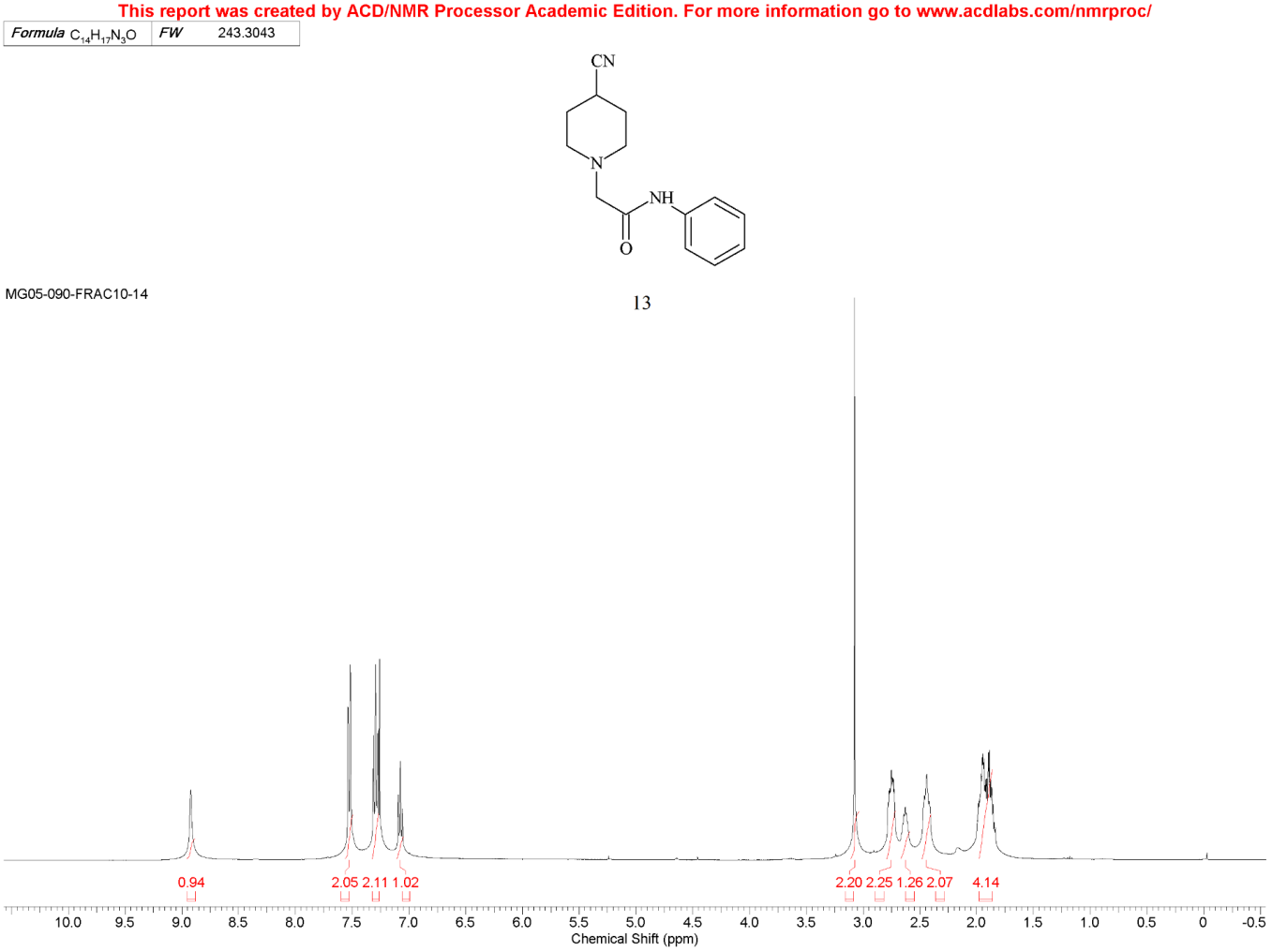

Figure S32. ^{1}H NMR spectrum of compound **13**.

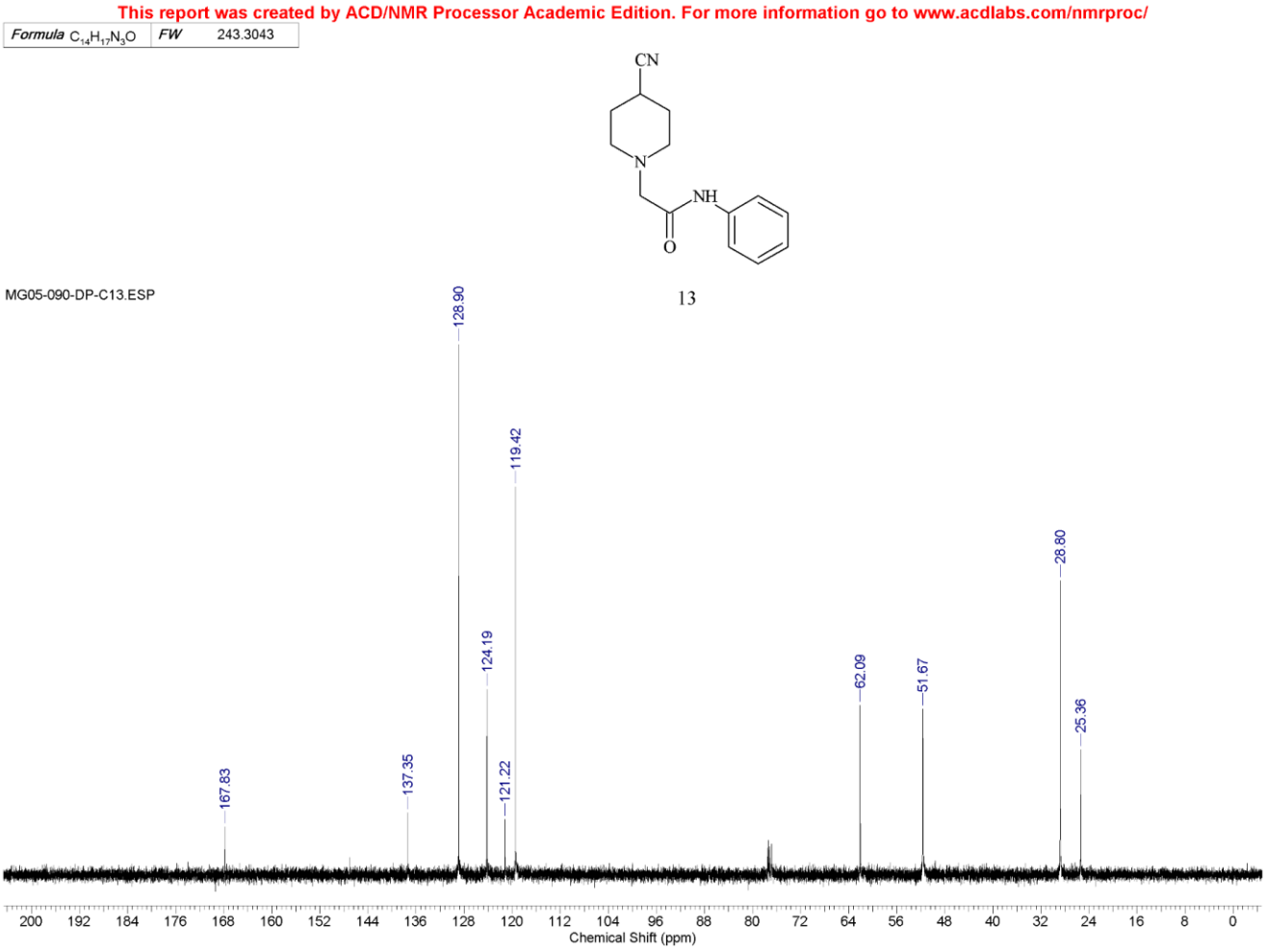

Figure S33. ^{13}C NMR spectrum of compound **13**.

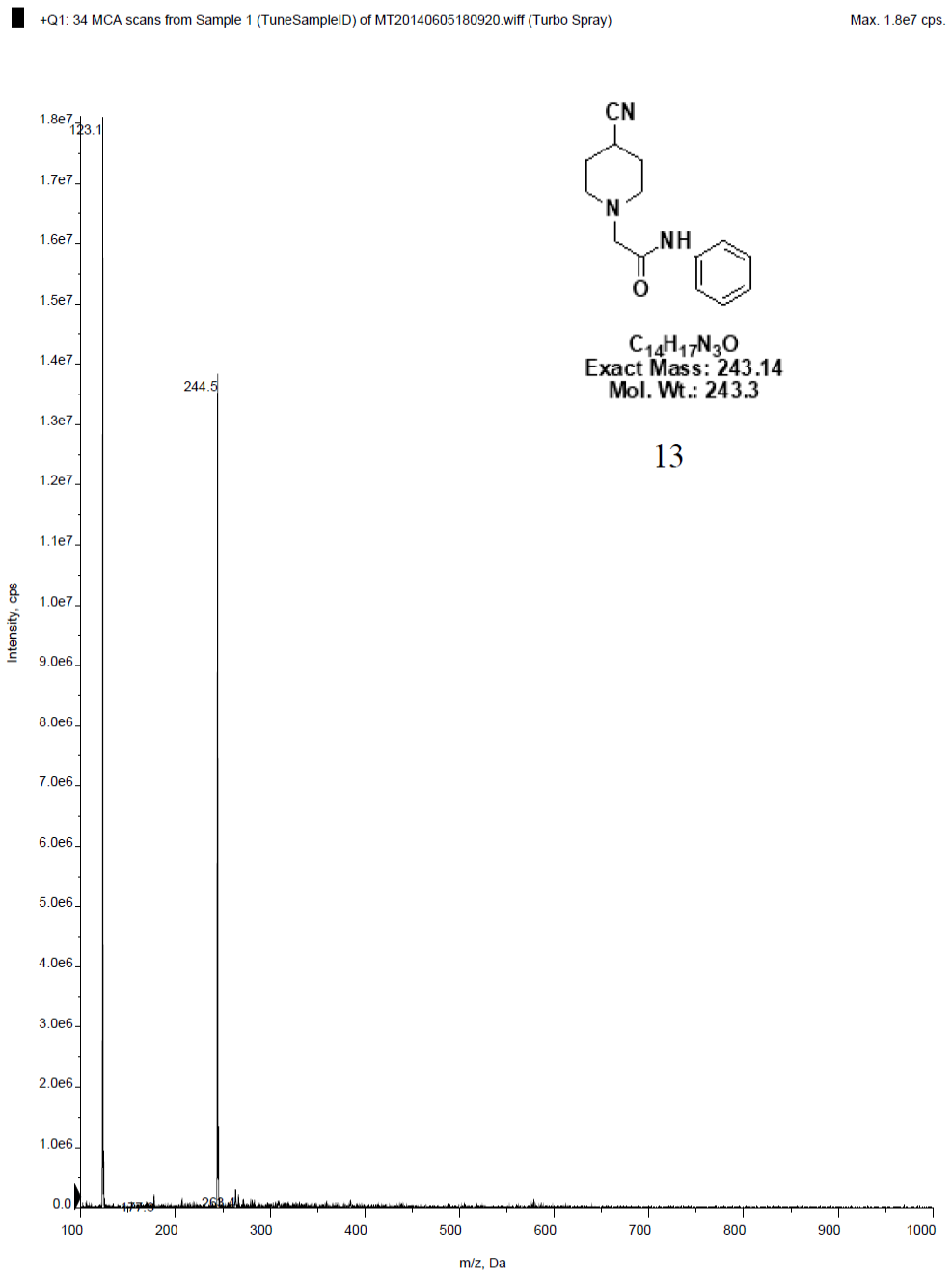

Figure S34. MS spectrum of compound **13**.

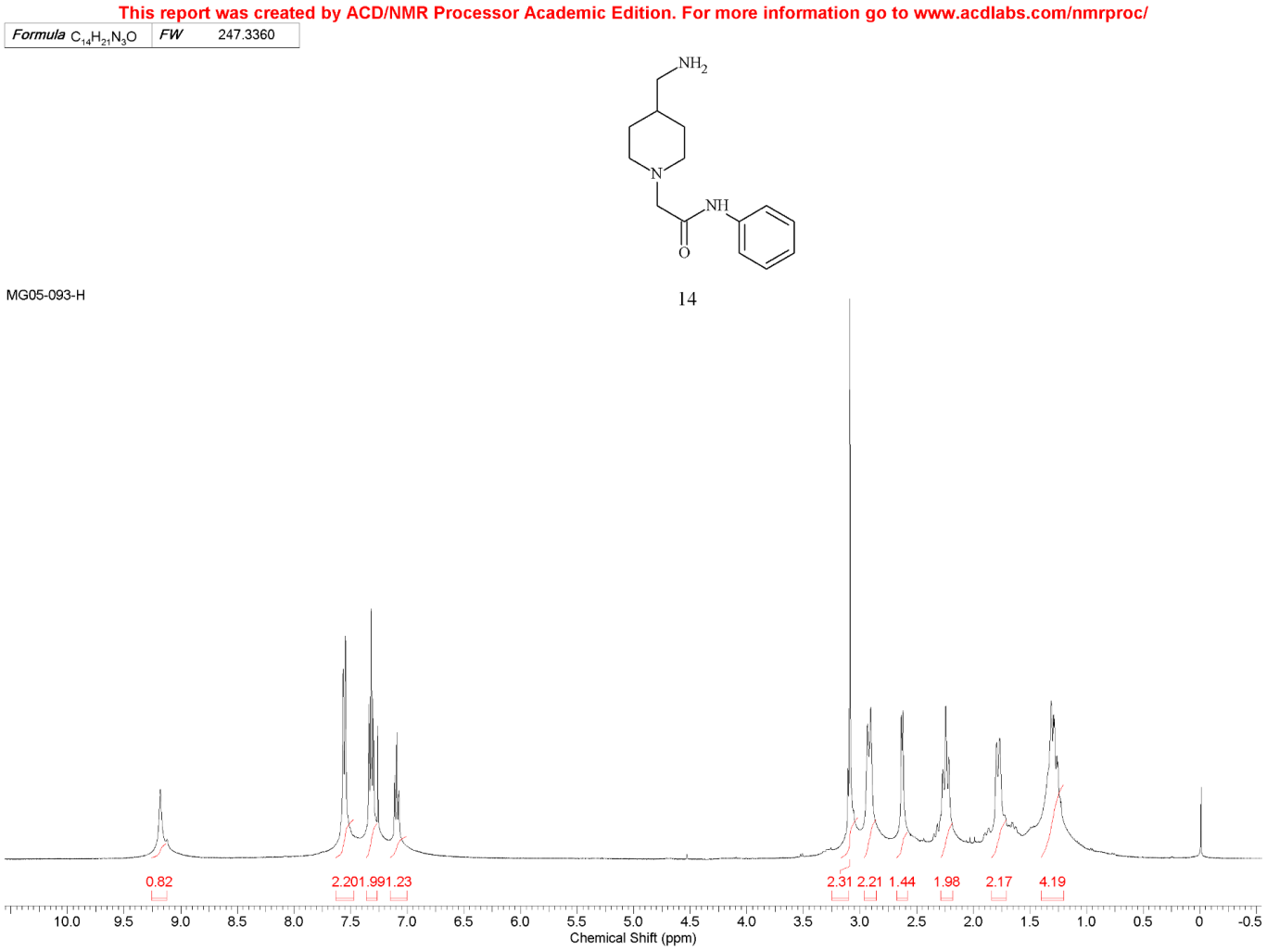

Figure S35. ^{1}H NMR spectrum of compound **14**.

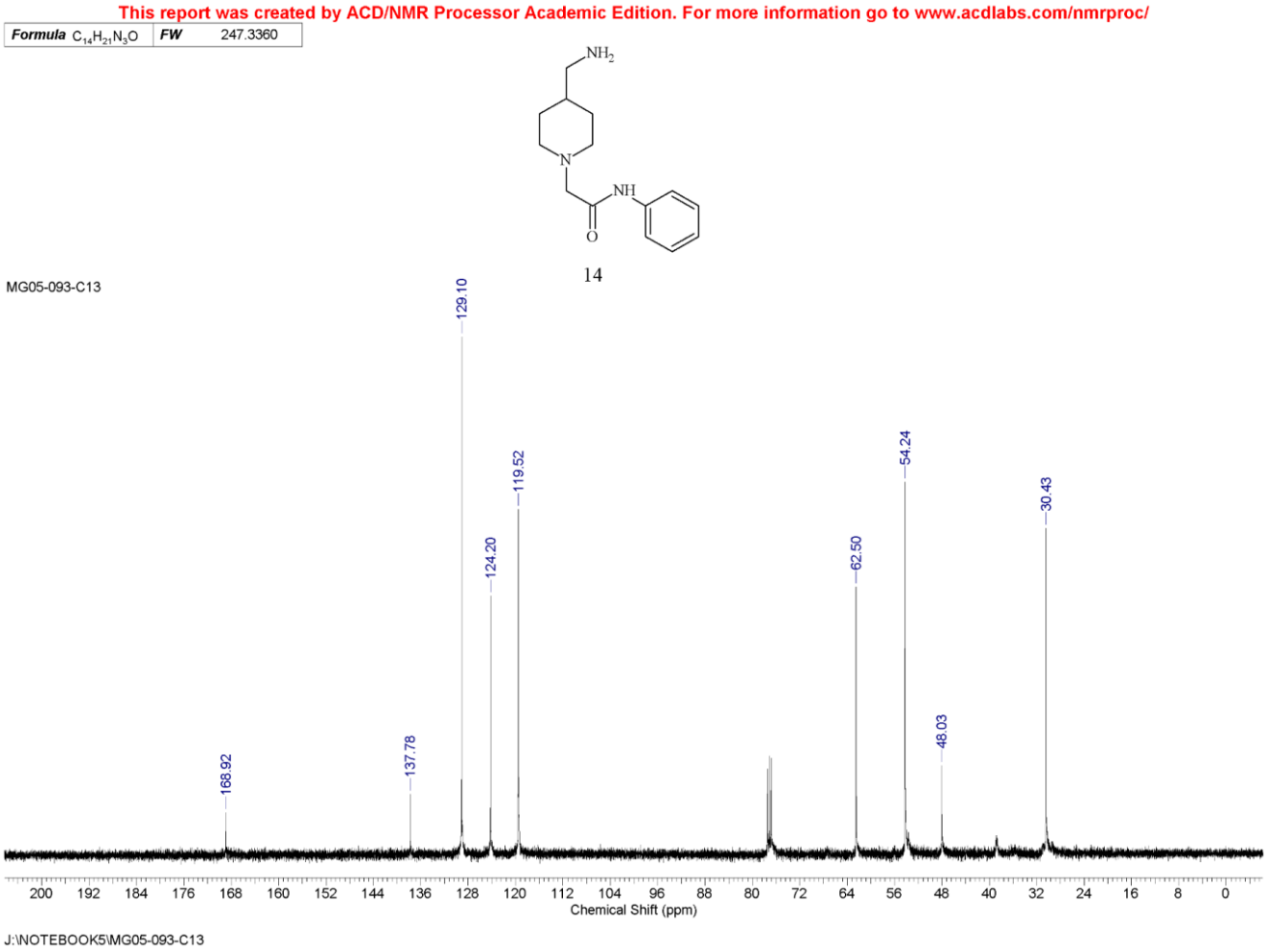

Figure S36. ^{13}C NMR spectrum of compound **14**.

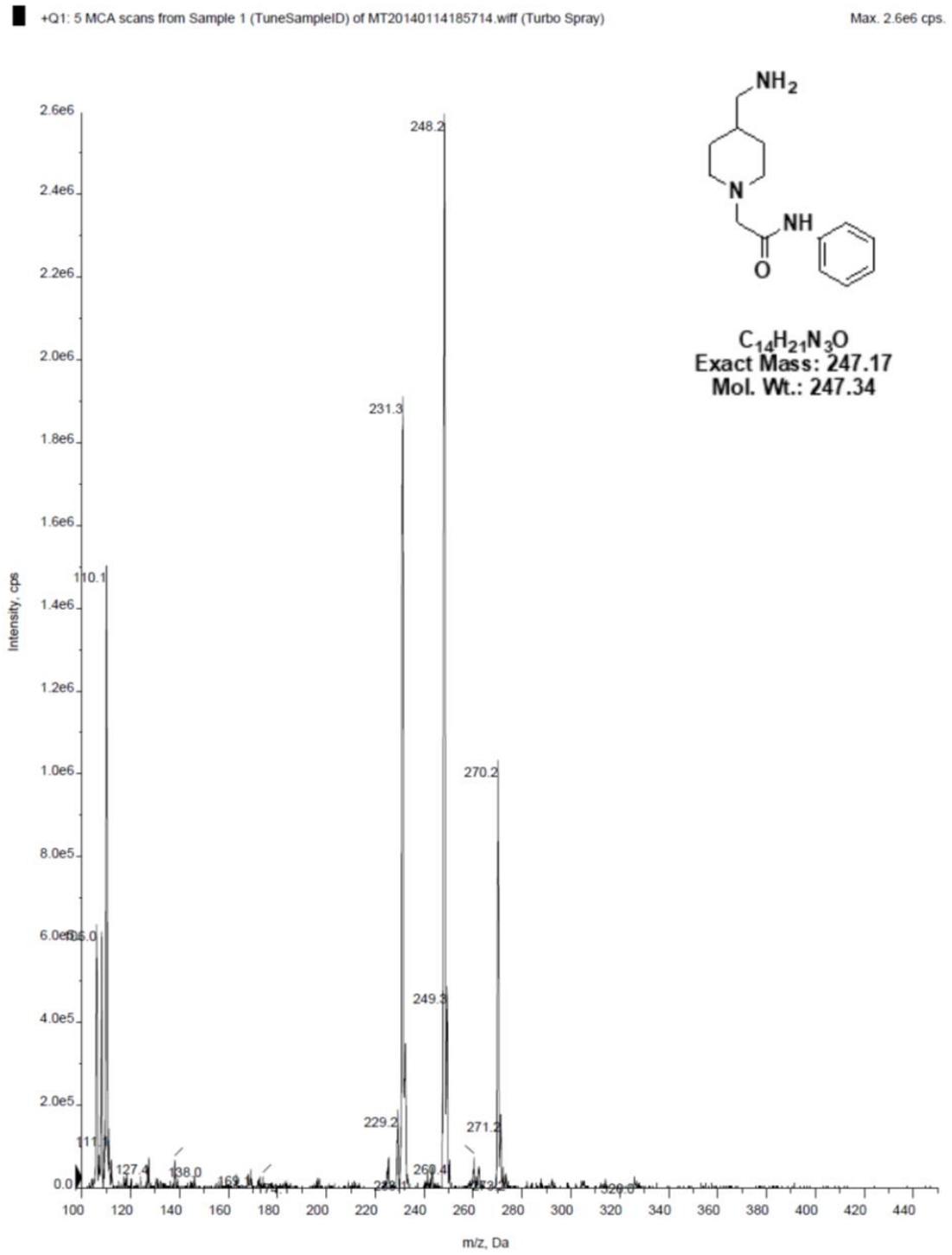

Figure S37. MS spectrum of compound **14**.

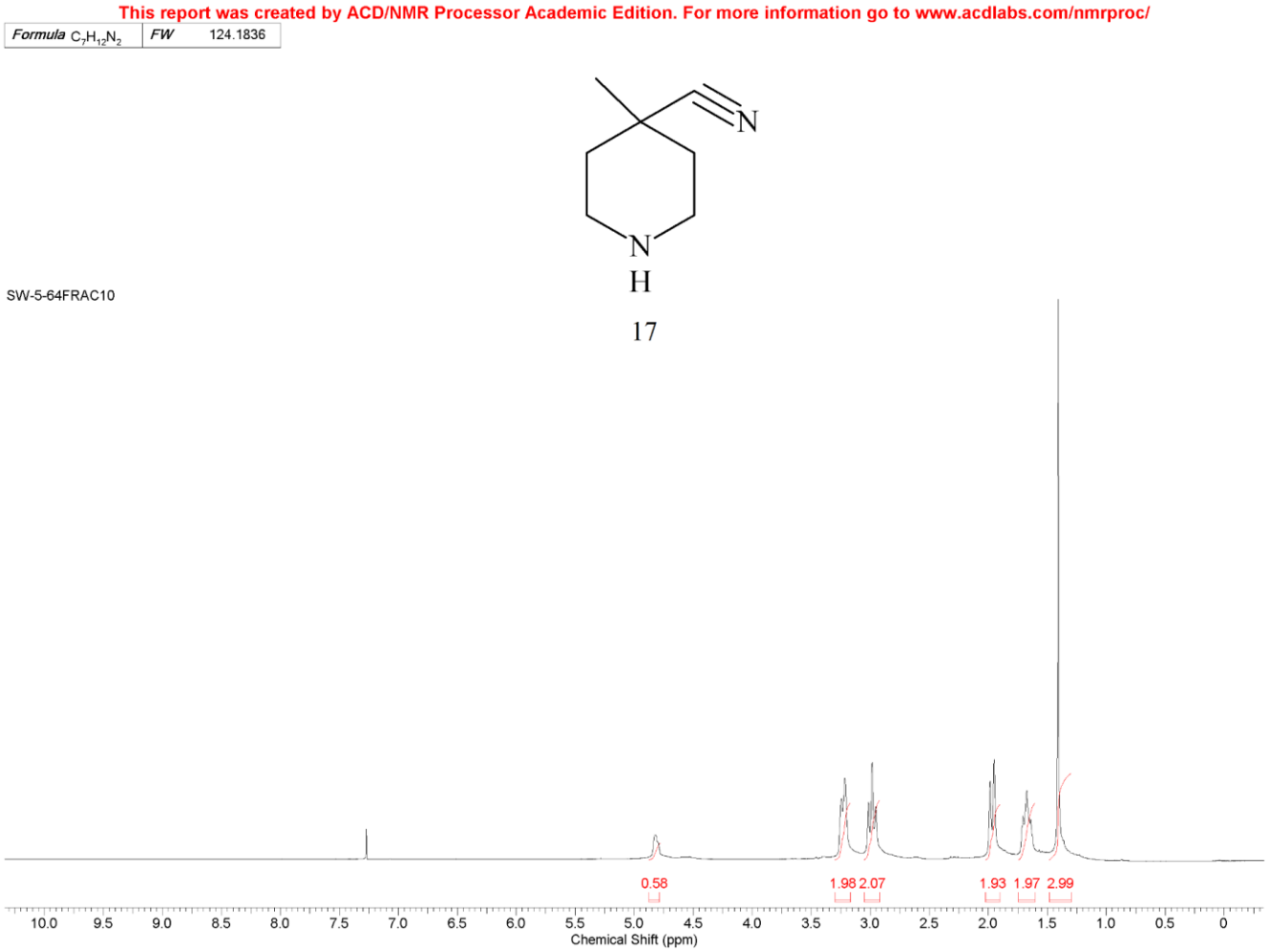

Figure S38. ^{1}H NMR spectrum of compound **17**.

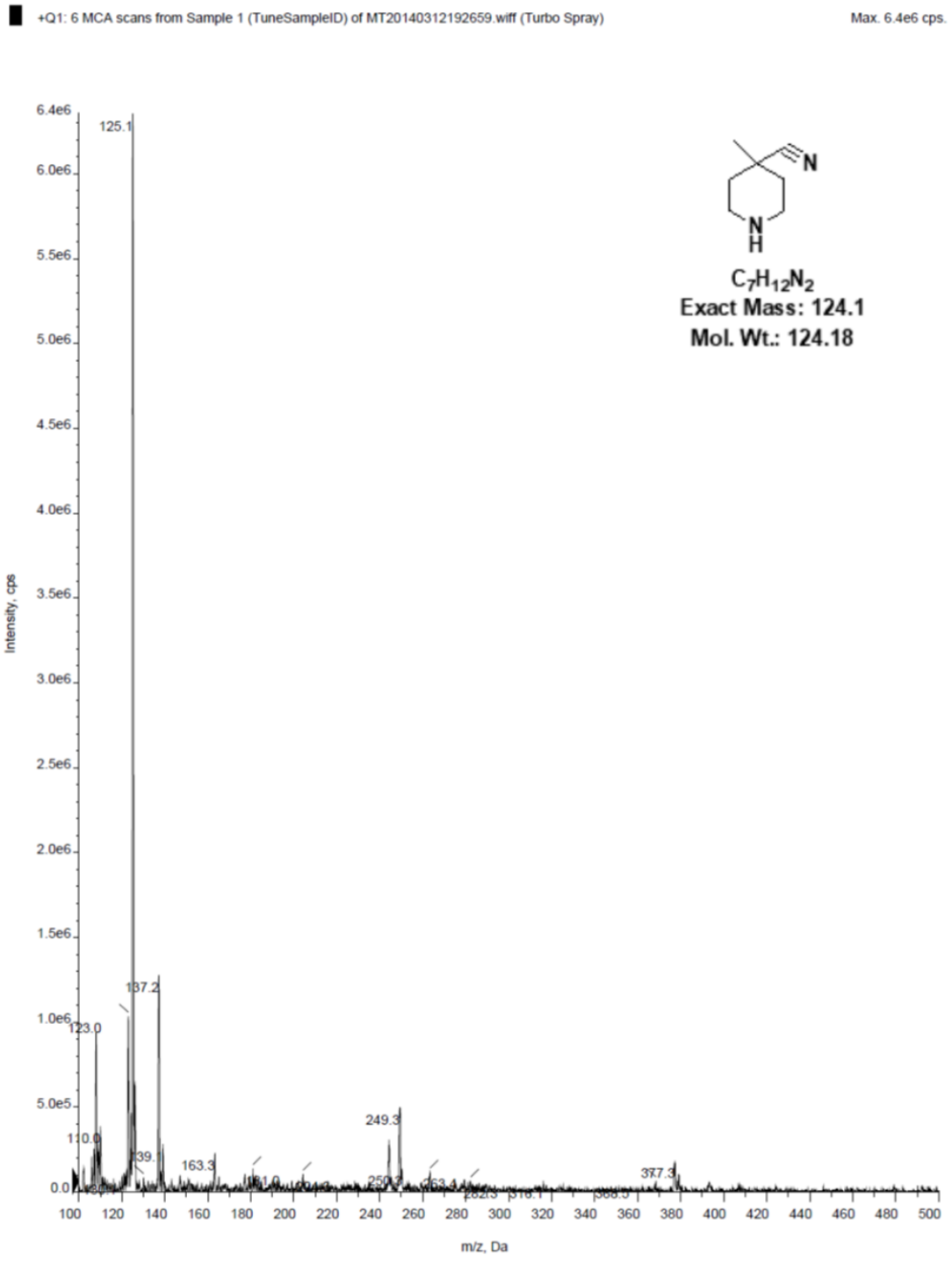

Figure S39. MS spectrum of compound **17**.

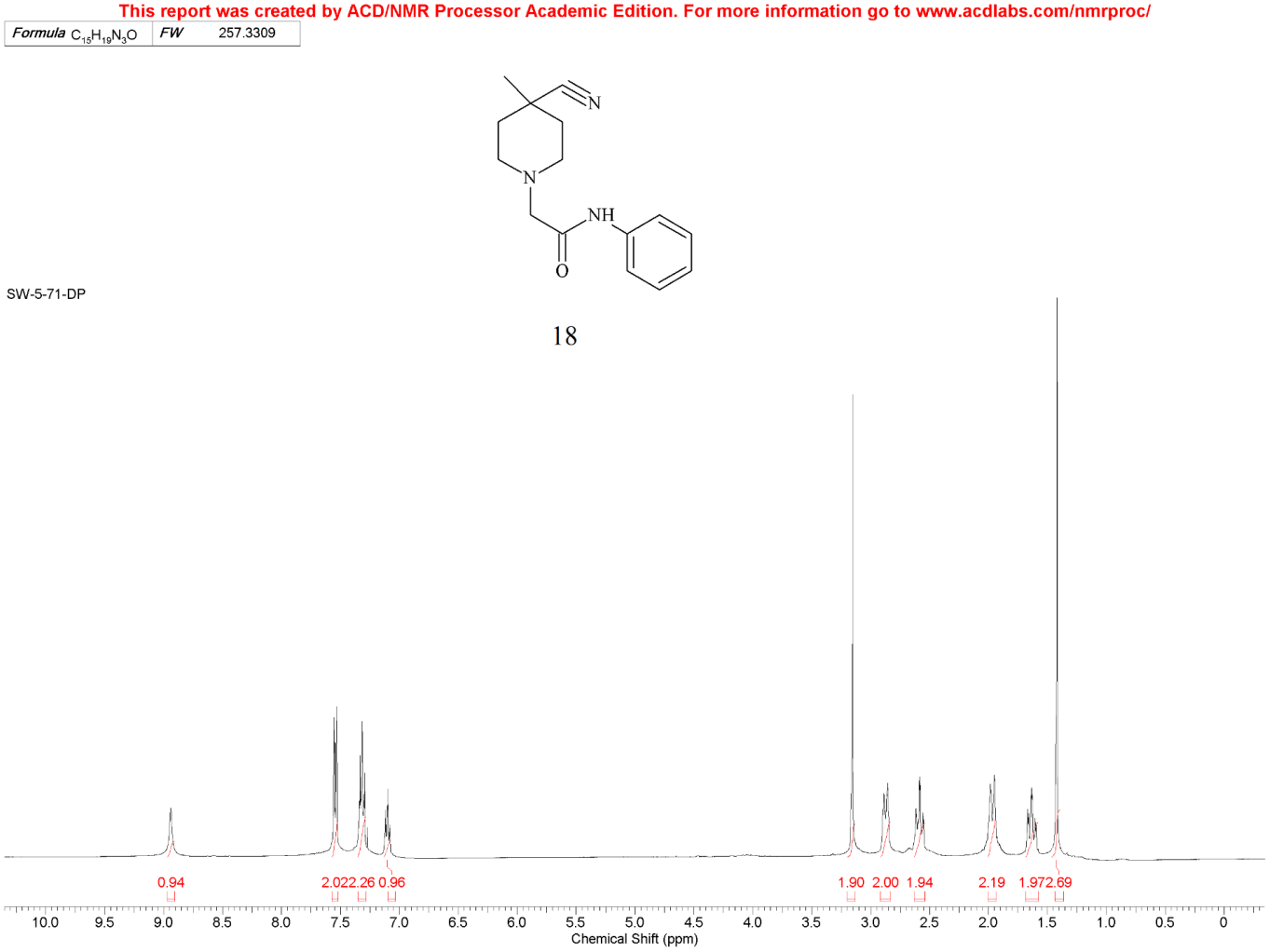

Figure S40. ^{1}H NMR spectrum of compound **18**.

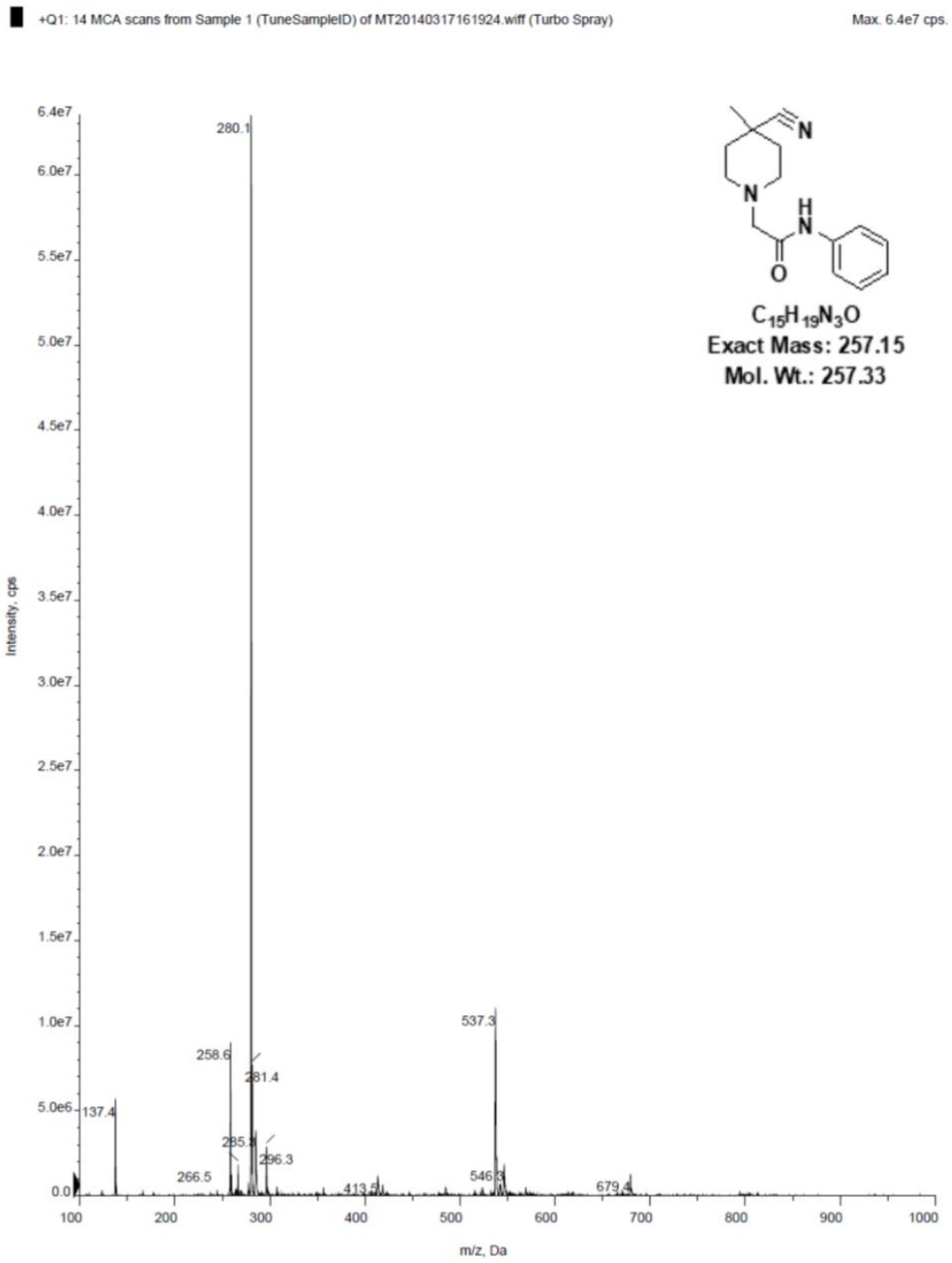

Figure S41. MS spectrum of compound **18**.

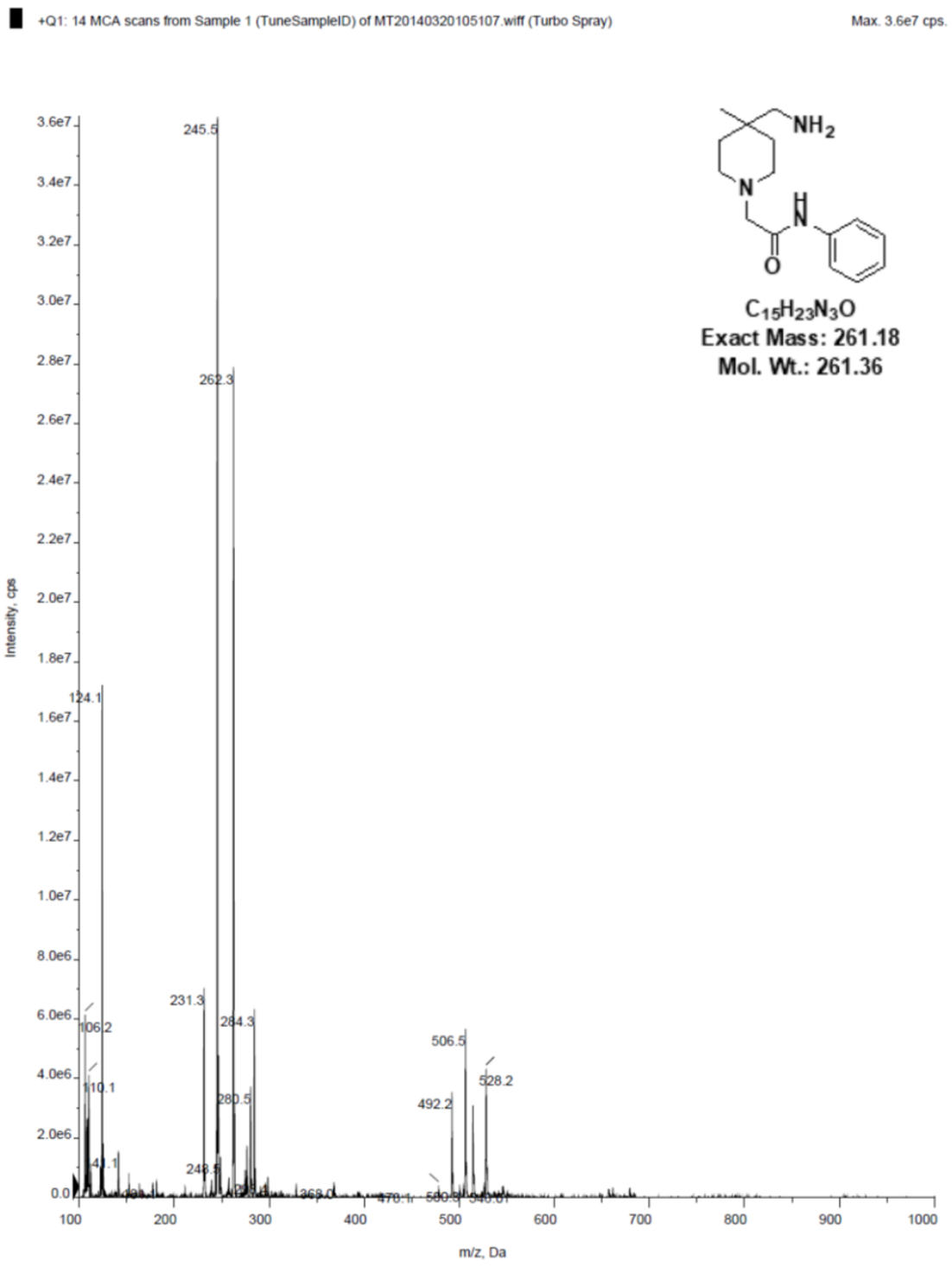

Figure S42. MS spectrum of compound **19**.

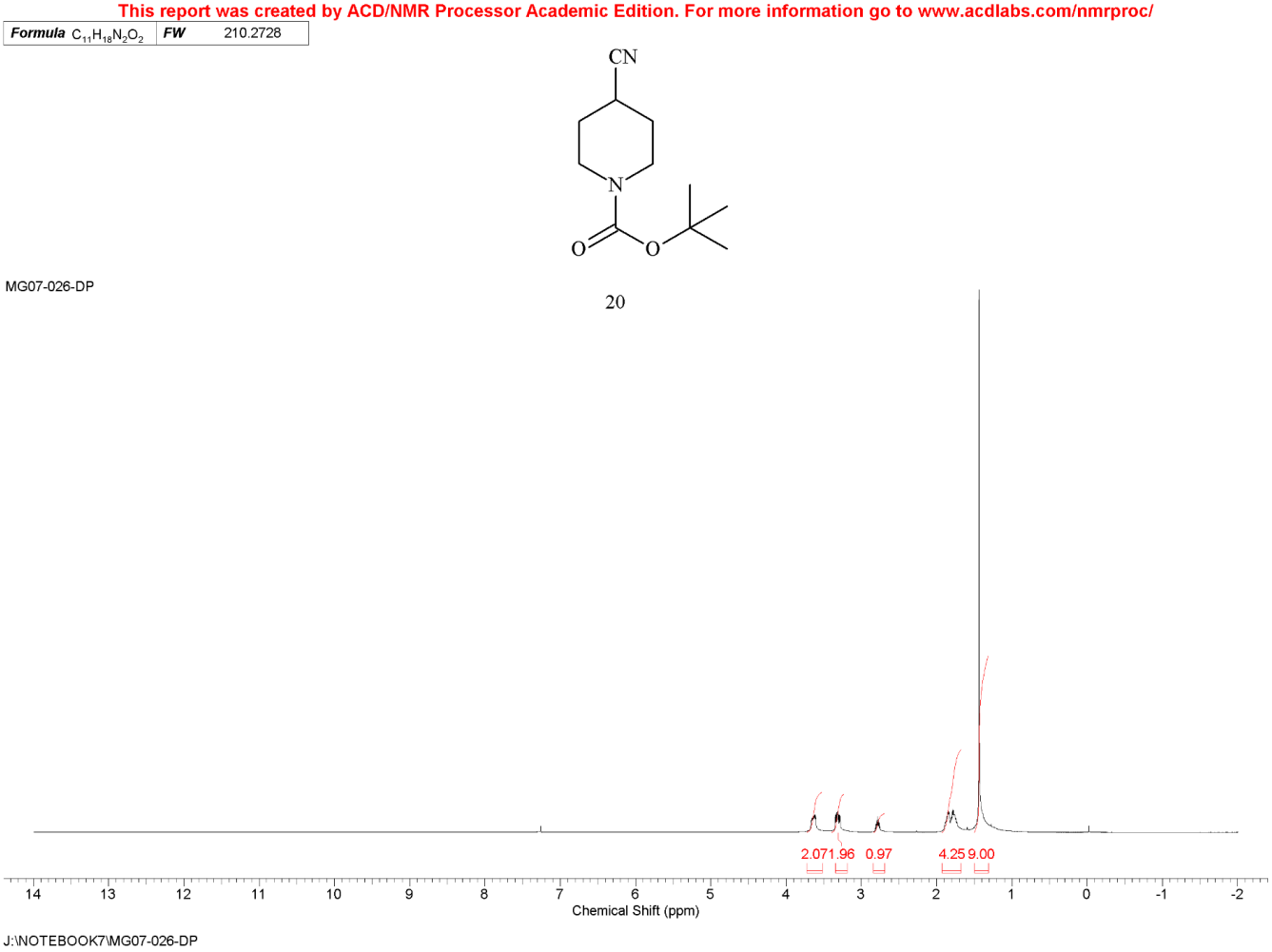

Figure S43. ^{1}H NMR spectrum of compound **20**.

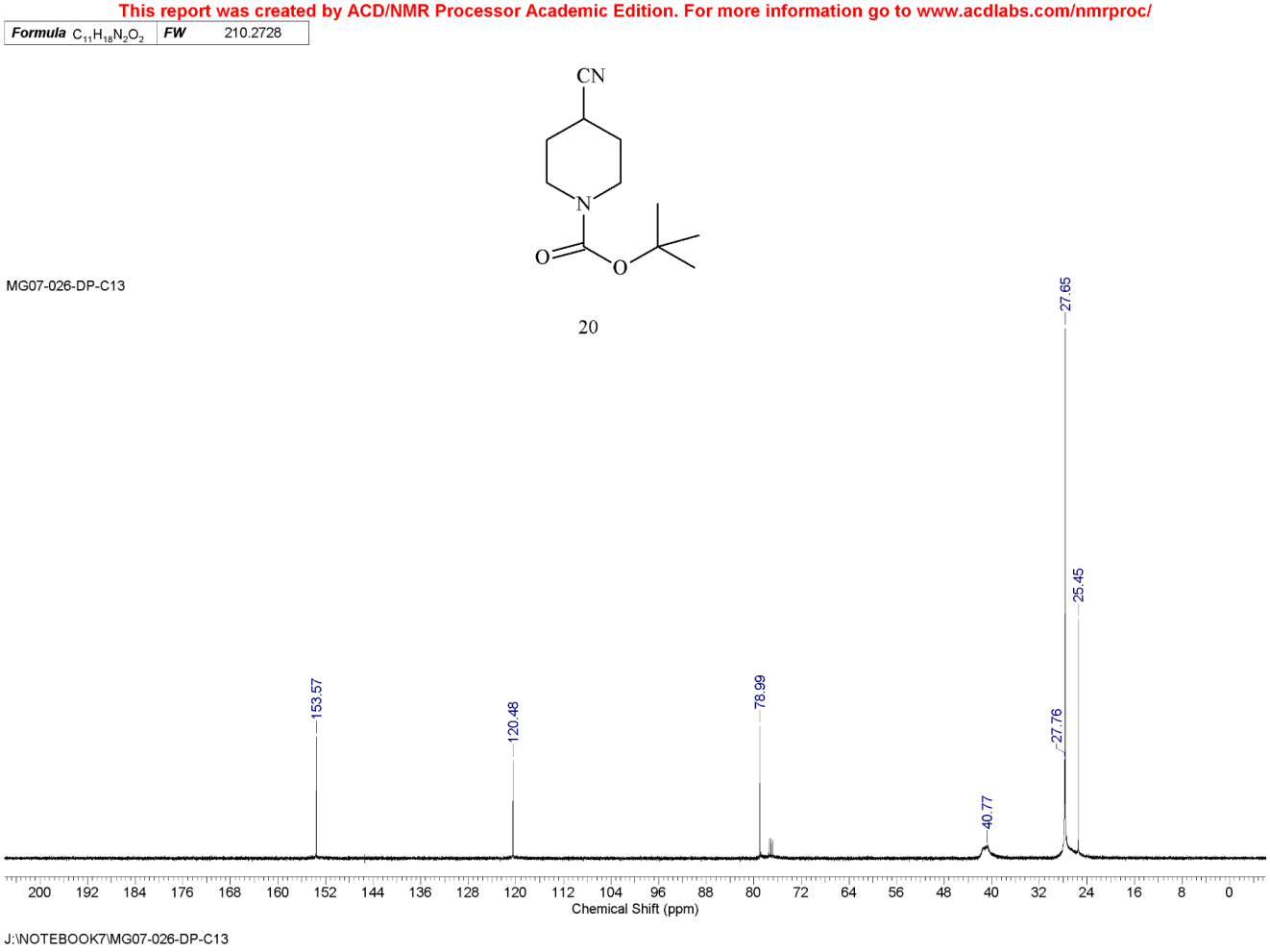

Figure S44. ^{13}C NMR spectrum of compound **20**.

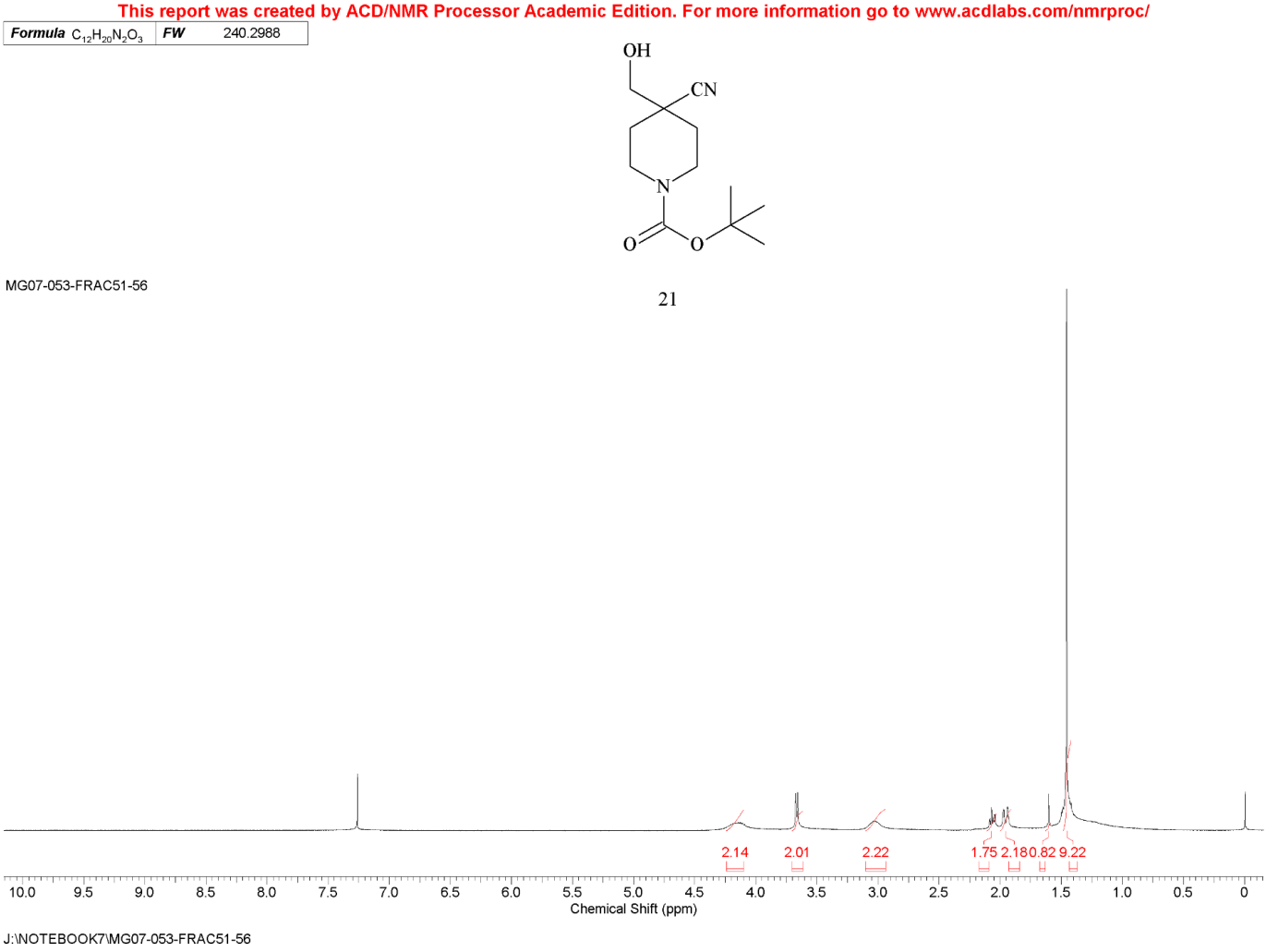

Figure S45. ^{1}H NMR spectrum of compound **21**.

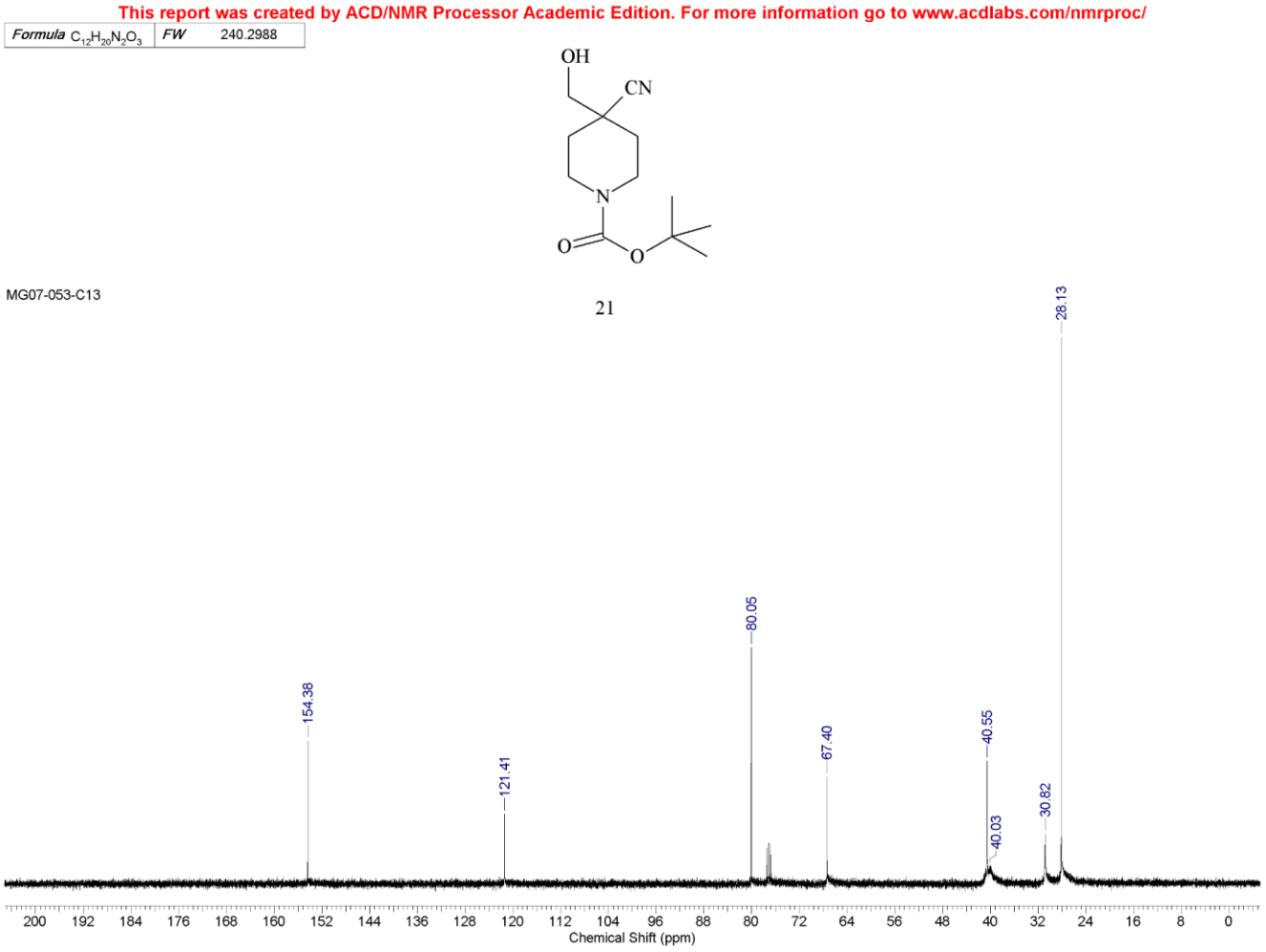

Figure S46. ^{13}C NMR spectrum of compound **21**.

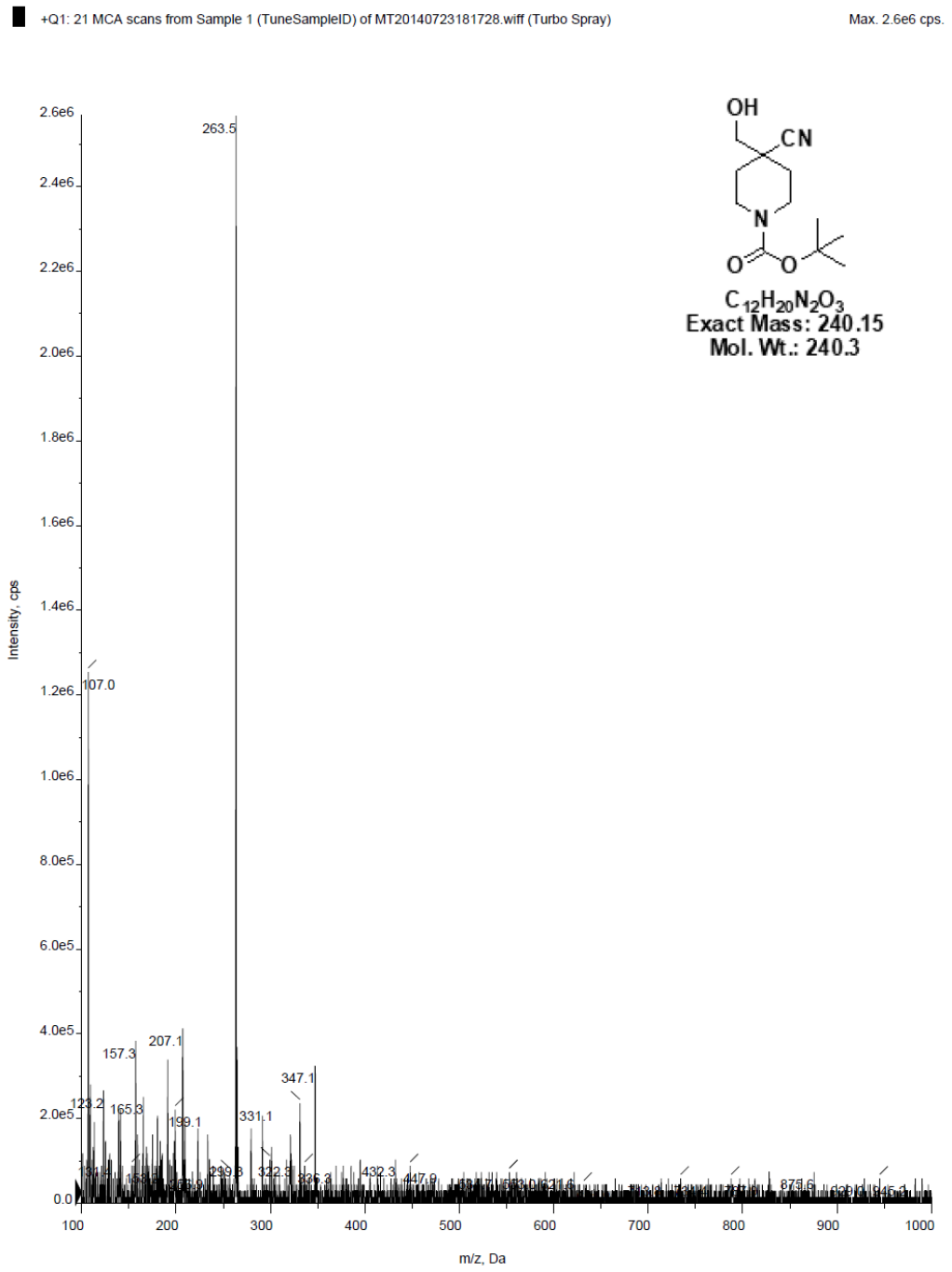

Figure S47. MS spectrum of compound **21**.

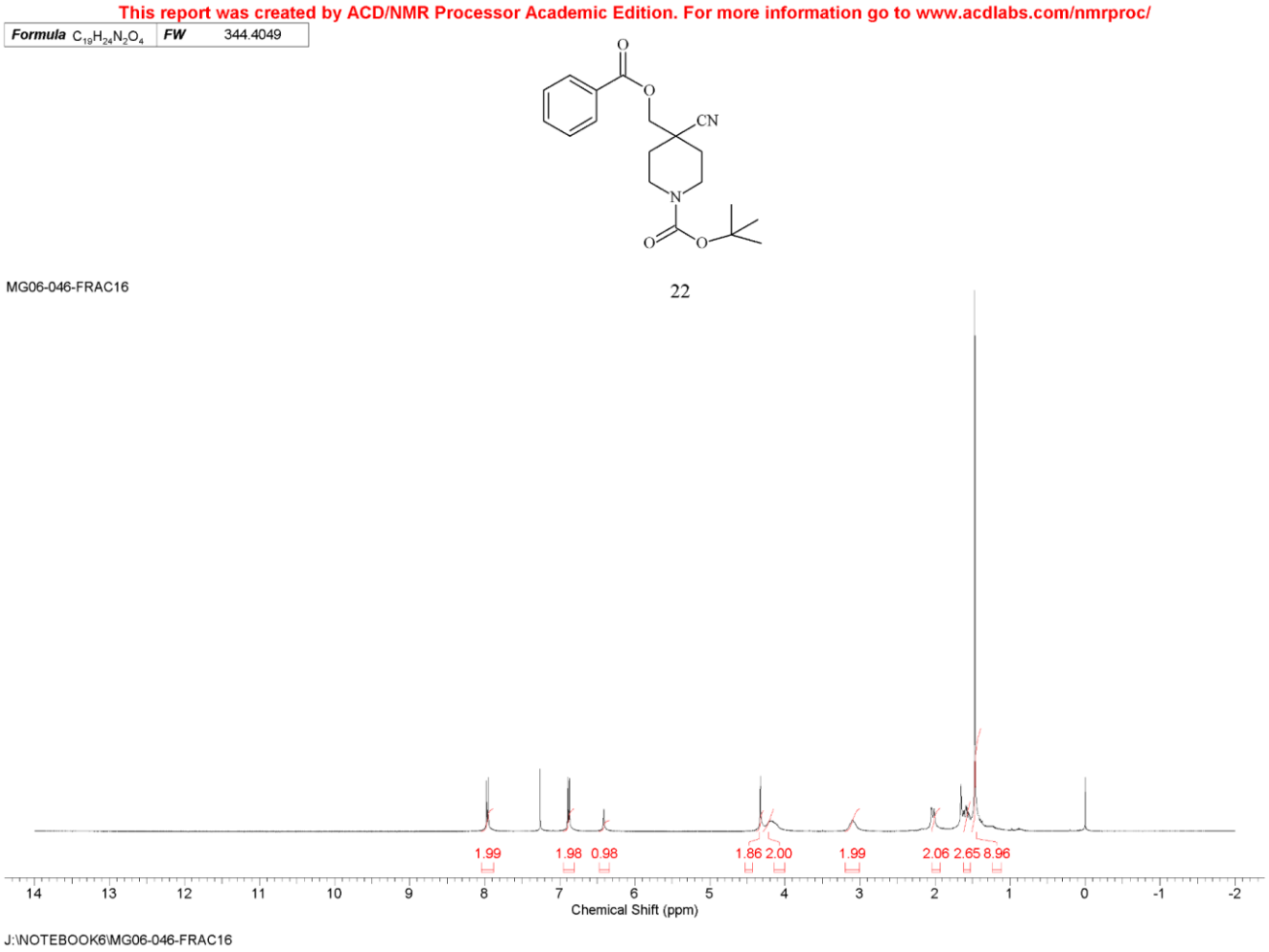

Figure S48. ^{1}H NMR spectrum of compound **22**.

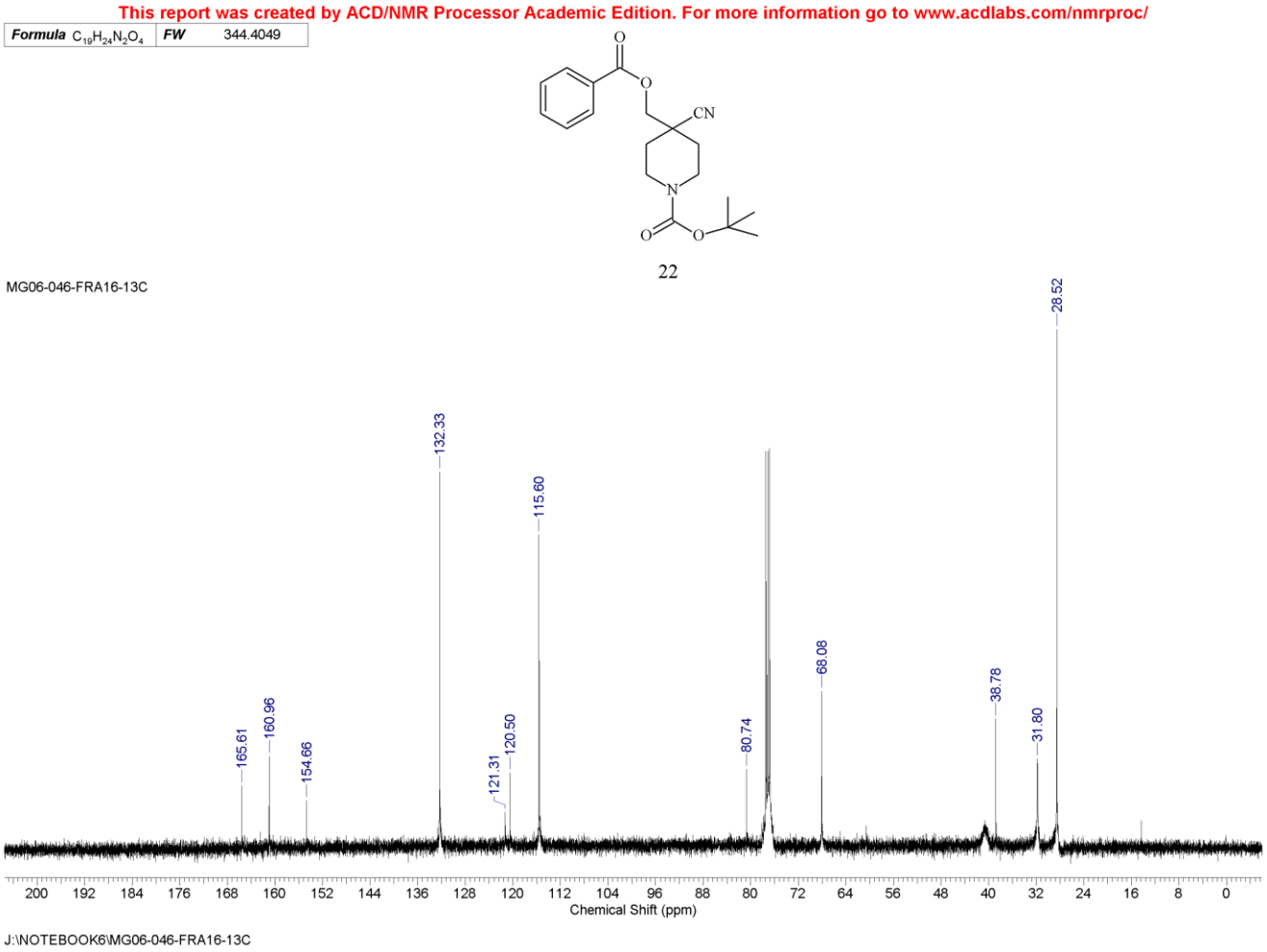

Figure S49. ^{13}C NMR spectrum of compound **22**.

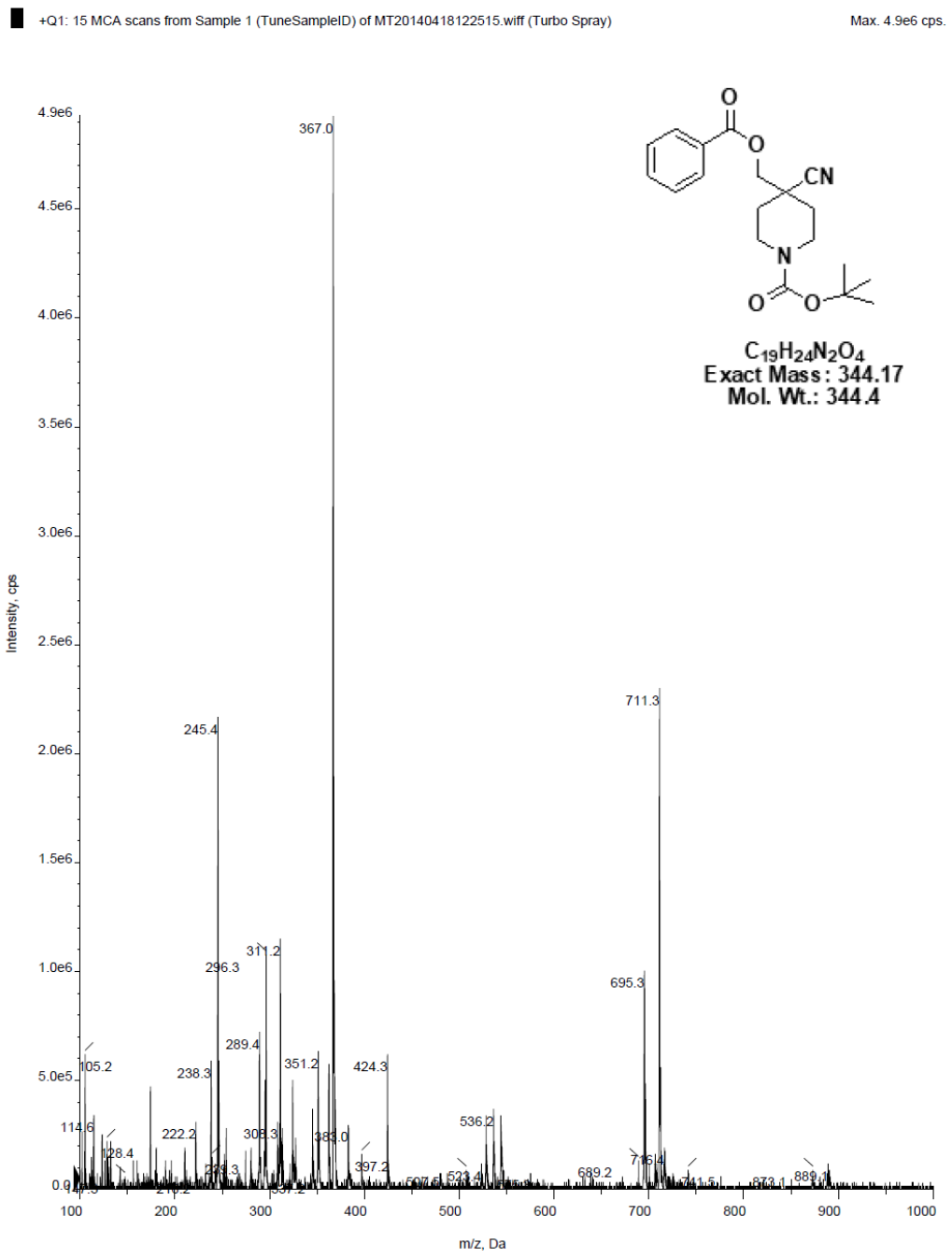

Figure S50. MS spectrum of compound **22**.

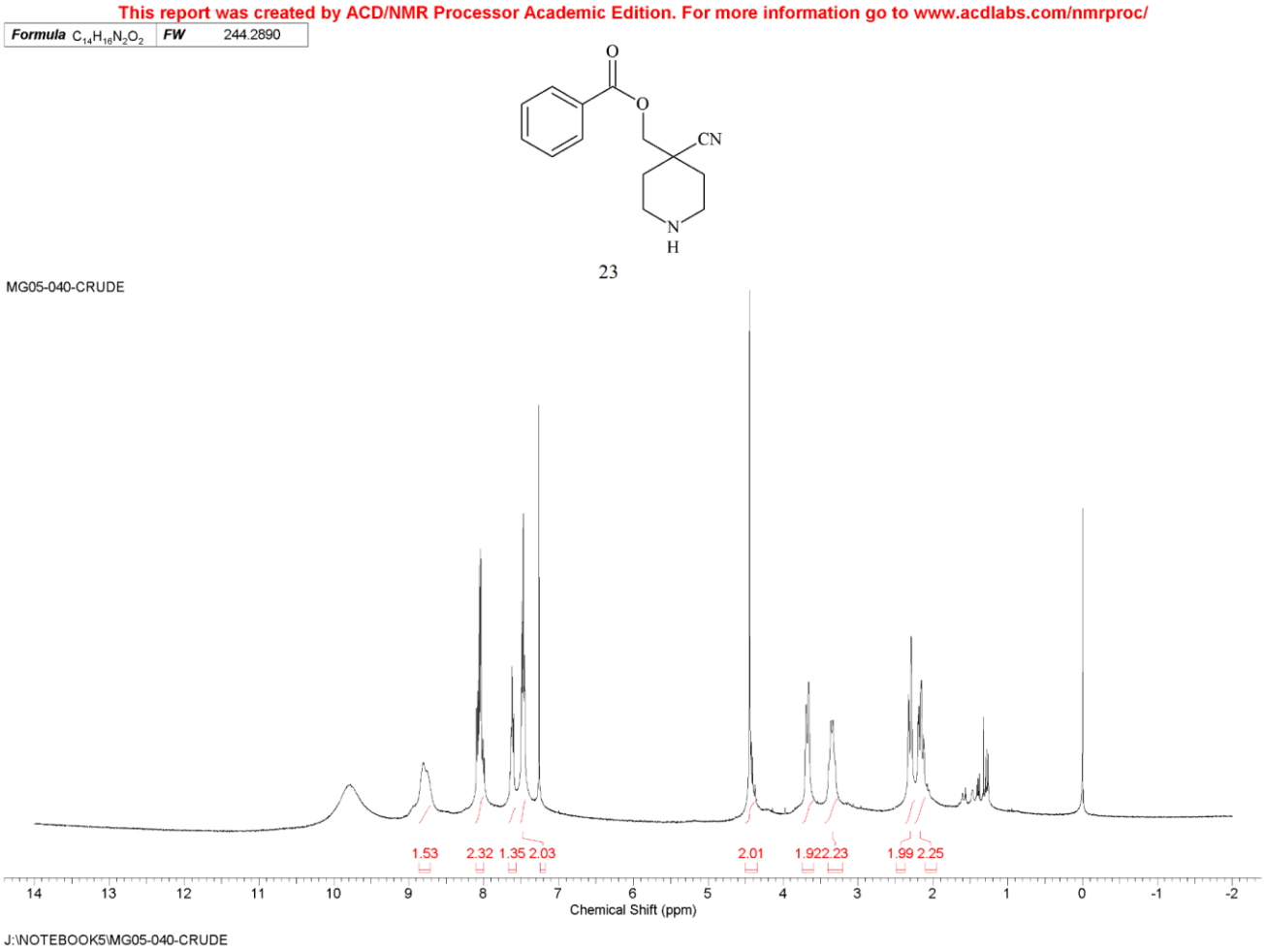

Figure S51. ^{1}H NMR spectrum of compound **23**.

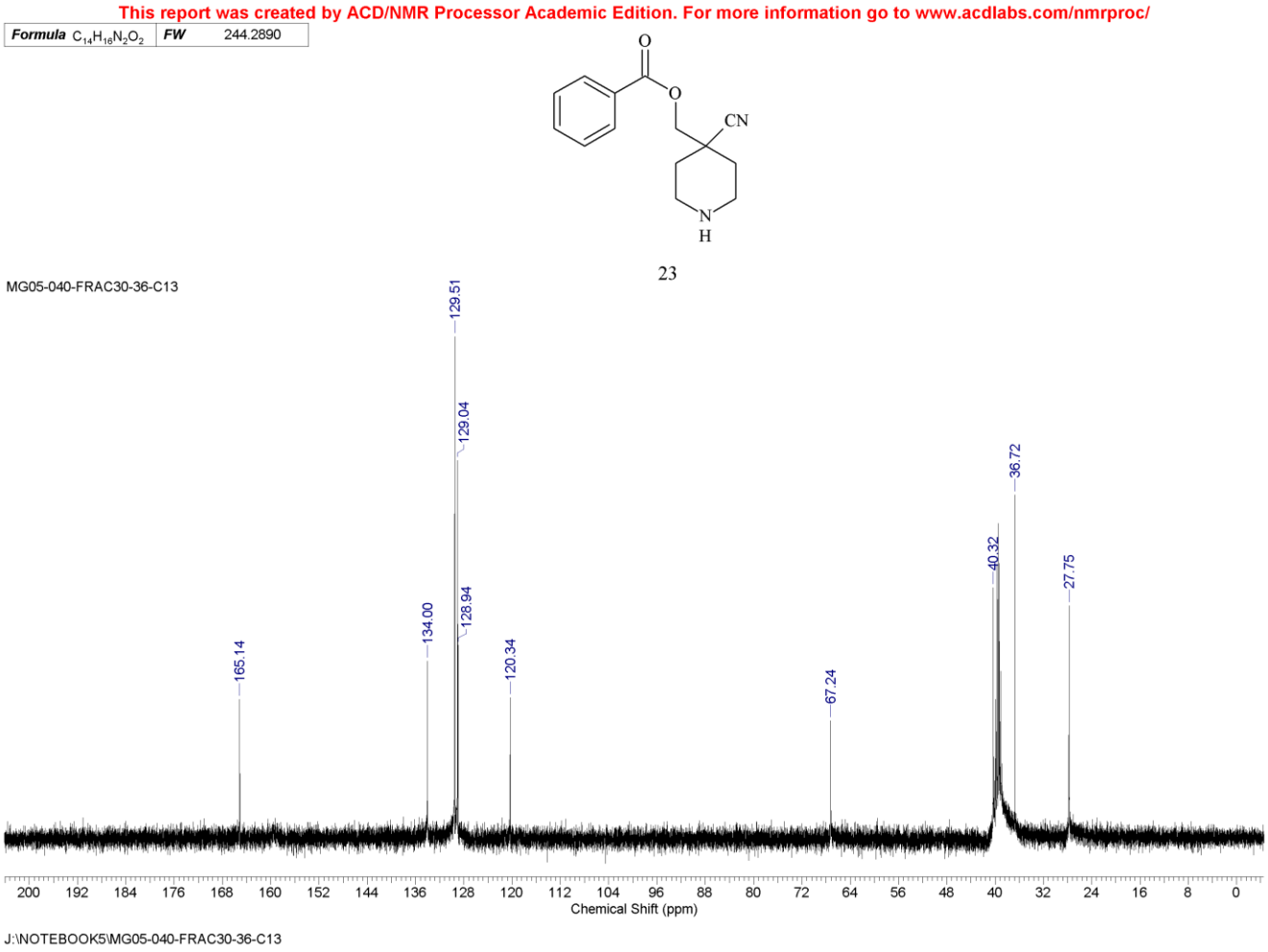

Figure S52. ^{13}C NMR spectrum of compound **23**.

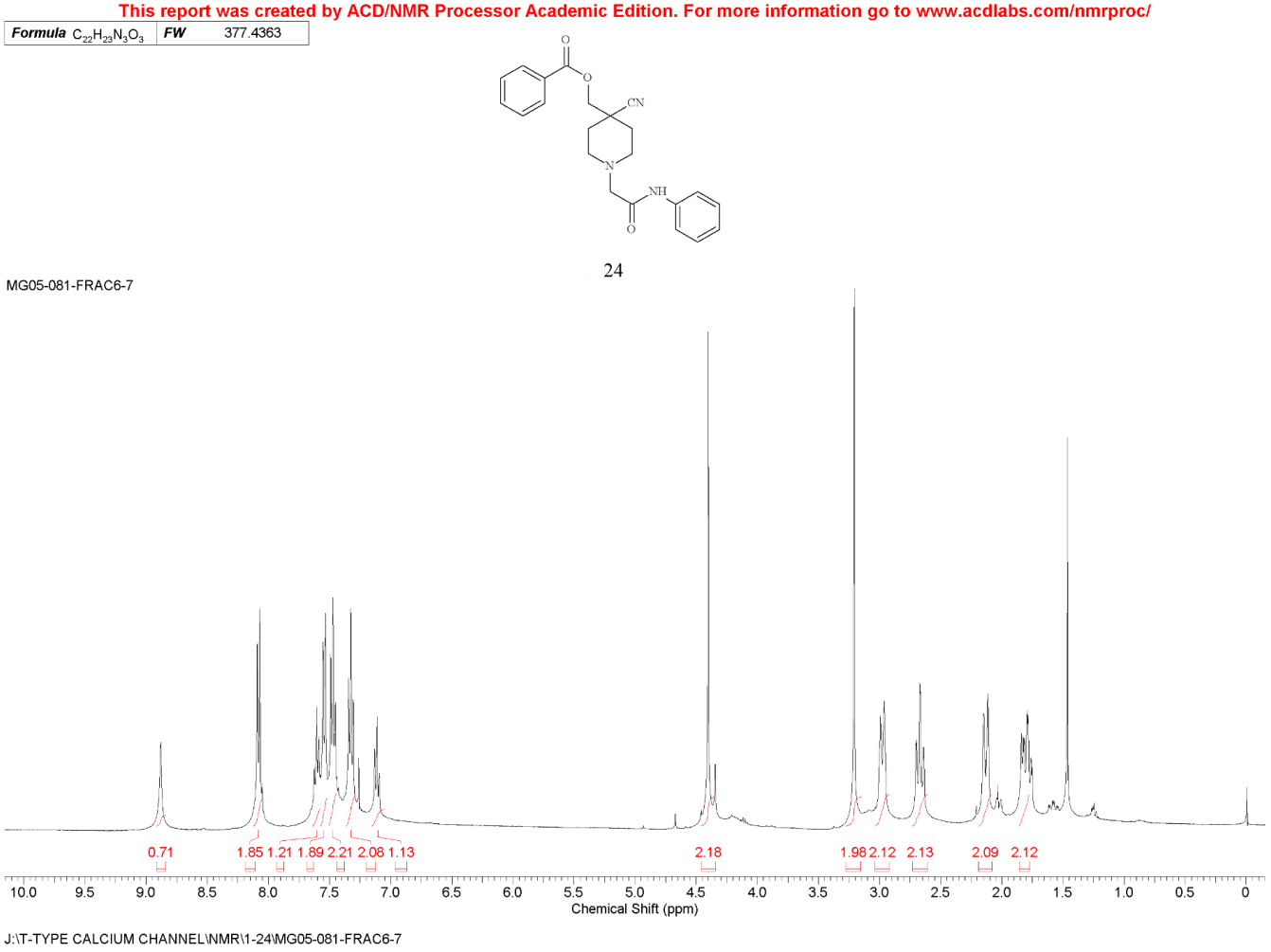

Figure S53. ^{1}H NMR spectrum of compound **24**.

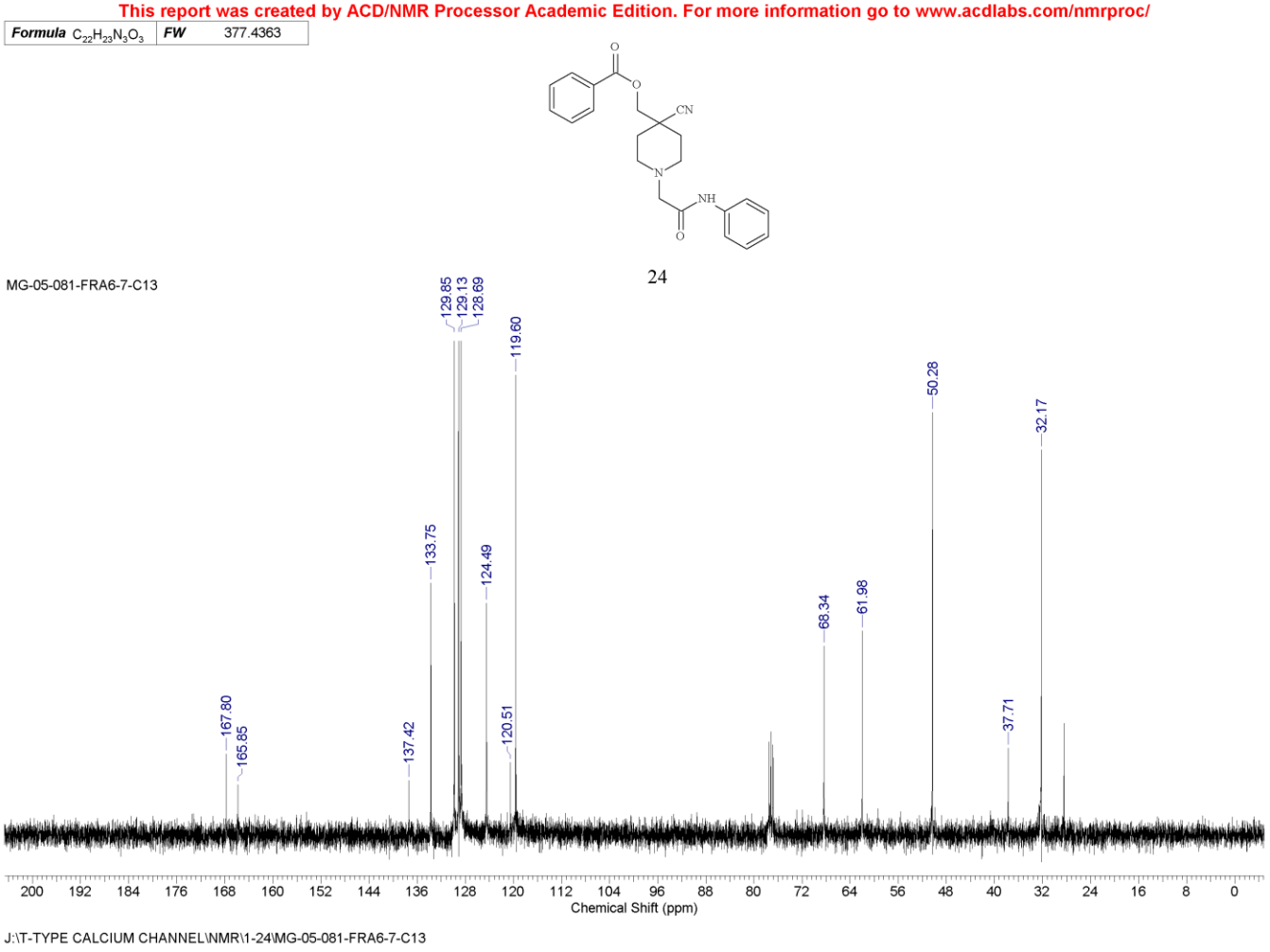

Figure S54. ^{13}C NMR spectrum of compound **24**.

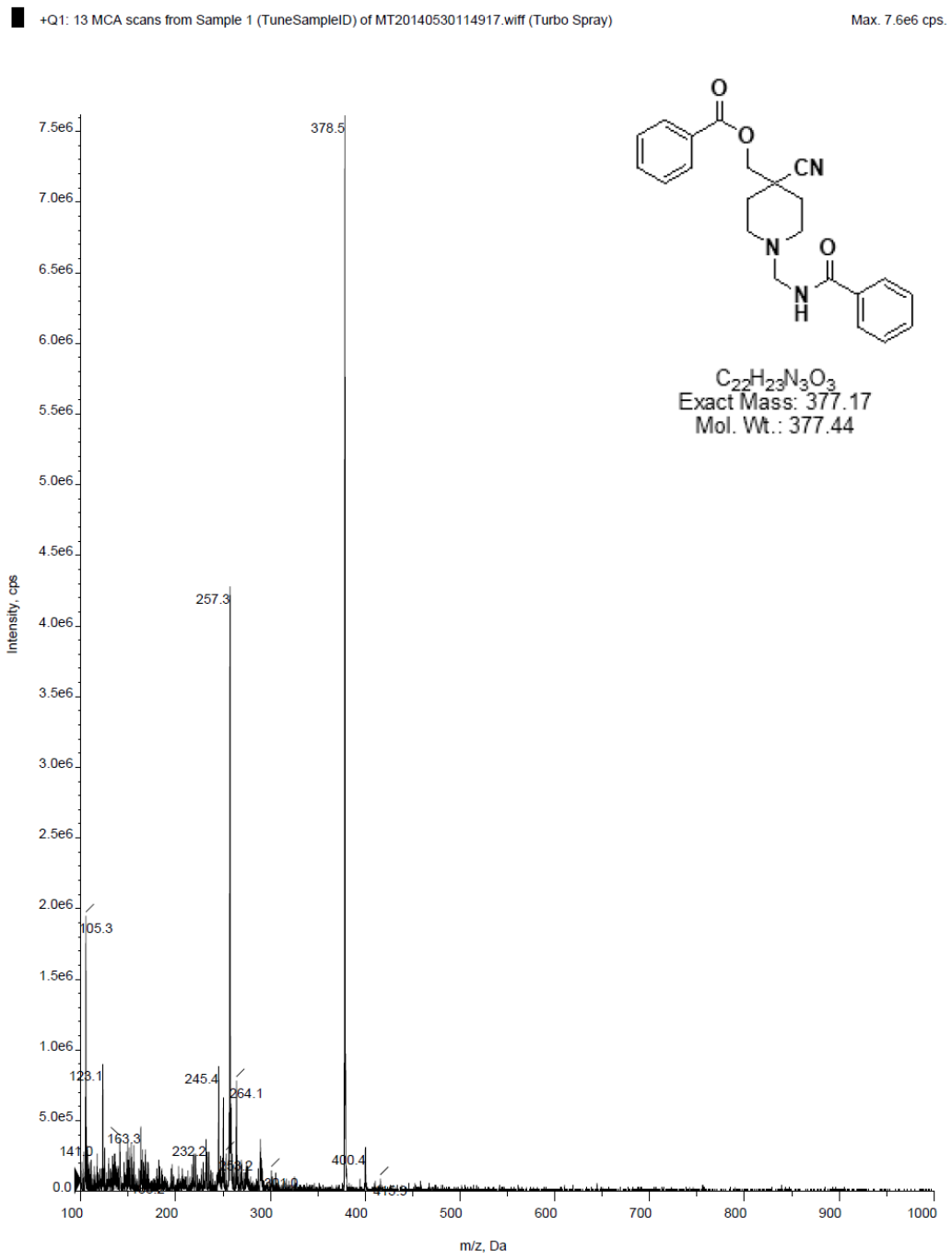

Figure S55. MS spectrum of compound **24**.

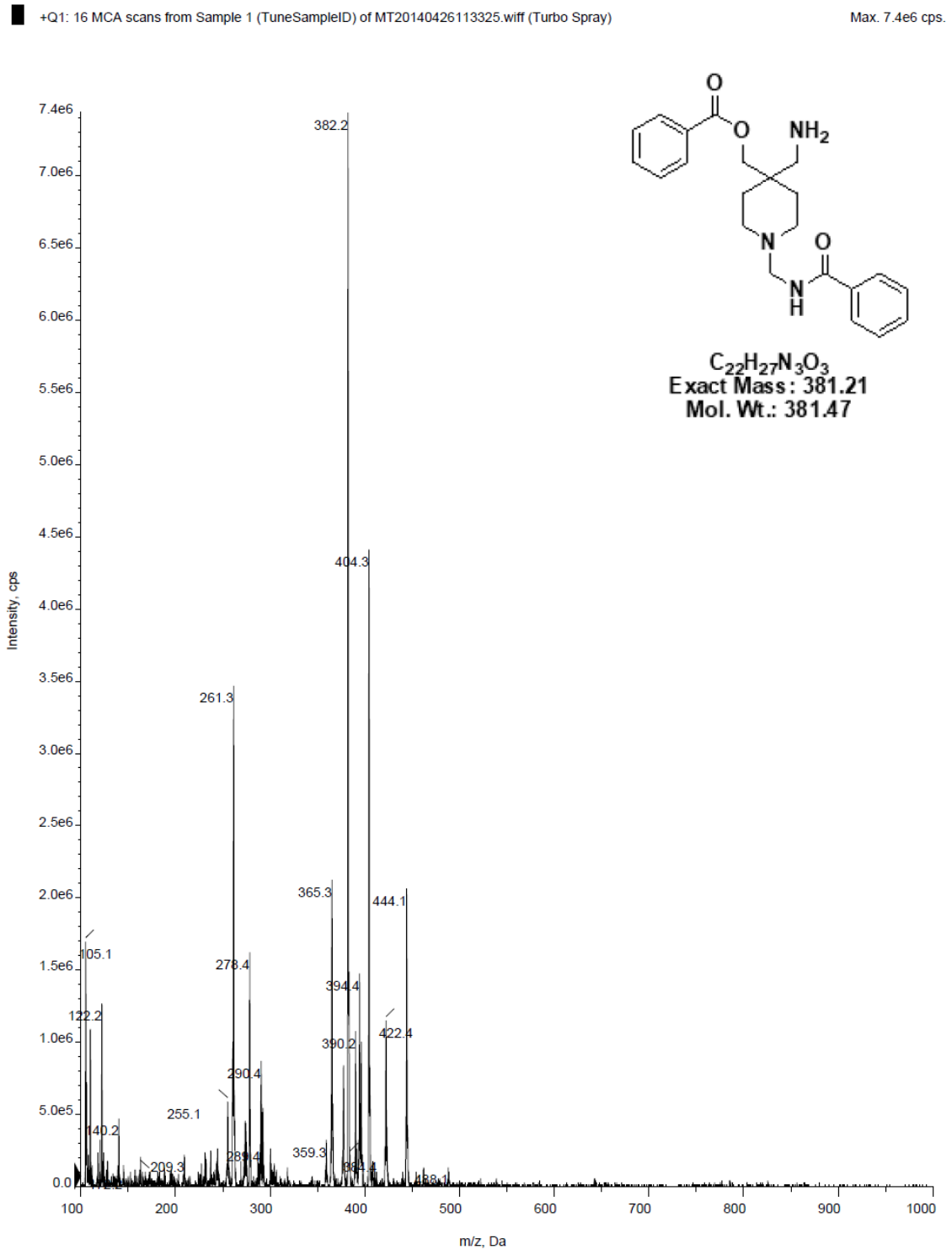

Figure S56. MS spectrum of compound **25**.

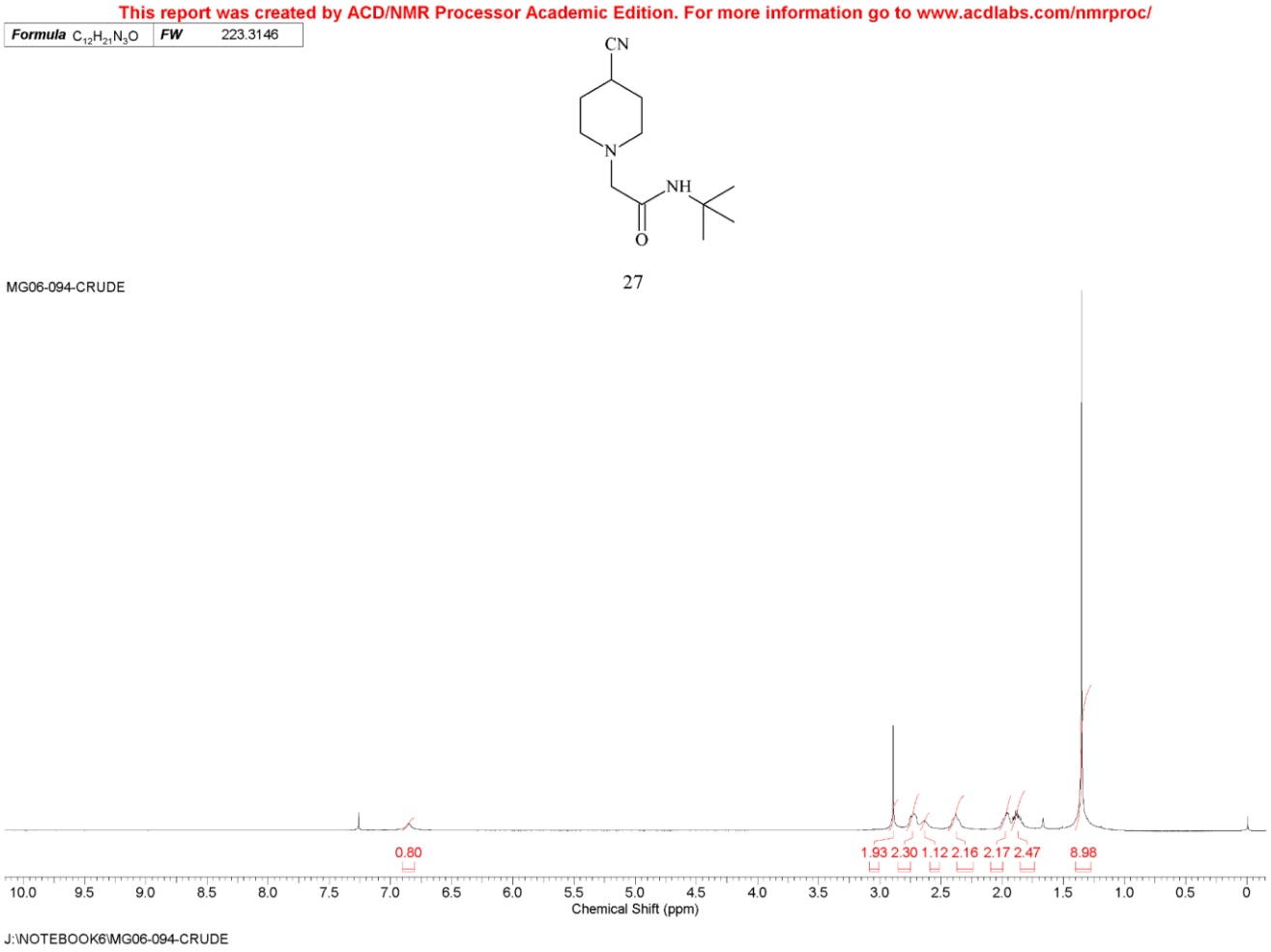

Figure S57. ^{1}H NMR spectrum of compound **27**.

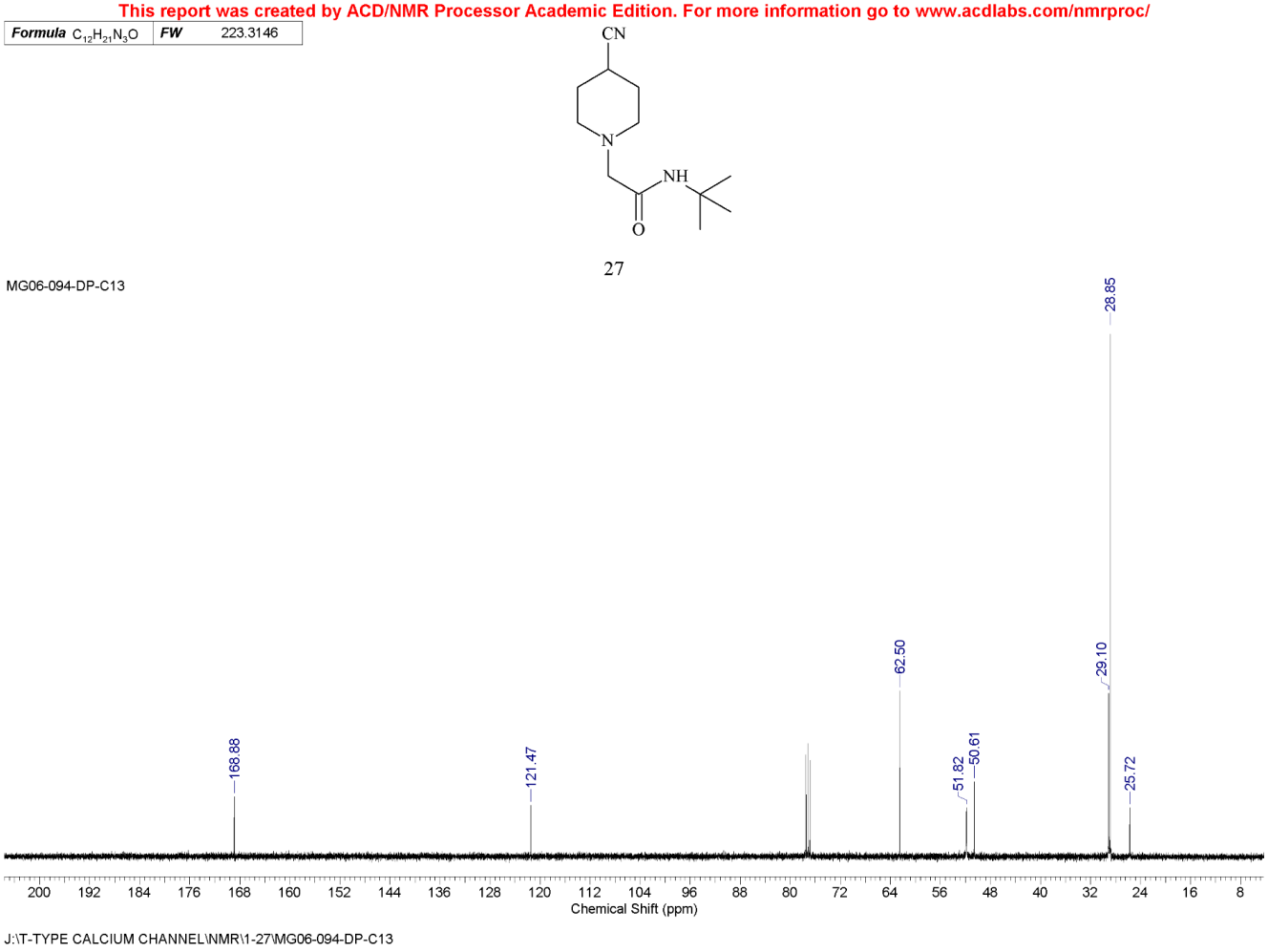

Figure S58. ^{13}C NMR spectrum of compound **27**.

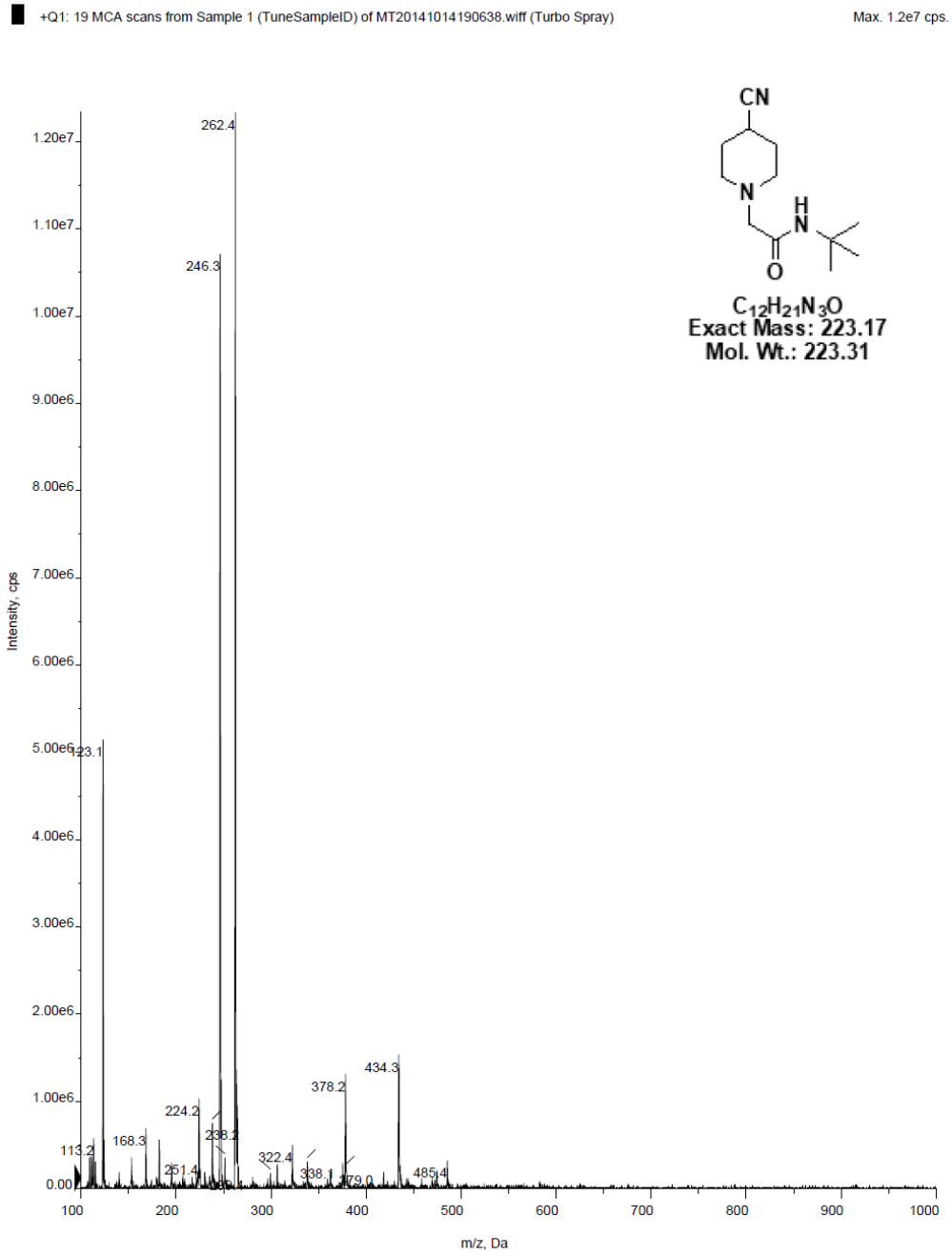

Figure S59. MS spectrum of compound **27**.

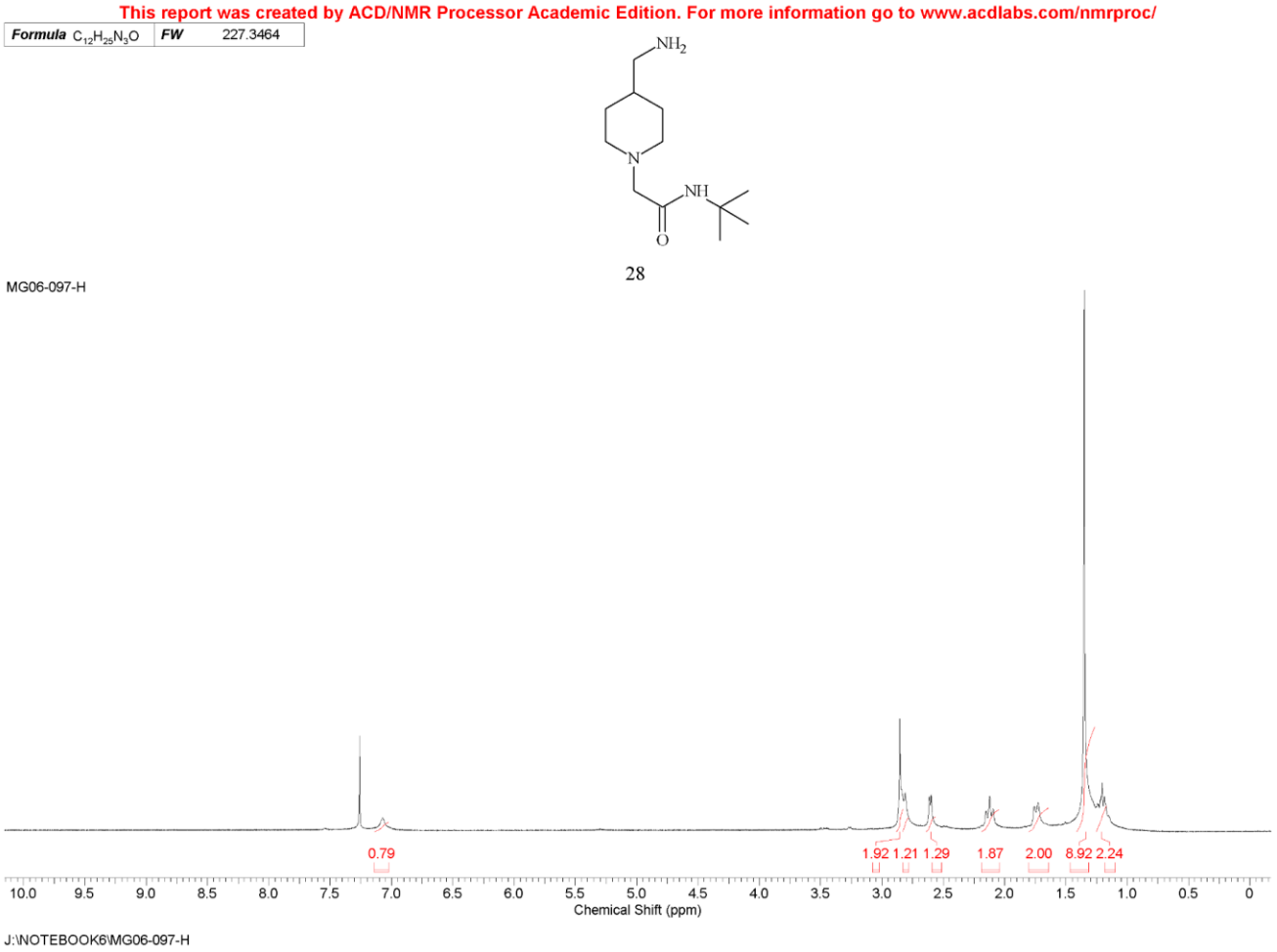

Figure S60. ^{1}H NMR spectrum of compound **28**.

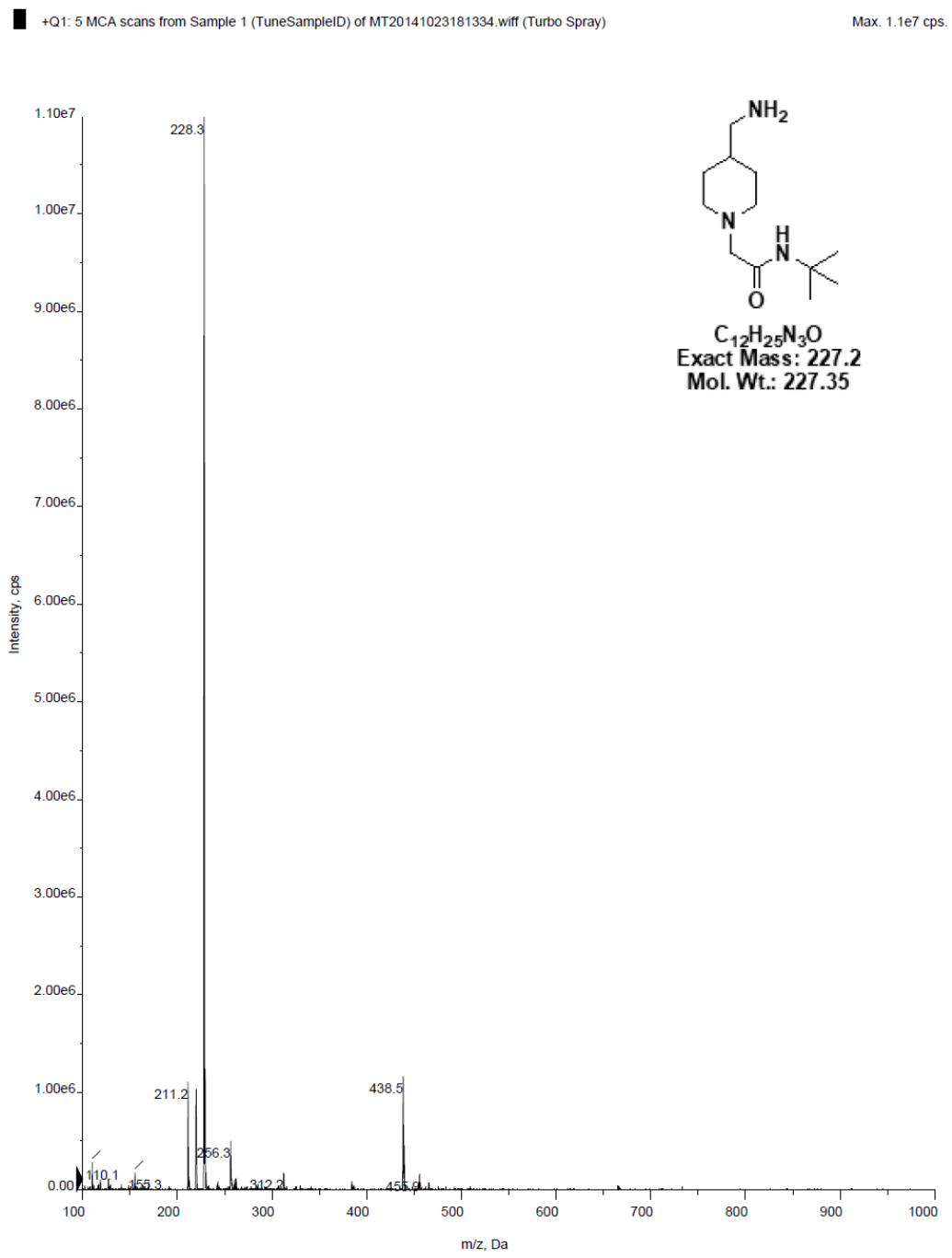

Figure S61. MS spectrum of compound **28**.